Project	**IEEE 802.16 Broadband Wireless Access Working Group <http://ieee802.org/16>**
Title	**Draft IEEE 802.16m Evaluation Methodology Document**
Date Submitted	**2007-06-18**

Source(s)	802.16m Evaluation Methodology Drafting Group Editor: Roshni Srinivasan, Intel Corporation Section Editors: Jeff Zhuang, Motorola Louay Jalloul, Beceem Communications Robert Novak, Nortel Jeongho Park, Samsung Electronics	 roshni.m.srinivasan@intel.com Jeff.Zhuang@motorola.com jalloul@beceem.com rnovak@nortel.com jeongho.jh.park@samsung.com

Re:	Update to C802.16m-07/080r1 by ad-hoc groups constituted in Session #49
Abstract	This document contains proposed evaluation methodology for IEEE 802.16m technical proposals.
Purpose	For discussion and approval by TGm
Notice	This document has been prepared to assist IEEE 802.16. It is offered as a basis for discussion and is not binding on the contributing individual(s) or organization(s). The material in this document is subject to change in form and content after further study. The contributor(s) reserve(s) the right to add, amend or withdraw material contained herein.
Release	The contributor grants a free, irrevocable license to the IEEE to incorporate material contained in this contribution, and any modifications thereof, in the creation of an IEEE Standards publication; to copyright in the IEEE's name any IEEE Standards publication even though it may include portions of this contribution; and at the IEEE's sole discretion to permit others to reproduce in whole or in part the resulting IEEE Standards publication. The contributor also acknowledges and accepts that this contribution may be made public by IEEE 802.16.
Patent Policy and Procedures	The contributor is familiar with the IEEE 802.16 Patent Policy and Procedures <http://ieee802.org/16/ipr/patents/policy.html>, including the statement "IEEE standards may include the known use of patent(s), including patent applications, provided the IEEE receives assurance from the patent holder or applicant with respect to patents essential for compliance with both mandatory and optional portions of the standard." Early disclosure to the Working Group of patent information that might be relevant to the standard is essential to reduce the possibility for delays in the development process and increase the likelihood that the draft publication will be approved for publication. Please notify the Chair <mailto:chair@wirelessman.org> as early as possible, in written or electronic form, if patented technology (or technology under patent application) might be incorporated into a draft standard being developed within the IEEE 802.16 Working Group. The Chair will disclose this notification via the IEEE 802.16 web site <http://ieee802.org/16/ipr/patents/notices>.

1
2

Table of Contents

Index of Tables

Index of Figures

1 Abbreviations and Acronyms

2

3GPP	3G Partnership Project
3GPP2	3G Partnership Project 2
AAS	Adaptive Antenna System also Advanced Antenna System
ACK	Acknowledge
AES	Advanced Encryption Standard
AG	Absolute Grant
AMC	Adaptive Modulation and Coding
A-MIMO	Adaptive Multiple Input Multiple Output (Antenna)
AMS	Adaptive MIMO Switching
ARQ	Automatic Repeat reQuest
ASN	Access Service Network
ASP	Application Service Provider
BE	Best Effort
CC	Chase Combining (also Convolutional Code)
CCI	Co-Channel Interference
CCM	Counter with Cipher-block chaining Message authentication code
CDF	Cumulative Distribution Function
CINR	Carrier to Interference + Noise Ratio
CMAC	block Cipher-based Message Authentication Code
CP	Cyclic Prefix
CQI	Channel Quality Indicator
CSN	Connectivity Service Network
CSTD	Cyclic Shift Transmit Diversity
CTC	Convolutional Turbo Code
DL	Downlink
DOCSIS	Data Over Cable Service Interface Specification
DSL	Digital Subscriber Line
DVB	Digital Video Broadcast
EAP	Extensible Authentication Protocol
EESM	Exponential Effective SIR Mapping
EIRP	Effective Isotropic Radiated Power
ErtVR	Extended Real-Time Variable Rate
FBSS	Fast Base Station Switch
FCH	Frame Control Header
FDD	Frequency Division Duplex
FFT	Fast Fourier Transform
FTP	File Transfer Protocol
FUSC	Fully Used Sub-Channel
HARQ	Hybrid Automatic Repeat reQuest
HHO	Hard Handover

HMAC	keyed Hash Message Authentication Code
HO	Handover
HTTP	Hyper Text Transfer Protocol
IE	Information Element
IEFT	Internet Engineering Task Force
IFFT	Inverse Fast Fourier Transform
IR	Incremental Redundancy
ISI	Inter-Symbol Interference
LDPC	Low-Density-Parity-Check
LOS	Line of Sight
MAC	Media Access Control
MAI	Multiple Access Interference
MAN	Metropolitan Area Network
MAP	Media Access Protocol
MBS	Multicast and Broadcast Service
MDHO	Macro Diversity Hand Over
MIMO	Multiple Input Multiple Output (Antenna)
MMS	Multimedia Message Service
MPLS	Multi-Protocol Label Switching
MS	Mobile Station
MSO	Multi-Services Operator
NACK	Not Acknowledge
NAP	Network Access Provider
NLOS	Non Line-of-Sight
NRM	Network Reference Model
nrtPS	Non-Real-Time Packet Service
NSP	Network Service Provider
OFDM	Orthogonal Frequency Division Multiplex
OFDMA	Orthogonal Frequency Division Multiple Access
PER	Packet Error Rate
PF	Proportional Fair (Scheduler)
PKM	Public Key Management
PUSC	Partially Used Sub-Channel
QAM	Quadrature Amplitude Modulation
QPSK	Quadrature Phase Shift Keying
RG	Relative Grant
RR	Round Robin (Scheduler)
RRI	Reverse Rate Indicator
RTG	Receive/transmit Transition Gap
rtPS	Real-Time Packet Service
RUIM	Removable User Identify Module
SDMA	Space (or Spatial) Division Multiple Access

SF	Spreading Factor
SFN	Single Frequency Network
SGSN	Serving GPRS Support Node
SHO	Soft Handover
SIM	Subscriber Identify Module
SINR	Signal to Interference + Noise Ratio
SISO	Single Input Single Output (Antenna)
SLA	Service Level Agreement
SM	Spatial Multiplexing
SMS	Short Message Service
SNIR	Signal to Noise + Interference Ratio
SNR	Signal to Noise Ratio
S-OFDMA	Scalable Orthogonal Frequency Division Multiple Access
SS	Subscriber Station
STC	Space Time Coding
TDD	Time Division Duplex
TEK	Traffic Encryption Key
TTG	Transmit/receive Transition Gap
TTI	Transmission Time Interval
TU	Typical Urban (as in channel model)
UE	User Equipment
UGS	Unsolicited Grant Service
UL	Uplink
UMTS	Universal Mobile Telephone System
USIM	Universal Subscriber Identify Module
VoIP	Voice over Internet Protocol
VPN	Virtual Private Network
VSF	Variable Spreading Factor
WiFi	Wireless Fidelity
WAP	Wireless Application Protocol
WiBro	Wireless Broadband (Service)
WiMAX	Worldwide Interoperability for Microwave Access

References

[1] IST-4-027756 WINNER II, D 5.10.2, “Spectrum requirements for systems beyond IMT-2000”, v.0.5

[2] A. F. Molisch, “Wireless Communications”, IEEE-Press Wiley, 2005.

[3] Erceg, et al, “Channel models for fixed wireless applications”, IEEE 802.16.3c-01/29r4, 17/7/2001

[4] Recommendation ITU-R M.1225, “Guidelines for evaluation of radio transmission technologies for IMT-2000”, 1997

[5] 3GPP-3GPP2 Spatial Channel Ad-hoc Group, “Spatial Channel Model Text Description,” V7.0, August 19, 2003

[6] 3GPP TR 25.996, “Spatial channel model for Multiple Input Multiple Output (MIMO) Simulations”

[7] Daniel S. Baum et al, “An Interim Channel Model for Beyond-3G Systems – Extending the 3GPP Spatial Channel Model (SCM)”, Proc. IEEE VTC'05, Stockholm, Sweden, May 2005.

[8] A. F. Molisch, H. Asplund, R. Heddergott, M. Steinbauer, and T. Zwick, “The COST259 directional channel model – I. overview and methodology,” IEEE Trans. Wireless Comm., vol. 5, pp. 3421–3433, 2006.

[9] H. Asplund, A. A. Glazunov, A. F. Molisch, K. I. Pedersen, and M. Steinbauer, “The COST259 directional channel model II - macrocells,” IEEE Trans. Wireless Comm., vol. 5, pp. 3434–3450, 2006.

[10] L. Correia (ed.), “Flexible Personalized Wireless Communications”, Wiley, 2001.

[11] A. F. Molisch and H. Hofstetter, “The COST273 Channel Model,” in “Mobile Broadband Multimedia Networks “, (L. Correia, ed.), Academic Press, 2006.

[12] IST-WINNER II Deliverable D1.1.1 v1.0, “WINNER II Interim Channel Models”, December 2006.

[13] M. Steinbauer, A. F. Molisch, and E. Bonek, “The double-directional radio channel,” IEEE Antennas and Propagation Mag., pp. 51–63, August 2001.

[14] G. J. Foschini and M. J. Gans, “On limits of wireless communications in a fading environment when using multiple antennas,” Wireless Personal Communications, vol. 6, pp. 311–335, Feb. 1998.

[15] P. Almers, et al. “Survey of channel and radio propagation models for wireless mimo systems,” Eurasip J. Wireless Comm. Networking, vol. in press, 2007.

[16] T-S Chu, L.J.Greenstein, “A quantification of link budget differences between the cellular and PCS bands”, IEEE Trans VT-48, No.1, January 1999, pp.60-65

[17] “Digital mobile radio towards future generation systems”, COST Action 231 Final Report, EUR 18957

[18] D.Parsons, “The Mobile Radio Propagation Channel”, Chap.4, p.88, Pentech Press, 1992

[19] Y.Oda, K.Tsunekawa, M.Hata, “Advanced LOS path-loss model in microcellular mobile communications” , IEEE Trans AP-51, pp.952-956, May 2003

[20] “Universal Mobile Telecommunications System (UMTS) ; Selection procedures for the choice of radio transmission technologies of the UMTS (UMTS 30.03 version 3.2.0)”, ETSI technical report TR 101 112 v3.2.0 (1998-04)

[21] Jakes, W.C “Microwave mobile communications”, Wiley, New York, 1974

[22] M. Patzold, “Mobile Fading Channels”, John Wiley, 2002

[23] 3GPP, R1-061001 “LTE Channel Models and link simulations”

[24] https://www.ist-winner.org/phase_model.html

[25] RUNCOM, “Coverage capacity simulateons for OFDMA PHY in ITU-T channel models, “ IEEE C802.16d-03/78r1, November, 2003

[26] RUNCOM, “Coverage simulation for OFDMA PHY mode,” IEEE C8021.6e-03/22r1.

[27] Sony, Intel, “TGn Sync TGn Proposal MAC Simulation Methodology”, IEEE 802.11-04/895r2, November 2004.

[28] ST Micro-Electronics “Time Correlated Packet Errors in MAC Simulations”, IEEE Contribution, 802.11-04-0064-00-000n, Jan. 2004.

[29] Atheros, Mitsubishi, ST Micro-Electronics and Marvell Semiconductors, “Unified Black Box PHY Abstraction Methodology”, IEEE Contribution 802.11-04/0218r1, March 2004.

[30] 3GPP TR 25.892 V2.0.0 “Feasibility Study for OFDM for UTRAN enhancement,”

[31] WG5 Evaluation Ad-hoc Group, “1x EV-DV Evaluation Methodology – Addendum (V6),” July 25, 2001

[32] Ericsson, “System level evaluation of OFDM- further considerations”, TSG-RAN WG1 #35, R1-03-1303, November, 2003

[33] Nortel, “Effective SIR Computation for OFDM System-Level Simulations,” TSG-RAN WG1 #35, R03-1370, November 2003.

[34] Nortel “OFDM Exponential Effective SIR Mapping Validation, EESM Simulation Results for System-Level Performance Evaluations,” 3GPP TSG-RAN1 Ad Hoc, R1-04-0089, January, 2004.

[35] K. Brueninghaus et al, “Link performance models for system level simulations of broadband radio access,” IEEE PIMRC, 2005.

[36] L. Wan, et al, “A fading insensitive performance metric for a unified link quality model,” WCNC, 2006.

[37] DoCoMo, Ericsson, Fujitsu, Mitsubishi Electric, NEC, Panasonic, Sharp, Toshiba Corporation, R1-060987, “Link adaptation schemes for single antenna transmissions in the DL, 3GPP-LTE WG1 meeting #44-bis, Athens, March 2006.

[38] G. Caire, “Bit-Interleaved Coded Modulation”, *IEEE Transactions on Information Theory*, Vol. 44, No.3, May 1998.

[39] J. Kim, et al, “Reverse Link Hybrid ARQ: Link Error Prediction Methodology Based on Convex Metric”, Dan Gal et al. Technologies, 3GPP2, TSG-C WG3.

[40] S. Tsai, “Effective-SNR Mapping for Modeling Frame Error Rates in Multiple-State Channels”, Ericsson, 3GPP2-C30-20030429-010.

[41] Reference not provided. Reference [33] from C80212m-07_069.doc.

[42] IEEE P 802.20™ PD-09 Version 1.0, “802.20 Evaluation Criteria – version 1.0,” September 23, 2005

[43] P. Barford and M Crovella, "Generating Representative Web Workloads for Network and Server Performance Evaluation" In Proc. ACM SIGMETRICS International Conference on Measurement and Modeling of Computer Systems, pp. 151-160, July 1998.

[44] S. Deng. “Empirical Model of WWW Document Arrivals at Access Link.” In Proceedings of the 1996 IEEE International Conference on Communication, June 1996

[45] R. Fielding, J. Gettys, J. C. Mogul, H. Frystik, L. Masinter, P. Leach, and T. Berbers-Lee, "Hypertext Transfer Protocol - HTTP/1.1", RFC 2616, HTTP Working Group, June 1999. ftp://ftp.Ietf.org/rfc2616.txt.

[46] B. Krishnamurthy and M. Arlitt, "PRO-COW: Protocol Compliance on the Web", Technical Report 990803-05-TM, AT&T Labs, August 1999, http://www.research.att.com/~bala/papers/procow-1.ps.gz. 29 30 31 32 33 34 35 36 37

[47] B. Krishnamurthy, C. E. Wills, "Analyzing Factors That Influence End-to-End Web Performance", http://www9.org/w9cdrom/371/371.html

[48] H. K. Choi, J. O. Limb, "A Behavioral Model of Web Traffic", Proceedings of the seventh International Conference on Network Protocols, 1999 (ICNP '99), pages 327-334.

[49] F. D. Smith, F. H. Campos, K. Jeffay, D. Ott, "What TCP/IP Protocol Headers Can Tell Us About the Web", Proc. 2001 ACM SIGMETRICS International Conference on Measurement and Modeling of Computer Systems, pp. 245-256, Cambridge, MA June 2001.

[50] 3GPP2/TSG-C30-20061204-062A, “cdma2000 Evaluation Methodology (V6)”, Maui, HI., December 2006

[51] J. Cao, William S. Cleveland, Dong Lin, Don X. Sun., "On the Non-stationarity of Internet Traffic", Proc. ACM SIGMETRICS 2001, pp. 102-112, 2001.

[52] K. C. Claffy, "Internet measurement and data analysis: passive and active measurement", http://www.caida.org/outreach/papers/Nae/4hansen.html.

[53] 3GPP2-TSGC5, HTTP and FTP Traffic Model for 1xEV-DV Simulations

[54] 3GPP TSG-RAN1#48 R1-070674, LTE physical layer framework for performance verification, Orange, China Mobile, KPN, NTT DoCoMo, Sprint, T-Mobile, Vodafone, Telecom Italia, February 2007.

[55] WINNER Project, IST-2003-507581 WINNER D1.3 version 1.0, “Final usage scenarios.”

[56] 3GPP TS 25.101v7.7.0, “User Equipment (UE) Radio Transmission and Reception (FDD)”

[57] 3GPP TSG RAN WG1#44, R1-060385, “Cubic Metric in 3GPP-LTE”, February 13-17, 2006, Denver, USA

[58] Bong Ho Kim, “Application traffic model,” http://www.flyvo.com/archive/Posdata-application_traffic_model.pdf , 2007

[59] ComScore Media Metrix Releases January Top 50 Web Rankings and Analysis; http://www.comscore.com/press/release.asp?press=1214

[60] http://www-tkn.ee.tu-berlin.de/research/trace/ltvt.html

[61] F. Fitzek and M. Reisslein. MPEG-4 and H.263 traces for network performance evaluation (extended version). Technical Report TKN-00-06, Technical University Berlin, Dept. of Electrical Eng., Germany, October 2000.

[62] W. R. Stevens, "TCP/IP Illustrated, Vol. 1", Addison-Wesley Professional Computing Series, 1994.

[63] M. Krunz and S. Tripathi, “On the Characterization of VBR MPEG Stream,” ACM, pp. 192-202, 1997

[64] A. Matrawy, I. Lambadaris, and C. Huang, “MPEG4 Traffic Modeling Using The Transform Expand Sample Methodology,” Proceedings of the IEEE 4th International Workshop on Networked Appliances, pp. 249-256, 2001.

[65] A. A. Lazar, G. Pacifici, and D. E. Pendarakis. Modeling video sources for real-time scheduling. In Proc. of IEEE GLOBECOM ‘93, volume 2, pages 835-839, 1993.

[66] F. H. P. Fitzek and M. Reisslein, “MPEG-4 and H.263 Video Traces for Network Performance Evaluation,” IEEE Network, Vol. 15, Issue 6, pp. 40-54, 2001.

Editor's Notes

This document is a harmonized contribution that has been developed from C802.16m-07_080r1 and contributions submitted to TGm in Sessions #48 and #49.

Major sections of this document have been edited by members of the ad-hoc groups constituted Session #48 and subsequently reconstituted in Session #49. Contributions that have been harmonized and section editors are listed at the top of each section.

The drafting group has marked some text with brackets and left other text unbracketed. Unbracketed text in black identifies content that has been harmonized. Square brackets [ ] identify text that requires further harmonization. This may include situations where the specified text is proposed for removal by one or more contributors or there are contradictory contributions related to that text. Bracketed text has also been color coded in green.

Editors' notes in red capture actions that may be necessary for further updates.

1. Introduction

A great deal can be learned about an air interface by analyzing its fundamental performance in a link-level setting which consists of one base station and one mobile terminal. This link-level analysis can provide information on the system's fundamental performance metrics. The actual performance, in real-world settings, where multiple base stations are deployed in a service area and operating in the presence of a large number of active mobile users, can only be evaluated through a system-level analysis. The extension of the link-level analysis methods to a system-level analysis may start with adding multiple users in a single-cell setting. This technique is generally straightforward and provides a mechanism for initial understanding of the multiple-access characteristics of the system. Ultimately, however, quantifying the system level performance, although difficult, carries with it the reward of producing results that are more indicative of the system performance.

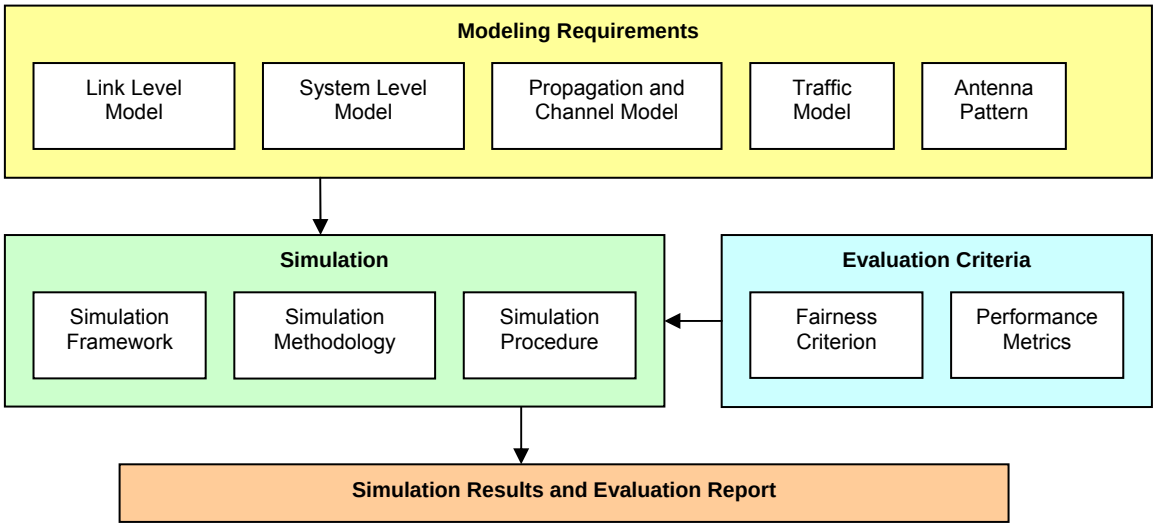

Figure 1 : Simulation Components

Since system level results vary considerably with different propagation and interference environments, as well as with the number and distribution of users within the cells, it is important that the assumptions and parameters, used in the analysis, be reported carefully lest the quoted network-level performance be misleading.

The objective of this evaluation methodology is to define link-level and system-level simulation models and associated parameters that shall be used in the evaluation and comparison of technology proposals for IEEE 802.16m. Proponents of any technology proposal using this methodology shall follow the evaluation methods defined in this document and report the results using the metrics defined in this document. The methods provided in this evaluation methodology document may be extended or enhanced in order to align with IMT EVAL or to further evaluate specific proposals not covered by this document.

Evaluation of system performance of a mobile broadband wireless access technology requires system simulation that accurately captures the dynamics of a multipath fading environment and the architecture of the air-interface. The main simulation components are illustrated in Figure 1

2. System Simulation Requirements

Editor: Roshni Srinivasan, roshni.m.srinivasan@intel.com

Sources	Document Reference
Sassan Ahmadi et al.	C80216m-07_069.doc
Dan Gal et al.	C80216m-07_063.doc
Robert Novak et al.	C80216m-07_074r1.pdf
Wookbong Lee et al.	C80216m-07_075r1.doc
Roshni Srinivasan et al.	C80216m-07_101.doc C80216m-07_102.doc

2.1. Antenna Characteristics

This section specifies the antenna characteristics, e.g. antenna pattern, orientation, etc. for antennas at the BS and the MS.

2.1.1. BS Antenna

2.1.1.1. BS Antenna Pattern

The antenna pattern used for each BS sector is specified as

$$\mathrm{A}(\theta) = -\min\left[12\left(\frac{\theta}{\theta_{3\mathrm{dB}}}\right)^2, A_m\right]$$

where $A(\theta)$ is the antenna gain in dBi in the direction $\theta, -180 \le \theta \le 180$, and min [.] denotes the minimum function, θ_{3dB} is the 3 dB beamwidth (corresponding to θ_{3dB} = 70 degrees), and A_m = 20 dB is the maximum attenuation. Figure 2 shows the BS antenna pattern for 3 sector cells to be used in system level simulations.

Figure 2: Antenna Pattern for 3-Sector Cells

2.1.1.2. BS Antenna Orientation

The antenna bearing is defined as the angle between the main antenna lobe center and a line directed due east given in degrees. The bearing angle increases in a clockwise direction. Figure 3 shows the hexagonal cell and its three sectors with the antenna bearing orientation proposed for the simulations. The main antenna lobe center directions each point to the sides of the hexagon.

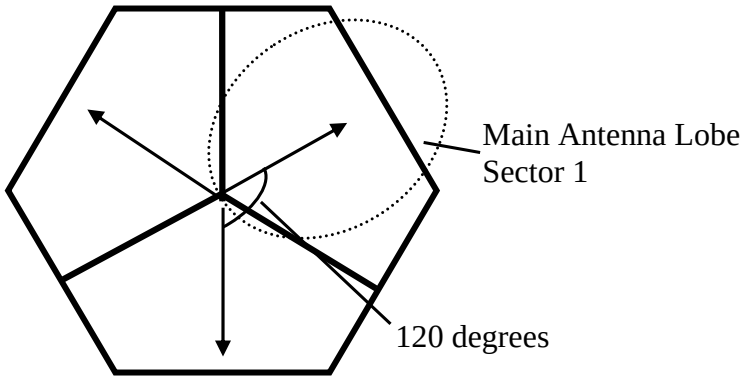

Figure 3 : Antenna bearing orientation diagram

2.1.2. MS Antenna

The MS antenna is assumed to be omni directional.

2.2. Simulation Assumptions

The purpose of this section is to outline simulation assumptions that proponents will need to provide in order to facilitate independent assessment of their proposals. The current tables for downlink and uplink simulation assumptions are templates that may be extended for a complete description of simulation assumptions. Baseline assumptions are specified for comparison with the reference system as defined by the 802.16m requirements. Additional assumptions relevant to a proposal may be provided by proponents to describe details that may be necessary for an evaluation of the proposal.

Topic	Description	Baseline System Assumptions	Proposal Specific Assumptions (To be provided by Proponent)
Basic modulation	Modulation schemes for data and control	QPSK, 16QAM, 64QAM	
Duplexing scheme	TDD, HD-FDD or FD-FDD	TDD	
Subchannelization	Subcarrier permutation	PUSC/AMC	
Resource Allocation Granularity	Smallest unit of resource allocation	PUSC: Non-STC: 1 slot, STC: 2 slots (1 slot = 1 subchannel x 2 OFDMA symbols) AMC: Non-STC: 1 slot, (1 slot = 2 bins x 3 OFDMA symbols)	

Downlink pilot structure	Pilot structure, density etc.	Specific to subchannelization scheme PUSC/AMC	
Multi-antenna Transmission format	Multi-antenna configuration and transmission scheme	MIMO 2x2 (Adaptive MIMO Switching Matrix A & Matrix B) Beamforming (2x2)	
Receiver Structure	MMSE/ML/MRC/ Interference Cancellation	MMSE (Matrix B data zone) MRC (MAP)	
Data Channel coding	Channel coding schemes and block sizes	Convolutional Turbo Coding (CTC)	
Control Channel Coding	Channel coding schemes and block sizes	Convolutional Turbo Coding (CTC), Convolutional Coding (CC) for FCH only	
Scheduling	Demonstrate performance / fairness criteria in accordance to traffic mix	Proportional Fairness for full buffer data only	
Link adaptation	Modulation and Coding Schemes, CQI Feedback Delay / Error	QPSK(1/2) with repetition 1/2/4/6, QPSK(3/4), 16QAM(1/2), 16QAM(3/4), 64QAM(1/2), 64QAM(2/3), 64QAM(3/4) 64QAM(5/6), CQI Feedback Delay of 2 frames	
Link to System Mapping	EESM/MI	EESM/MI	
H-ARQ	Chase Combining/ Incremental Redundancy, Synchronous Asynchronous, Adaptive/Non-Adaptive ACK/NACK Delay, Maximum Number of Retransmissions	Chase Combining Asynchronous, Non-adaptive, 1 frame ACK/NACK delay, Maximum 4 HARQ Retransmissions, 20% Target PER for Initial Transmission (BE data)	
Power Control	Subcarrier power allocation	Equal power per subcarrier	
Interference Model	Co-channel interference model, fading model for interferers, number of major interferers, threshold, receiver interference awareness	Frequency selective interference model for PUSC/AMC, no interference awareness at receiver	
Frequency Reuse	Frequency reuse pattern	3 Sectors with Frequency Reuse of 1 and Reuse 3	
Control signalling	Message/signaling format, overheads	Compressed MAP with sub-maps	

1
2

Table 1: System-level simulation assumptions for the downlink

Topic	Description	Baseline Assumptions Where Applicable	Proposal Specific Assumptions (To be filled by Proponent)
Basic modulation	Modulation schemes for data and control	QPSK, 16QAM	
Duplexing scheme	TDD, HD-FDD or FD-FDD	TDD	
Subchannelization	Subcarrier permutation	PUSC/AMC	
Resource Allocation Granularity	Smallest unit of resource allocation	PUSC: 1 slot, (1 slot = 1 subchannel x 3 OFDMA symbols) AMC: 1 slot, (1 slot = 2 bins x 3 OFDMA symbols)	
Uplink pilot structure	Pilot structure, density etc.	Specific to subchannelization scheme PUSC/AMC	
Multi-antenna Transmission format	Multi-antenna configuration and transmission scheme	Collaborative SM for two MS with single antenna	
Receiver Structure	MMSE/ML Interference Cancellation	MMSE	
Data Channel coding	Channel coding schemes and block sizes	Convolutional Turbo Coding (CTC)	
Control Channel Coding	Channel coding schemes and block sizes	CDMA Codes (PUSC 2 symbols) for Initial Ranging and Handover, CDMA Codes (PUSC 1 symbol) for Periodic Ranging and Bandwidth Request, CQICH (6 bits)	
Scheduling	Demonstrate performance / fairness criteria in accordance to traffic mix	Proportional Fairness for full buffer data only	
Link adaptation	Modulation and Coding Schemes	QPSK(1/2) with repetition 1/2/4/6, QPSK(3/4), 16QAM(1/2), 16QAM(3/4)	
Link to System Mapping	EESM/MI	EESM/MI	

H-ARQ	Chase Combining/ Incremental Redundancy, Synchronous Asynchronous, Adaptive/Non-Adaptive ACK/NACK Delay, Maximum Number of Retransmissions	Chase Combining Asynchronous, Non-adaptive, ACK/NACK delay N/A, , Maximum 4 HARQ Retransmissions, 20% Target PER for Initial Transmission (BE data)	
Power Control	Open Loop / Closed Loop		
Interference Model	Co-channel interference model, fading model for interferers, number of major interferers, threshold, receiver interference awareness	Frequency selective interference model for PUSC/AMC, no interference awareness at receiver	
Frequency Reuse	Frequency reuse pattern	3 Sectors with Frequency Reuse of 1 and Reuse 3	
Control signalling	Message/signaling format, overheads	Initial Ranging, Periodic Ranging, Handover Ranging, Bandwidth Request, Fast Feedback/CQI Channel	

Table 2: System-level simulation assumptions for the uplink

2.3. Deployment Scenarios

The following table summarizes the channel environments and associated assumptions and parameters that are required for system level simulations.

[Editor's note: The table entries in the following template have been populated based on text from the channel models section. The template may be extended to cover additional parameters. Entries corresponding to bracketed text in the channel models sections are bracketed. Entries that need specification are marked TBD.]

Scenario/ Parameters	Urban Macrocell	Suburban Macrocell	Urban Microcell	[Indoor Small Office]	[Outdoor to Indoor]
BS-BS distance	1.5 km	1.5 km	0.5 km	[50 m]	[TBD]
BS Height	32 m	32 m	12.5 m	[1-2.5m]	[TBD]
BS Tx Power	46 dBm	46 dBm	46 dBm	[TBD]	[46 dBm]
MS Tx	23 dBm	23 dBm	23 dBm	[23 dBm]	[23 dBm]

Power					
MS Height	1.5 m	1.5 m	1.5 m	[1.5m]	[1.5m]
Path Loss Model	Refer to Section 3.2.3.1	Refer to Section 3.2.3.2	Refer to Section 3.2.3.3	[Refer to Section 3.2.3.4]	[Refer to Section 3.2.3.5]
Lognormal Shadowing Standard Deviation	8 dB	NLOS 8 dB LOS 4 dB	NLOS 4 dB LOS 3 dB	[NLOS (Room to corridor) 8 dB NLOS (Through light wall) 6 dB NLOS (Through heavy wall) 8 dB]	[7 dB]
Mobility	0-350 kmph	0-350 kmph	0-120 kmph	[TBD]	[TBD]
Channel Mix	TBD	TBD	TBD	[TBD]	[TBD]

Table 3: Channel Environments

2.4. Reference System Calibration

This purpose of this section is to provide guidelines for simulation parameters that proponents will need to use in order to evaluate performance gains of their proposals relative to the reference system as defined in the 802.16m requirements document. The purpose of calibration is to ensure that, under a set of common assumptions and models, the simulator platforms that will be used by various proponents can produce results that are similar.

2.4.1. Base Station Model

Parameter	Description	Value
P_{BS}	MAX transmit power per sector/carrier	46 dBm @ 10 MHz bandwidth
H_{BS}	Base station height	32m
G_{BS}	Gain (boresight)	17 dBi
S	Number of sectors	3
θ_{BS}	3-dB beamwidth	$S = 3 : \theta_{BS} = 70^0$

G_{FB}	Front-to-back power ratio	20 dB
M_{TX}	Number of transmit antennas	2
M_{RX}	Number of receive antennas	2
d_{BS}	BS antenna spacing	4λ
NF_{BS}	Noise figure (transmit & receive)	5 dB
HW_{BS}	Hardware loss (cable, implementation, etc.)	2 dB

Table 4: BS equipment model

2.4.2. Mobile Station Model

Parameter	Description	Value
P_{SS}	RMS transmit power/per SS	23 dBm
H_{SS}	Subscriber station height	1.5 m
G_{SS}	Gain (boresight)	0 dBi
$\{\theta_{SS}\}$, $G(\{\theta_{SS}\})$	Gain as a function of Angle-of-arrival	Omni
N_{TX}	Number of transmit antennas	1
N_{RX}	Number of receive antennas	2
d_{SS}	SS antenna spacing	$\lambda / 2$
NF_{SS}	Noise figure (transmit & receive)	7 dB
HW_{SS}	Hardware loss (cable, implementation, etc.)	2 dB

Table 5: MS Equipment Model

2.4.3. OFDMA Numerology

Parameter	Description	Value : 802.16e Reference System	Value: 802.16m
f_c	Carrier frequency	2.5 GHz	
BW	Total bandwidth	10 MHz	
N_{FFT}	Number of points in full FFT	1024	
F_S	Sampling frequency	11.2 MHz	
Δ_f	Subcarrier spacing	10.9375 kHz	
$T_o = 1/\Delta_f$	OFDMA symbol duration without cyclic prefix	91.43 us	
CP	Cyclic prefix length (fraction of T_o)	1/8	
T_s	OFDMA symbol duration with cyclic prefix	102.86 us for CP=1/8	
T_F	Frame length	5 ms	
N_F	Number of OFDMA symbol in frame	47	
R_{DL-UL}	Ratio of DL to UL (TDD mode)	32 symbols: 15 symbols (without sounding) 31 symbols: 16 symbols (with sounding)	
T_{duplex}	Duplex time	TTG: 296 PS for 10 MHz RTG: 168 PS for 10 MHz PS = $4/F_S$	
DL_{Perm}	DL permutation type	PUSC/AMC	
UL_{Perm}	UL permutation type	PUSC/AMC	

Table 6: OFDMA Air Interface Parameters

3. Channel Models

Editor: Jeff Zhuang, Jeff.Zhuang@motorola.com

Sources	Document Reference
Mark Cudak et al. Jeff Zhuang et al.	C80216m-07_061.pdf, C80216m-07_062.pdf,
Sassan Ahmadi et al.	C80216m-07_069.doc,

Sassan Ahmadi et al.	C80216m-07_070.doc
Dan Gal et al.	C80216m-07_063.doc
Robert Novak et al. Dean Kitchener et al.	C80216m-07_074r1.pdf C80216m-07_073
Liu Ting et al.	C80216m-07_064r1.doc
Wookbong Lee et al.	C80216m-07_075r1.doc
Andreas F. Molisch et al.	C80216m-07_065r1.doc
Dean Kitchener et al.	C80216m-07_093r1.doc
Will Sun et al.	C80216m-07_098.doc
Rob Nikides et al.	C80216m-07_099r4.doc
Pekka Kyösti et al.	C80216m-07_104.doc

Editor's notes:

1. The following contributions were discussed in the ad-hoc: 07/061, 062, 069, 070, 063, 074r1, 073, 064r1, 075r1, 104, 098, 093r1, 065r1, 099r4, as well as notes
2. Editor's notes in "*< red text >*" are based on ad-hoc discussion.
3. Text discussed but have not reached consensus is captured in "[green text]"

3.1. Introduction

Channel models suitable for evaluation of 802.16m system proposals are described in this section, wherein the model considers parameters specific to 802.16m including bandwidths, operating frequencies, cell scenario (environment, cell radius, etc), and multi-antenna configurations.

High-level considerations are discussed first in order to adopt/modify/develop proper channel models for the performance evaluation of 802.16m systems. An overview of generic MIMO channel modeling is then given. Both system level and link level models are described in detail with a purpose of fulfilling the needs to conduct effective link and system level simulations that can generate trustworthy and verifiable results to assess performance related to the 802.16m system requirements.

3.1.1. General Considerations

The channel models defined in this document are to provide sufficient details for the purpose of evaluating the system proposals to 802.16m. Since 802.16m is also targeting IMT-Advanced, the system requirements, deployment scenario, and operational bandwidth and frequency of a future IMT-advanced system should also be considered.

In the ITU-R recommendation ITU-R M.1645 the framework for systems beyond IMT-2000 (IMT-Advanced) envisions data rates of up to 1Gbps for nomadic/local area wireless access, and up to 100 Mbps for mobile access. As a reference, the European WINNER project has devised a method for determining spectrum requirements for IMT-Advanced, and their conclusions are given in [1]. In that report it is stated that in order to achieve the above performance targets of IMT-Advanced, sufficiently wide bandwidth and possibly multiple such wideband RF channels may be needed. Candidate bands for

IMT-Advanced are to be considered in 2007 at the WRC-07 conference. When considering candidate bands, the WINNER report further suggests that the utilization of bands above 3 GHz may be necessary, but these bands could present significant technical challenges if used for wide area mobile access, due to the increase in path loss with frequency.

The terrain environment in which 802.16m systems may be deployed (i.e., outdoor/indoor, macro/micro/pico-cell, etc.) dictates the channel modeling, affecting not only parameters but also the model itself. Therefore, channel modeling needs to consider various radio environments and propagation scenarios in which 802.16m system may be deployed.

3.1.2. Overview of Channel Modeling Methodology

The channel behavior is described by its long-term and short-term fading characteristics where the former often depends on the geometrical location of a user in a wireless network and the latter defines the time-variant spatial channels.

In general, there are two ways of modeling a channel: *deterministic* and *stochastic* [2]. The deterministic category encompasses all models that describe the propagation channel for a specific transmitter location, receiver location, and environment. Deterministic channel models are site-specific, as they clearly depend on the location of transmitter, receiver, and the properties of the environment. They are therefore most suitable for network planning and deployment.

In many cases, it is not possible or desirable to model the propagation channel in a specific environment. Especially for system testing and evaluation, it is more appropriate to consider channels that reflect “typical”, “best case”, and “worst case” propagation scenarios. A stochastic channel model thus prescribes *statistics* of the channel impulse responses (or their equivalents), and during the actual simulation, impulse responses are generated as *realizations* according to those statistics.

For a simulation-based study, stochastic channel modeling is more suitable. Almost all the existing channels models are stochastic ones, such as the SUI model proposed for IEEE 802.16d [3], the ITU model for IMT-2000 [4], the 3GPP SCM model [5] [6] and SCME (Spatial Channel Model Extensions) model [7], the COST 259 model [10][8][9], the COST 273 model [11], and the WINNER model [12].

Essential to the evaluation of multiple-antenna techniques, which are envisioned to be a key enabling technology for 802.16m and IMT-Advanced, is the modeling of MIMO channels that can be represented as double-directional channels [13] or as vector (matrix) channels [14]. The former representation is more related to the physical propagation effects, while the latter is more on the “mathematical” effect of the channel on the system [15]. The double-directional model is a physical model in which the channel is constructed from summing over multiple waves/rays. Thus it can also be referred to as a “ray-based model”. The vector/matrix channel is a mathematical or analytical model in which the space-time channel as seen by the receiver is constructed mathematically, assuming certain system and antenna parameters. In this approach, the channel coefficients are correlated random process in both space and time, where the correlation is defined mathematically.

A realization of a *double-directional channel* is characterized by its double-directional impulse response. It consists of N propagation waves between the transmitter and the receiver sites. Each wave is delayed in accordance to its excess-delay τ_ℓ, weighted with the proper complex amplitude $a_\ell e^{j\phi_\ell}$. Note that the amplitude is a two-by-two matrix, since it describes the vertical and horizontal polarizations and the cross-polarization; neglecting a third possible polarization direction is admissible in macro- and micro-cells. Finally, the waves are characterized by their angle-of-departure (AOD) $\Omega_{T,\ell}$ and angle-of-arrival (AOA) $\Omega_{R,\ell}$.[1] The channel impulse response matrix $\underline{h}$, describing horizontal and vertical polarization is then

$$\underline{h}(t,\tau,\Omega_T,\Omega_R)=\sum_{\ell=1}^{N}\underline{h}_\ell(t,\tau,\Omega_T,\Omega_R)=\sum_{\ell=1}^{N}\underline{a}_\ell e^{j\phi_\ell}\delta(\tau-\tau_\ell)\delta(\Omega-\Omega_{T,\ell})\delta(\Psi-\Omega_{R,\ell}) \quad (1)$$

The number of waves N can become very large if all possible paths are taken into account; in the limit, the sum has to be replaced by an integral. For practical purposes, waves that are significantly weaker than the considered noise level can be neglected. Furthermore, waves with similar AODs, AOAs, and delays can also be merged into ”effective” paths, known also as taps or clusters.

In general, all multipath parameters in (1), $\tau_\ell,\Omega_{R,\ell},\ \Omega_{T,\ell},\underline{a}_\ell$, and $e^{j\phi_\ell}$ will depend on the absolute time t; also the set of waves or multipath components (MPCs) contributing to the propagation will vary, $N\to N(t)$. The variations with time can occur both because of movements of scatterers, and movement of the mobile station or MS (the BS is assumed fixed).

A mathematical wideband *matrix* channel response describes the channel from a transmit to a receive antenna array. It is characterized by a matrix $\underline{H}$ whose elements H_{ij} are the (non-directional) impulse responses from the $j-$th transmit to the i-th receive antenna element. They can be computed for any antenna constellation as

$$H_{i,j}=h(\tau,\vec{x}_{R,i},\vec{x}_{T,j})=\sum_{\ell=1}^{N}\vec{g}_R(\Omega_R)\cdot\underline{h}(\tau_\ell,\Omega_{R,\ell},\Omega_{T,\ell})\cdot\vec{g}_T(\Omega_T)\cdot e^{j\left\langle\vec{k}(\varphi_{R,\ell})\vec{x}_{R,i}\right\rangle}e^{j\left\langle\vec{k}(\varphi_{T,\ell})\vec{x}_{T,j}\right\rangle}, \quad (2)$$

where $\vec{x}_R$ and $\vec{x}_T$ are the vectors of the chosen element-position measured from an arbitrary but fixed reference points $\vec{x}_{R,0}$ and $\vec{x}_{T,0}$ (e.g., the centers of the arrays) and $\vec{k}$ is the wave vector so that

$$\left\langle\vec{k}(\Omega)\cdot\vec{x}\right\rangle=\frac{2\pi}{\lambda}(x\cos\vartheta\cos\varphi+y\cos\vartheta\sin\varphi+z\sin\vartheta). \quad (3)$$

where ϑ and φ denote elevation and azimuth, respectively. The functions $\vec{g}_R(\Omega_R)$ and $\vec{g}_T(\Omega_T)$ are the antenna patterns at transmitter and receiver, respectively, where the

[1]We stress that the (double-directional) channel is reciprocal. While the directions of multipath components at the base station and at the mobile station are different, the directions at one link end for the transmit case and the receive case must be identical. When we talk in the following about AOAs and AODs, we refer to the directions at two different link ends.

two entries of the vector $\vec{g}$ describe the antenna pattern for horizontal and vertical polarization.

3.1.3. System Level Channel Modeling Considerations

System level simulation is widely used to understand and assess the overall system performance. In link level modeling, typically only the short-term fading behavior of a point-to-point link is modeled which sometime extends to multiple links in the case of interference condition. So a link level study reveals the performance under a particular link condition (or a particular interference condition). In system-level modeling, on the other hand, all possible link conditions are modeled along with their occurrence probability. System models include additionally, the large-scale location-dependent propagation parameters such as path loss and shadowing, as well as the relationship among multiple point-to-point links.

Channel models that allow effective and efficient system level simulations are of particular interest in the evaluation methodology discussion. In a typical system level simulation, the geometry of a wireless deployment is first defined (e.g., typically a cellular topology is assumed), based on which the long-term fading behaviors and large-scale parameters are derived. After that, the short-term time-variant spatial fading channels are generated.

As mentioned previously, there are in general, two types of methodologies to generate short-term fading channels. The first is a physical model in which the channel is constructed from summing over multiple waves/rays that are parameterized according to the geometrics. The physical modeling is independent of the antenna configuration, which means that the actual mathematical channel perceived by a receiver will need to further incorporate the antenna configuration, traveling speed, velocity, and so on.

As an example of a physical model, the 3GPP SCM model [5] has been widely used in system simulation. It models the physical propagation environment using paths and sub-paths with randomly specified angles, delays, phases, and powers. The MIMO channel coefficients for simulation is derived after defining the antenna configuration and array orientation at both MS and BS. Time-variation is realized after defining MS travel direction and speed. Other ray-based channel models for system level simulation include, but not limited to, SCME [7] and WINNER channel model [12]. The ray-based physical models are powerful as they are independent from any particular assumption of antenna configurations.

The other modeling methodology is mathematical or analytical modeling in which the space-time channel as seen by the receiver is constructed mathematically, assuming certain system and antenna parameters. In this method, the channel coefficients are correlated random process in both space and time, where the correlation is defined mathematically.

Mathematical modeling tries to analytically model the statistical behavior of a channel, represented by probability distributions and/or power profiles of delays and angles. On the other hand, in a ray-based modeling, the statistical behavior is satisfied through the summation of multiple rays with random parameters. The two approaches can be viewed as two different simulation implementations, especially if they are based on the

same probability distributions and/or power profiles. The system performance results are expected to be very close with both models.

Both approaches could be considered for system simulation purpose. A few important considerations for system simulations are:

- *Simulation run-time*. A system level simulation typically involves the generation of spatial channels from a MS position to multiple base stations (e.g., 19 cells or 57 sectors in a three-sector cellular network). Multi-user scheduling is also commonly simulated, in which the channel conditions of multiple MSs (e.g., 10, 20, or more) are required in the scheduler to determine how to distribute resources among them. Therefore, it is important if a model can result in the reduction of run-time without sacrificing the truthfulness to reality.
- *Consistency with link-level models*. Link level models should reflect particular (e.g., typical) link conditions experienced in various propagation scenarios. A link level study relies on the system level model to understand the likelihood of the particular link condition, while system level study sometimes relies on the link-level study results in order to model the actual link performance.
- *Results comparability and statistical convergence*. A channel model should facilitate comparison of system study results from independent sources. A channel model should ensure the statistical behavior of a channel to converge quickly without having to run a larger number of realizations (run-time concern). As an example, if a model defines some second order statistics as random variables themselves (e.g., angular spread, delay spread, etc.), the simulation may require more realizations and thus longer time to get convergence.

3.1.4. Link Level Channel Modeling Considerations

A link level channel model is used mainly for calibrating point-to-point MIMO link performance at various SINR points of interest, with extensions to multiple links in the case of interference. Note that any particular link level channel does not contain the information of large-scale fading or how often a particular kind of link condition occurs in a wireless system.

A link level channel can be naturally developed as a typical representation of a propagation scenario under a particular system setting (e.g., a macro-cell outdoor system with a representative BS and MS antenna configuration). A link-level channel modeling methodology should be consistent with the system level modeling methodology.

Conventional Tapped Delay Line (TDL) models, such as the three-tap ones used for the IEEE 802.16d SUI TDL [3] and the six-tap ITU models for IMT-2000 [4], need to be extended to include the spatial channel modeling to capture the relationship among all the channels between multiple transmit and receive antennas. For example, SCME models [7] define TDLs where each tap consists of multiple rays in the space that can be further grouped into 3 or 4 mid-taps. WINNER II clustered delay line (CDL) models [12] for beyond-3G systems also defined delay line model with additional angular information specified for each tap.

A few important observations need to be considered:

1. The six-tap ITU models were developed for 5 MHz bandwidth channels, and as the bandwidth increases, the resolution in the delay domain increases so that more taps are required for higher bandwidth channel models. Each resolvable tap consists of a number of multipath components so that the tap fades as the mobile moves. As bandwidth increases there will be less multipath components per resolvable tap so that the fading characteristics of the taps are likely to change. The tap fading is likely to become more Rician in nature (i.e., increasing K-factor with bandwidth) and the Doppler spectrum will not have the classic "bathtub" shape. This also means that the coherence times/distances for the tap fading will most likely be longer for higher bandwidths. The above observation suggests that measurement data under bandwidths up to 100MHz needs to be collected and analyzed to obtain the appropriate channel statistics which may vary according to transmission bandwidth.

2. The model should be flexible to incorporate various antenna effects such as the potential antenna gain imbalance, antenna coupling/correlations, and polarization. Ideally the model would include both azimuth and elevation angle (i.e., antenna tilt).

3.2. System Level Channel Model

This section focuses on the system-level simulation procedure and parameters for modeling the long- and short-term behavior of spatial channels between a MS position and one or more BS. The procedure and all the required parameters will be described in sufficient details for simulation purposes.

For deployment-related assumptions and parameters, as required in system level simulation, please refer to Section 2 of this evaluation methodology document. The deployment parameters include, among others, cell radius and topology, BS transmission power, BS antenna pattern, orientation, height, gain, and front-to-back ratio, MS transmission power, MS antenna pattern, height, and gain.

Once the deployment parameters are specified, a system level simulation typically involves the random drop of users in a radio environment of interest. The set of users comprises of a specified mix of different speeds and channel scenarios. Then, the long-term parameters of the link between a set of BS and a MS, such as path loss and shadowing factor, are generated. The short-term time-varying spatial fading channel coefficients are generated at last. Typically, multiple links between an MS to multiple BSs are needed, among which there is one desired link and multiple interference links. The shadowing factor of these links can be correlated.

After the introduction of the general approach for spatial modeling, the rest of the subsections will define the channel modeling procedure and parameters, as well as channel scenarios and speed mix recommended for a system simulation.

3.2.1. Spatial Channel Modeling

The general modeling approach is based on the geometry of a network layout. The large-scale parameters such as path loss and shadowing factor are generated

according to the geometric position of the BS and MS. Then the statistical channel behavior is defined by some distribution functions of delay and angle and also by the power delay and angular profiles. Typically, exponential power delay profile and Laplacian power angular profile are assumed with the function completely defined once the RMS delay spread and angular spread (both departure AOD and arrival AOA) are specified. The RMS delay and angular spread parameters can be random variables themselves, with a mean and deviation as in SCM. The RMS delay and angular spread can be mutually correlated, together with other large-scale parameters such as shadowing factors.

According to the exact profile and distribution functions defined by the particular RMS delay and angular spread values, a finite number of channels taps are generated randomly with a per-tap delay, mean power, mean AOA and AOD, and RMS angular spread. They are defined in a way such that the overall power profile and distribution function are satisfied. Each tap is the contribution of a number of rays (plane waves) arriving at the same time (or roughly the same time), with each ray having its own amplitude, AOA, and AOD.

The number of taps and their delay and angles may be randomly defined, but a reduced-complexity model can specify the delays, mean powers, and angles of the channel taps in a pre-determined manner when typical values are often chosen. Similar to the well-known TDL model where the power delay profile is fixed, a “spatial” TDL reduced-complexity model additionally defines the spatial information such as per-tap mean AOA, AOD, and per-tap angular spread (thus the power angular profile). Spatial TDL models are also referred to as Cluster Delay Line or CDL models as each tap is modeled as the effect of a cluster of rays arriving at about the same time. Each tap suffers from fading in space and over time. The spatial fading process will satisfy a pre-determined power angular profile. Due to the simplicity of reduced complexity modeling, it is recommended for system level simulation.

The actual realization of a time-varying spatial channel can be performed in two ways:

- Ray-based: The channel coefficient between each transmit and receive antenna pair is the summation of all rays at each tap and at each time instant, according to the antenna configuration, gain pattern, and the amplitude, AOA, AOD of each ray. The temporal channel variation depends on the traveling speed and direction relative to the AOA/AOD of each ray

- Correlation based: The antenna correlation for each tap is computed first according the per-tap mean AOA/AOD, per-tap power angular profile, and antenna configuration parameters (e.g.., spacing, polarization, etc.). The per-tap Doppler spectrum depends on the traveling speed and direction relative to the mean per-tap AOA/AOD, as well as the per-tap power angular profile. The MIMO channel coefficients at each tap can then be generated mathematically by transforming typically the i.i.d. Gaussian random variables according to the antenna correlation and the temporal correlation (correspondingly the particular Doppler spectrum). The approach of pre-calculating and storing all the correlations and time-varying fading processes may also be used in system simulation.

3.2.2. Radio Environment and Propagation Scenarios

The terrain or radio environment, such as indoor, urban, or suburban, dictates the radio propagation behavior. Even in similar terrain environments, there may be different propagation behavior or scenarios.

For the simulation of IEEE 802.16m systems, the following scenarios are defined:

1. **Urban macro-cell**: This scenario is characterized by large cell radius (approximately 1-6 km BS to BS distance), high BS antenna positions (above rooftop heights, between 10-80 m, typically 32 m), moderate to high delay and angle spread and high range of mobility (0 – 350 km/h). *<Editor's note: Text in { } are modified from IMT.EVAL>* { In typical urban macro-cell a mobile station is located outdoors at street level and fixed base station clearly above surrounding building heights. As for propagation conditions, non- or obstructed line-of-sight is a common case, since street level is often reached by a single diffraction over the rooftop. The building blocks can form either a regular Manhattan type of grid, or have more irregular locations. Typical building heights in urban environments are over four floors. Buildings height and density in typical urban macro-cell are mostly homogenous. } *<Editor's note: Bad urban macro-cell from WINNER could be used if longer delay spread is preferred. General view from ad-hoc is to include for further study>* As a variant, the **bad urban macro-cell** describes cities with buildings with distinctly inhomogeneous building heights or densities. The inhomogeneities in city structure can be the result of, for example, large water areas separating the built-up areas, or the high-rise skyscrapers in otherwise typical urban environment. Increased delay and angular dispersion can also be caused by mountainous surrounding the city. Base station is typically located above the average rooftop level, but within its coverage range there can also be several high-rise buildings exceeding the base station height. From the modeling point of view this differs from typical urban macro-cell by an additional far scatterer cluster.

2. **Suburban macro-cell**: This scenario is characterized by large cell radius (approximately 1-6 km BS to BS distance), high BS antenna positions (above rooftop heights, between 10-80 m, typically 32 m), moderate to high delay spreads and low angle spreads and high range of mobility (0 – 350 km/h). *<Editor's note: Text in { } are modified from IMT.EVAL>* {In suburban macro-cells, base stations are located well above the rooftops to allow wide area coverage, and mobile stations are outdoors at street level. Buildings are typically low residential detached houses with one or two floors, or blocks of flats with a few floors. Occasional open areas such as parks or playgrounds between the houses make the environment rather open. Streets do not form urban-like regular strict grid structure. Vegetation is modest. }

3. **Urban micro-cell**: This scenario is characterized by small cell radius (approximately 0.3 – 0.5 km BS to BS distance) BS antenna positions at rooftop heights or lower (typically 12.5m), high angle spread and moderate delay spread, and medium range of mobility (0 – 120 km/h). This model is sensitive to antenna height and scattering environment (such as street layout, LOS). *<Editor's note:*

Text in { } are modified from IMT.EVAL> { In urban micro-cell scenario, the height of both the antenna at the BS and that at the MS is assumed to be well below the tops of surrounding buildings. Both antennas are assumed to be outdoors in an area where streets are laid out in a Manhattan-like grid. The streets in the coverage area are classified as "the main street", where there is LOS from all locations to the BS, with the possible exception of cases in which LOS is temporarily blocked by traffic (e.g. trucks and busses) on the street. Streets that intersect the main street are referred to as perpendicular streets, and those that run parallel to it are referred to as parallel streets. This scenario is defined for both LOS and NLOS cases. Cell shapes are defined by the surrounding buildings, and energy reaches NLOS streets as a result of propagation around corners, through buildings, and between them. } *<Editor's note: Bad urban macro-cell from WINNER could be used if longer delay spread is preferred. General view from ad-hoc is to include for further study>* **Bad urban micro-cell** scenarios are identical in layout to Urban Micro-cell scenarios. However, propagation characteristics are such that multipath energy from distant objects can be received at some locations. This energy can be clustered or distinct, has significant power (up to within a few dB of the earliest received energy), and exhibits long excess delays. Such situations typically occur when there are clear radio paths across open areas, such as large squares, parks or bodies of water.

4. [**Indoor Small Office**: This scenario investigates isolated cells for home or small office coverage. In a typical small office environment, there are multiple floors and multiple rooms or areas. The channel modeling of typical small office scenario can be used together in the outdoor to indoor scenario. *<Editor's note: No consensus on the inclusion of Indoor Small Office scenario, regarding how important for 16m to target indoor comparing with others, say 802.11. If removed here, relevant text in other subsections will be removed as well>*]

5. [**Outdoor to indoor:** This scenario is the combination of an outdoor and an indoor scenario such as **urban micro-cell** and **indoor small office**. In this particular combination, the MS antenna height is assumed to be at 1 – 2 m (plus the floor height), and the BS antenna height below roof-top, at 5 - 15 m depending on the height of surrounding buildings (typically over four floors high). *<Editor's note: Some level of consensus on the inclusion of this scenario. Outdoor to indoor was typically modeled with additional path loss. But it is understood that the short-term fading could also change. So such a scenario may be useful. >]*

3.2.3. Path loss

The path loss model depends on the propagation scenario. For example, in a macro-cell environment, the COST-231 modified Hata model [17] is well known and widely used for systems with a carrier frequency less than or equal to 2.5GHz. The Erceg-Greenstein model [3] was proposed in IEEE802.16d for carrier frequencies up to 3.5GHz. Extension of these path loss models to carrier frequencies above 3.5GHz are also proposed in the WINNER model [12].

For the evaluation of the IEEE 802.16m systems, the following path loss models are specified:

3.2.3.1. Urban macro-cell

The modified COST231 Hata model define the following pathloss

$$PL[dB] = \left(44.9 - 6.55\log_{10}\left(h_{bs}\right)\right)\log_{10}\left(\frac{d}{1000}\right) + 45.5 + \left(35.46 - 1.1h_{ms}\right)\log_{10}(f) - 13.82\log_{10}(h_{bs}) + 0.7h_{ms} + C \quad (4)$$

where the constant *C* = 3dB for urban macro.

Assuming MS height of 1.5m and at f=2GHz carrier frequency, the model becomes

$$PL = \left(44.9 - 6.55\log_{10}(h_{BS})\right)\log_{10}(d) + 26.46 + 5.83\log_{10}(h_{BS}) \quad (5)$$

In addition, a frequency scaling factor of $26\log_{10}(f_c)$ is used to account for the path loss change according to the carrier frequency. The frequency correction factor was taken from some work done by Jakes and Reudink [16], where they used measurement data taken in New Jersey at frequencies of 450MHz, 900MHz, 3.7GHz, and 11.2GHz. They showed a frequency dependence for path loss of $f^{2.6}$, which is larger than the frequency correction being employed by the WINNER models (f^2). Note that the original Hata model has a frequency dependence of $(26.16\text{-}1.1h_{ms}+1.56)\log(f)$ (=26.07 when h_{ms}=1.5m) , which is very close to the dependence found by Jakes and Reudink. So the proposed path loss model becomes

$$PL = \left(44.9 - 6.55\log_{10}(h_{BS})\right)\log_{10}(d) + 26.46 + 5.83\log_{10}(h_{BS}) + 26\log_{10}(f[GHz]/2) \quad (6)$$
$$with \quad 50m < d < 5km \quad h_{BS} > 30m \quad f = 2...6GHz$$

With both a default BS and MS heights 32m and 1.5 respectively, the model reduces to

$$PL = 34.5 + 35\log_{10}(d) + 26\log_{10}(f[GHz]/2) \quad (7)$$

3.2.3.2. Suburban macro-cell

For the COST 231 Hata suburban pat loss model the path loss equation is identical to that of the urban macro model in (4), except for a C=0dB correction factor instead of 3dB. However, this offset itself is somewhat contradictory with the suburban offset used in the original Hata model derived for 150-1000MHz. The original Hata offset for suburban areas was [18]:

$$PL_{Suburban} = PL_{Urban} - 2\left[\log\left(\frac{f(MHz)}{28}\right)\right]^2 - 5.4 \quad (8)$$

Because the original Hata offset matches well with the experiments reported in the Erceg model [ref], is the adopted here. Again, a frequency scaling factor of $26\log_{10}(f_c)$ is used to account for the path loss change according to the carrier frequency.

3.2.3.3. Urban micro-cell

LOS case:

The recommended urban microcellular LOS path loss model is the following [19]:

$$\frac{P_r(r)}{P_t} = -20\log\left(\frac{e^{sr}\,4\pi r D(r)}{\lambda}\right)$$

where,

P_t = Transmit Power

$P_r(r)$ = Received power

r = Distance between Tx and Rx antennas

e^{sr} = Visibility factor ($s = 0.002$)

λ = Wavelength

$$D(r) = \begin{cases} 1 & \text{if } r \le r_{bp} \\ \dfrac{r}{r_{bp}} & \text{if } r > r_{bp} \end{cases}$$

$$r_{bp} = \frac{4(h_t - h_0)(h_r - h_0)}{\lambda} = \text{breakpoint distance}$$

h_t = Height of transmit antenna above the road

h_r = Height of transmit antenna above the road

h_0 = Effective road height = 1.0m (9)

This is effectively a two ray model, which has an effective road height to account for the effect of traffic on the ground reflected ray. It also includes a visibility factor, which adds additional path loss at longer ranges as visibility in the street becomes more obscured. The model has been validated by measurements at several frequencies in Japan [19].

NLOS Case:

The WINNER path loss model for this case assumes that the dominant propagation path is around the streets, and therefore only has a 'round-the-streets' component. However, in practice there is also an over-the-rooftop component, as given in the ETSI model for UMTS in [20]. The ETSI model combines a round-the-streets model (Berg model) with an over-the-rooftop model, taking the minimum of these two models at any given mobile location. The ETSI model was modified to include the advanced LOS model [19] which is described below.

$$PL_{Berg}(dB) = 20\log\left(\frac{4\pi d_n D\left(\sum_{j=1}^{n} r_{j-1}\right)\prod_{j=1}^{n} e^{sr_{j-1}}}{\lambda}\right)$$

$R = \sum_{j=1}^{n} r_{j-1}$ = Distance along streets between Tx and Rx

r_j = Length of the street between nodes j and $j+1$ (there are $n+1$ nodes in total)

$$r_{bp} = \begin{cases} r_0 \text{ if } r_0 \le \dfrac{4(h_t - h_0)(h_r - h_0)}{\lambda} \\ \dfrac{4(h_t - h_0)(h_r - h_0)}{\lambda} \text{ if } r_0 > \dfrac{4(h_t - h_0)(h_r - h_0)}{\lambda} \end{cases}$$

$$D(R) = \begin{cases} 1 \text{ if } R \le r_{bp} \\ \dfrac{R}{r_{bp}} \text{ if } R > r_{bp} \end{cases}$$

The distance d_n is the illusory distance and is defined by the recursive expression,

$k_j = k_{j-1} + d_{j-1} q_{j-1}$

$d_j = k_j r_{j-1} + d_{j-1}$

with $k_0 = 1$ and $d_0 = 0$

$$q_j(\theta_j) = \left(|\theta_j| \frac{q_{90}}{90}\right)^{\nu}$$

θ_j = Angle between streets at junction j

$q_{90} = 0.5$, and $\nu = 1.5$

$PL_{over\_the\_rooftop}(dB) = 24 + 45\log(r_{Eu} + 20)$

r_{Eu} = Euclidean distance between Tx and Rx

$PL(dB) = \min\left(PL_{Berg}(dB), PL_{over\_the\_rooftop}(dB)\right)$ (10)

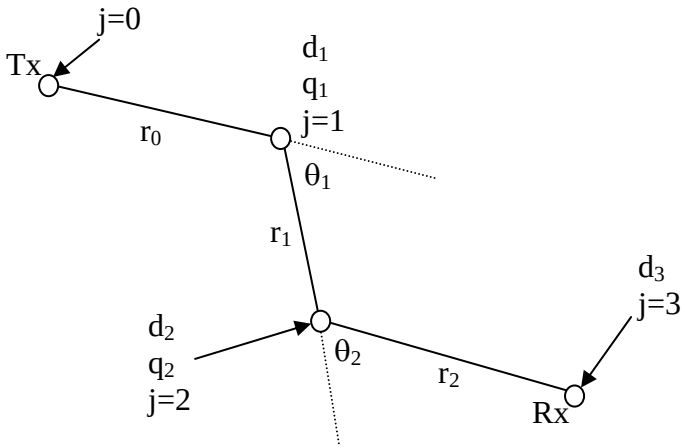

Figure 4: Geometry of street sections used for microcellular NLOS path loss model.

3.2.3.4. Indoor Small Office

<Editor's notes: LOS case is not included for simplicity>

WINNER model [12] defines the following model for NLOS case under the condition of 3 m < *d* < 100 m, $h_{BS} = h_{MS} = 1 \sim 2.5$m,

NLOS (Room to Corridor):

PL = 36.8 $\log_{10}$ (*d*[m]) + 43.8 + 20$\log_{10}$ (f [GHz]/5.0)

NLOS (through-wall):

PL = 20 $\log_{10}$ (d[m]) + 46.4 + $n_W \cdot 5$ + 20$\log_{10}$ (f [GHz]/5.0) (Light wall)

PL = 20 $\log_{10}$ (d[m]) + 46.4 + $n_W \cdot 12$ + 20$\log_{10}$ (f[GHz]/5.0) (Heavy wall)

where n_w is the number of walls between BS and MS.

3.2.3.5. Outdoor to indoor

WINNER model [12] defines the following path loss model for the NLOS case.

$PL = PL_b + PL_{tw} + PL_{in}$

Where $PL_b = PL_{B1}(d_{out} + d_{in})$, $PL_{tw} = 14 + 15(1 - \cos(\theta))^2$, $PL_{in} = 0.5\, d_{in}$

3 m $< d_{out} + d_{in} <$ 1000 m, $h_{BS} = 3n_{Fl} + 2$ m, $h_{MS} = 1.5$ m

PL_{B1} is path-loss of urban-micro cell, d_{out} is the distance between the outside terminal and closest point of the wall to the inside terminal, d_{in} is the distance from wall to the inside terminal , θ is the angle between the outdoor path and the normal of the wall. n_{Fl} is the number of the floor. (Ground floor is the number 1.)

3.2.4. Shadowing Factor (SF)

The shadowing factor has a log-normal distribution and the standard deviation that are defined as follow based on the WINNER parameters [12], for different scenarios.

Urban macro-cell: 8dB
Suburban macro-cell: NLOS: 8dB

Urban micro-cell: NLOS: 4dB, LOS 3dB

[Indoor Small Office: NLOS (Room to Corridor) 4dB, NLOS (through-wall) 6dB (light wall), 8dB (heavy-wall)]

[Outdoor to indoor: 7dB]

The site-to-site shadowing correlation is 0.5. The SF of closely positioned MS is typically observed similar or correlated. Therefore, the SF can be obtained via interpolation in the following way.

For each base station, a uniformly spaced grid is generated using the pre-defined de-correlation distance as shown in Figure 5. Each node $S_{n,l}$ on the grid represents the shadowing factor corresponding to base station *l* at the geographic location *n* with (*x, y*) coordinate. All nodes $\{S_{n,0},\cdots,S_{n,L}\}$, where *L* represents the set of base stations in the simulation, correspond to a single geographical location *n* in a simulated system. The distance between closest nodes, D_{cor}, in the grid is the pre-defined de-correlation distance (e.g. 50 meters).

For a mobile location, either from a random drop or a result of mobility, the shadowing factor from the mobile to a base station *l* should be calculated by interpolating the shadowing factors of the closest four nodes, $S_{0,l}$-$S_{3,l}$ for the corresponding base station *l* in FIGURE. Specifically, the shadowing factor $g_{k,l}$ at a location corresponding to base station *l* is determined by

$$SF(g_{k,l}) = \left(1-\sqrt{\frac{x_{pos}}{D_{cor}}}\right)\left[S_{0,l}\sqrt{\frac{y_{pos}}{D_{cor}}}+S_{3,l}\left(1-\sqrt{\frac{y_{pos}}{D_{cor}}}\right)\right]+\left[S_{1,l}\sqrt{\frac{y_{pos}}{D_{cor}}}+S_{2,l}\left(1-\sqrt{\frac{y_{pos}}{D_{cor}}}\right)\right]\sqrt{\frac{x_{pos}}{D_{cor}}} \quad (11)$$

Note that the linear interpolation above guarantees smooth change of shadowing factors around the nodes on the grid, and moving from one square to another square. Additionally, the linear interpolation above guarantees the same standard deviation of shadowing factors at all points in the simulated system.

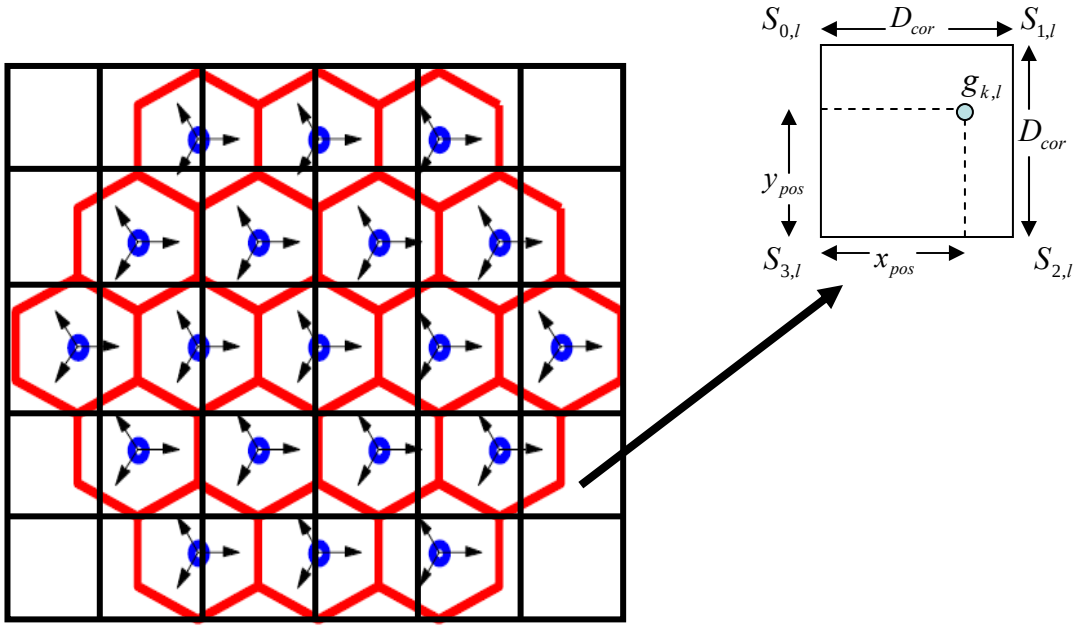

Figure 5: Shadowing factor grid example showing interpolation operation.

3.2.5. "Spatial" TDL or Cluster-Delay-Line Models

A spatial TDL model or CDL model as referred in the WINNER report defines the spatial information such as per-tap mean AOA, AOD, and per-tap angular spread (thus the power angular profile). The CDL models specify the number of taps (clusters), their delays and powers, the mean AOA and AOD of each cluster, and the arrival and departure angular spread (AS). So they offer well-defined radio channels with fixed parameters to obtain comparable simulation results with relatively non-complicated channel models.

For each propagation scenario, the corresponding CDL is given as follows that includes a power delay profile and the corresponding per-tap power angular profile. Note that the AOA and AOD values given in the following tables are the mean AOA/AOD of each cluster (i.e., tap or path). The mean power of each tap and its delay is also given. The ray power is 1/20 of the mean tap power (i.e., ~13dB).

In a spatial TDL or CDL model, each tap may be simulated via generating 20 equal-power rays with fixed offset angles, as suggested in WINNER. The offset angles are the same as those defined in SCM and they are specified in a way such that by adjusting the interval between these equal-power rays a Laplacian power angular profile can be approximated. Note that the offset angles are the deviation from the mean AOA/AOD (see appendix-2 for the offset). In the case when a ray of dominant power exists, the cluster has 20+1 rays. This dominant ray has a zero angle offset. The departure and arrival rays are coupled randomly.

Spatial TDL or CDL model also allows for the generation of spatial correlation mathematically, which can be used directly to generate the matrix channel coefficients. The spatial correlation for each tap can be derived from the mean AOA/AOD and the

Laplacian power angular profile with the specified angular spread. Per-tap correlation can also be derived numerically based on the 20 equal-power rays used to approximate the Laplacian power angular profile.

Most of the taps have a single delay. In case a tap has three delays values, these correspond to sub-clusters as defined in the table below:

Sub-cluster #	Mapping to rays	Power	Delay Offset
1	2,3,4,5,6,7,8,19,20	10/20	0
2	9,10,11,12,17,18	6/20	5
3	13,14,15,16	4/20	10

Table 7: Sub-cluster model used for some taps in Spatial TDL or CDL model

The sub-cluster can be easily simulated with a ray-based model. [But if a spatial correlation is preferred in a mathematical model, the three sub-taps could be approximated to have the same correlation.] *<Editor's note: In addition to the text in [], another alternative could be using the 4/6/10 rays in the table to numerically compute the spatial correlation>*

<Editor's note: The addition of the following text on XPR and their values for CDL was proposed by Electrobit>

[The cross polarization ratio XPR_V is the power ratio of vertical-to-vertical polarized component to vertical-to-horizontal polarized component, XPR_H is the power ratio of horizontal-to-horizontal polarized component to horizontal-to-vertical polarized component. In the model tables the cross polarization ratios are assumed the same for all clusters.]

3.2.5.1. Urban macro-cell

Cluster #	Delay [ns]			Power [dB]			AoD [°]	AoA [°]	Ray power [dB]	Cluster ASD = 2°	Cluster ASA = 15°
1	0			-6.4			11	61	-19.5		
2	60			-3.4			-8	44	-16.4		
3	75			-2.0			-6	-34	-15.0		
4	145	150	155	-3.0	-5.2	-7.0	0	0	-13.0		
5	150			-1.9			6	33	-14.9		
6	190			-3.4			8	-44	-16.4		
7	220	225	230	-3.4	-5.6	-7.4	-12	-67	-13.4		
8	335			-4.6			-9	52	-17.7		
9	370			-7.8			-12	-67	-20.8		
10	430			-7.8			-12	-67	-20.8		
11	510			-9.3			13	-73	-22.3		
12	685			-12.0			15	-83	-25.0		
13	725			-8.5			-12	-70	-21.5		
14	735			-13.2			-15	87	-26.2		
15	800			-11.2			-14	80	-24.2		

16	960	-20.8	19	109	-33.8		
17	1020	-14.5	-16	91	-27.5		
18	1100	-11.7	15	-82	-24.7		
19	1210	-17.2	18	99	-30.2		
20	1845	-16.7	17	98	-29.7		

Table 8: Urban macro-cell CDL[, XPRV = 4dB, XPRH = 6dB]

Cluster #	Delay [ns]	Power [dB]	AoD [º]	AoA [º]	Ray power [dB]	Cluster ASD = 2º	Cluster ASA = 15º
1	0	-4.7	-10	61	-17.7		
2	0 5 10	-3 -5.2 -7	0	0	-13		
3	10	-7.2	12	-75	-20.2		
4	10	-6.3	-11	-70	-19.3		
5	30 35 40	-4.8 -7 -8.8	-12	76	-14.8		
6	50	-3.7	-9	53	-16.7		
7	80	-7.4	-12	76	-20.4		
8	110	-7.2	12	-75	-20.2		
9	155	-9.6	14	-87	-22.7		
10	165	-5.2	-10	64	-18.3		
11	165	-6.3	11	70	-19.3		
12	250	-8.9	14	83	-21.9		
13	280	-8.5	13	-81	-21.5		
14	440	-8.4	13	-81	-21.4		
15	490	-8.5	-13	81	-21.5		
16	525	-5	10	62	-18		
17	665	-10.9	15	92	-23.9		
18	685	-10.9	15	92	-24		
19	4800	-9.7	-135	25	-22.7		
20	7100	-13	80	40	-26		

Table 9: Bad urban macrocell CDL[, XPRV = 4dB, XPRH = 6dB]

3.2.5.2. Suburban macro-cell

Cluster #	Delay [ns]	Power [dB]	AoD [º]	AoA [º]	Ray power [dB]	Cluster ASD = 2º	Cluster ASA = 10º
1	0 5 10	-3.0 -5.2 -7.0	0	0	-13.0		
2	25	-7.5	13	-71	-20.5		

3	35			-10.5			-15	-84	-23.5		
4	35			-3.2			-8	46	-16.2		
5	45	50	55	-6.1	-8.3	-10.1	12	-66	-16.1		
6	65			-14.0			-17	-97	-27.0		
7	65			-6.4			12	-66	-19.4		
8	75			-3.1			-8	-46	-16.1		
9	145			-4.6			-10	-56	-17.6		
10	160			-8.0			-13	73	-21.0		
11	195			-7.2			12	70	-20.2		
12	200			-3.1			8	-46	-16.1		
13	205			-9.5			14	-80	-22.5		
14	770			-22.4			22	123	-35.4		

Table 10: Suburban macro-cell CDL[, XPRV = 8dB, XPRH = 3dB]

3.2.5.3. Urban micro-cell

In the LOS model Ricean K-factor is 3.3 dB, which corresponds to 20m distance between Tx and Rx.

Cluster #	Delay [ns]			Power [dB]			AoD [°]	AoA [°]	Ray power [dB]		Cluster ASD = 3°	Cluster ASA = 18°
1	0			0.0			0	0	-0.31*	-24.7**		
2	30	35	40	-10.5	-12.7	-14.5	5	45	-20.5			
3	55			-14.8			8	63	-27.8			
4	60	65	70	-13.6	-15.8	-17.6	8	-69	-23.6			
5	105			-13.9			7	61	-26.9			
6	115			-17.8			8	-69	-30.8			
7	250			-19.6			-9	-73	-32.6			
8	460			-31.4			11	92	-44.4			

Table 11: Urban micro-cell CDL (LOS) [, XPRV = 9dB, XPRH = 10dB]

* Power of dominant ray,
** Power of each other ray

Cluster #	Delay [ns]			Power [dB]			AoD [°]	AoA [°]	Ray power [dB]	Cluster ASD =10°	Cluster ASA = 22°
1	0			-1.0			8	-20	-14.0		
2	90	95	100	-3.0	-5.2	-7.0	0	0	-13.0		
3	100	105	110	-3.9	-6.1	-7.9	-24	57	-13.9		
4	115			-8.1			-24	-55	-21.1		
5	230			-8.6			-24	57	-21.6		
6	240			-11.7			29	67	-24.7		
7	245			-12.0			29	-68	-25.0		
8	285			-12.9			30	70	-25.9		
9	390			-19.6			-37	-86	-32.6		
10	430			-23.9			41	-95	-36.9		

11	460	-22.1	-39	-92	-35.1		
12	505	-25.6	-42	-99	-38.6		
13	515	-23.3	-40	94	-36.4		
14	595	-32.2	47	111	-45.2		
15	600	-31.7	47	110	-44.7		
16	615	-29.9	46	-107	-42.9		

Table 12: Urban micro-cell CDL (NLOS) [, XPRV = 8dB, XPRH = 7dB]

Bad Urban micro-cell

Cluster #	Delay [ns]			Power [dB]			AoD [°]	AoA [°]	Ray power [dB]	Cluster ASD = 3°	Cluster ASA = 5°
1	0	5	10	-3.0	-5.2	-7.0	0	0	-13.0		
2	25	30	35	-3.4	-5.6	-7.3	-14	31	-13.4		
3	25			-1.7			-13	30	-14.7		
4	35			-1.9			-14	31	-14.9		
5	45			-2.2			15	-34	-15.2		
6	70			-5.0			22	51	-18.0		
7	70			-3.6			19	44	-16.6		
8	90			-3.8			-19	-45	-16.8		
9	155			-6.4			-25	-58	-19.4		
10	170			-2.7			-17	-38	-15.7		
11	180			-7.5			-27	-63	-20.5		
12	395			-16.5			-41	93	-29.5		
13	1600			-5.7			-110	15	-18.7		
14	2800			-7.7			75	-25	-20.7		

Table 13: Bad urban micro-cell CDL (NLOS)[, XPRV = 8dB, XPRH = 7dB]

3.2.5.4. Indoor Small Office

Only NLOS condition is given below.

Cluster #	Delay [ns]			Power [dB]			AoD [°]	AoA [°]	Ray power [dB]	Cluster ASD = 5°	Cluster ASA = 5°
1	0	5	10	-3.0	-5.2	-7.0	0	0	-13.0		
2	5			-4.0			59	-55	-17.0		
3	20			-4.7			-64	-59	-17.7		
4	25			-9.0			89	-82	-22.0		
5	30			-8.0			83	-77	-21.0		
6	30	35	40	-4.0	-6.2	-8.0	-67	62	-14.0		
7	35			-1.1			32	29	-14.2		
8	45			-5.2			-67	62	-18.2		
9	55			-9.5			-91	-84	-22.5		
10	65			-7.9			-83	77	-20.9		
11	75			-6.8			-77	-71	-19.8		
12	90			-14.8			-113	105	-27.8		

13	110	-12.8	-106	98	-25.8		
14	140	-14.1	111	-103	-27.2		
15	210	-26.7	-152	141	-39.7		
16	250	-32.5	-168	-156	-45.5		

Table 14: Indoor Small Office (NLOS)[, XPRV = 10dB, XPRH = 10dB]

3.2.5.5. Outdoor to Indoor

Cluster #	Delay [ns]	Power [dB]	AoD [°]	AoA [°]	Ray power [dB]	Cluster ASD = 5°	Cluster ASA = 8°
1	0	-7.7	29	102	-20.8		
2	10 15 20	-3.0 -5.2 -7.0	0	0	-13.0		
3	20	-3.7	20	70	-16.7		
4	35	-3.0	-18	-64	-16.0		
5	35	-3.0	18	-63	-16.0		
6	50	-3.7	20	70	-16.7		
7	55 60 65	-5.4 -7.6 -9.4	29	100	-15.4		
8	140	-5.3	24	84	-18.3		
9	175	-7.6	29	100	-20.6		
10	190	-4.3	-21	76	-17.3		
11	220	-12.0	36	-126	-25.0		
12	585	-20.0	46	163	-33.0		

Table 15: Outdoor to indoor CDL (NLOS)[, XPRV = 8dB, XPRH = 8dB]

3.2.6. Channel Type and Velocity Mix

In system level simulation, users may be associated with a set of different channel types and velocities. In such cases, a mix of user speeds and channel types is evaluated.

For IMT-Advanced system that will deliver high data rate multimedia services, it is expected that many users will be stationary, since the user will need to look at the information being received. This has been taken into account in the specification of parameters for HSDPA simulations. In this case it can be seen that 14% of users are stationary and 51% of users have speeds ≤ 1kph. It is recommended that this distribution also be used for macro-cellular system simulations for IEEE 802.16m. For the hotspot layer this distribution will be different again, where in this case all users are likely to be walking or stationary (all ≤ 3kph).

The speed mix, based on the similar parameters used in HSDPA simulation, is defined in the following table:

Speed (km/h)	0	3	30	120
Percentage	51%	17%	25%	7%

Table 16: Speed mix (modified from HSDPA speed distribution)

<Editor's notes: The following text in [ ] is for further discussion, regarding to what scenario is the above speed mix relevant to and the channel type mix to be used.>

[The above speed mix is generally applicable to a macro-cell environment, which may differ from that for a micro-cell or an indoor scenario. The speed mix for other scenarios is for future specification. Also for future definition is the mix of propagation scenarios in a system level simulation.]

If the TX and the RX are stationary, and the channel at time *t* is to be computed, then each cluster is made of a number of coherent (fixed) rays N_c and a number of scattered (variable) rays N_s (N_c + N_s = total number of rays per clusters).

The variable rays are ascribed a bell-shaped Doppler spectrum as described in [3]:

$$S(f) = \begin{cases} 1 - 1.72 f_0^2 + 0.785 f_0^4 & f_0 \le 1 \\ 0 & f_0 > 1 \end{cases} \qquad \text{where} \quad f_0 = \frac{f}{f_m}$$

where f_m is the maximum Doppler rate (suggested value: 2 Hz in [3]). The fixed rays within a cluster share the same amplitude and phase, and their Doppler spectrum is a Dirac impulse at f = 0 Hz.

3.2.7. Generation of Spatial Channels

The following procedure describes the simulation procedure based on the spatial TDL or CDL models. In the correlation based implementation, the spatial and temporal correlation need to be derived first and then generate the channel coefficients. In the ray-based approach, the time-variant matrix channels are constructed from all the rays.

Step 1: *Choose a propagation scenario (e.g. Urban Macro, Suburban Macro etc.). After dropping a user, determine the various distance and orientation parameters.*

The placement of the MS with respect to each BS is to be determined according to the cell layout. From this placement, the distance between the MS and the BS (d) and the LOS directions with respect to the BS and MS (θ_{BS} and θ_{MS}, respectively) can be determined. Note that θ_{BS} and θ_{MS} are defined relative to the broadside directions. The MS antenna array orientations (Ω_{MS}), are i.i.d., drawn from a uniform 0 to 360 degree distribution.

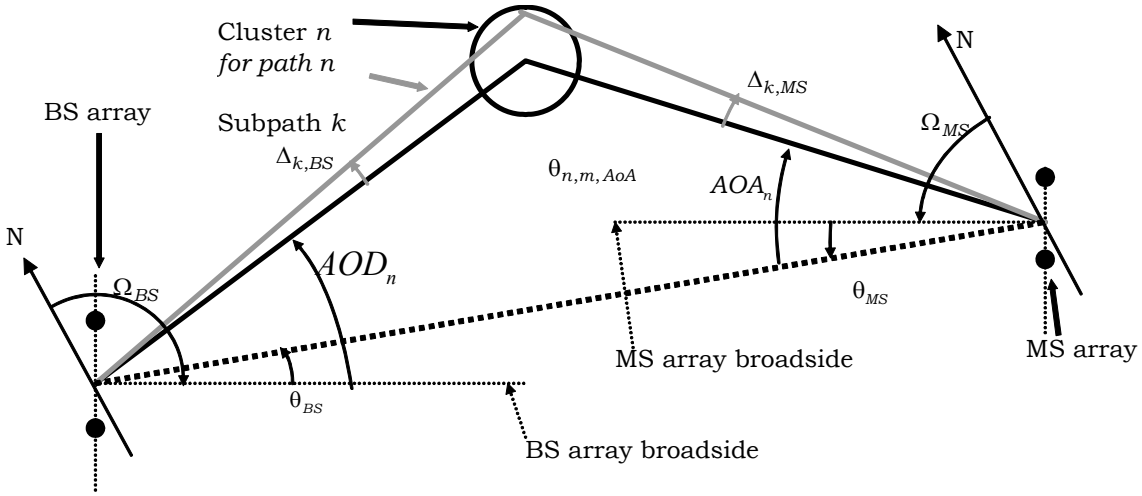

Figure 6: The MIMO channel model angle parameters

Step 2: *Calculate the bulk path loss associated with the BS to MS distance.*

Step 3: *Determine the Shadowing Factor (SF).*

SF is randomly generated from a log-normal distribution with a pre-specified standard deviation. Generate the SF according to section 1.2.4

If ray-based implementation, go to step 8 directly and skip steps in between

Step 4: *Calculate the per-tap spatial correlation matrix based on per-tap $AS_{BS,\ path}$ at the BS and the per-tap $AS_{MS,\ path}$ at the MS, both of which are specified in the reduced complexity models. The spatial correlation also depends on the BS/MS antenna configurations (a random broadside direction, number and spacing of antennas, polarization, etc.)*

Once the per-tap AS, mean AOA, and mean AOD are defined, the theoretical spatial correlation at both BS and MS can be derived, assuming Laplacian power angular distribution. In particular, the antenna spatial correlations between the p-th and q-th antenna at the BS and MS, respectively, are

$$r_{n,BS}(p,q) = \int_{-\infty}^{\infty} p(\alpha)\exp\left\{ j\frac{2\pi d_{BS}}{\lambda}(p-q)\sin(AOD_n+\alpha)\right\} d\alpha$$

$$r_{n,MS}(p,q) = \int_{-\infty}^{\infty} p(\beta)\exp\left\{ j\frac{2\pi d_{MS}}{\lambda}(p-q)\sin(AOA_n+\beta)\right\} d\beta$$

where d_{BS} (d_{MS}) is the antenna spacing at BS (MS) and λ is the wavelength. α is the angular offset around the mean AOD at BS, and β is the angular offset around the mean AOA at MS. The pdf of angular offsets is

$$p(\alpha) = \frac{1}{\sqrt{2}AS_{BS,Path}} \exp\left\{-\frac{\sqrt{2}|\alpha|}{AS_{BS,Path}}\right\}$$

$$p(\beta) = \frac{1}{\sqrt{2}AS_{MS,Path}} \exp\left\{-\frac{\sqrt{2}|\beta|}{AS_{MS,Path}}\right\}$$

The above integration can be computed with two approaches (other alternatives may also exist). See Appendix-A for details. In summary, the first approach is to approximate the Laplacian PDF with 20 rays, after which the integration is reduced to a summation. The second approach is to compute the integration using a numerical method. Either using 20-ray approximation or numerical integration, it is possible to quantize the AOA or AOD and then pre-compute the spatial correlation for each quantized AOA and AOD values. Using pre-stored correlation matrices may reduce the simulation run-time.

Denoting the spatial correlation matrix at BS and MS as $\mathbf{R}_{BS,n}$ and $\mathbf{R}_{MS,n}$, the per-tap spatial correlation is determined as

$$\mathbf{R}_n = \mathbf{R}_{BS,n} \otimes \mathbf{R}_{MS,n} \text{(Kronecker product)}$$

In the case that the antenna elements are cross-polarization antennas, the per-tap channel correlation is determined as

$$\mathbf{R}_n = \mathbf{R}_{BS,n} \otimes \boldsymbol{\Gamma} \otimes \mathbf{R}_{MS,n}$$

where $\boldsymbol{\Gamma}$ is a cross-polarization matrix based on the cross polarization defined in Appendix-B.

Step 5: *Determine the antenna gains of the BS and MS paths as a function of their respective AoDs and AoAs. Calculate the per-tap average power with BS/MS antenna gain as*

$$P_n^{"} = P_n * G_{BS}(AOD_n) * G_{MS}(AOA_n)$$

Step 6: *Determine the Doppler spectrum of each tap, based on a random traveling direction, the array broadside direction defined in step 4, a Laplacian power angular profile with the RMS angular spread AS defined in the CDL models.*

From the Doppler spectrum defined for any arbitrary Doppler spectrum in [21], the Doppler spectrum at tap-n for the case of Laplacian power angular profile is :

$$S_n(f) \propto \begin{cases} \dfrac{1}{\sqrt{f_{\max}^2 - f^2}} \exp\left\{-\dfrac{\sqrt{2}\left|\cos^{-1}(f/f_{\max}) + \vartheta_n\right|}{AS_{MS,Path}}\right\}, & |f| \le f_{\max} = f_c v/c \\ 0, & \text{otherwise} \end{cases}$$

where ϑ_n is the angle between the traveling direction and the mean AOA for tap-n.

<Editor's notes: Nortel expressed the simulation convenience of using Jakes spectrum as an option. So the text in [.] reflects that option> [Generating the time-varying fading process from a Doppler spectrum based on the traveling direction and mean AoA can

be computationally expensive. The impact on the overall system level performance with this more accurate method may be small. Therefore, the Jakes spectrum should be used as a tradeoff between simulation complexity and model accuracy. This will facilitate easy generation of such a time-varying process (e.g. offline generation)]

Step 7: *Generate time-variant MIMO channels with above-defined per-tap spatial correlations*.

For each tap, generate NxM i.i.d. channels first that satisfies the specified Doppler spectrum H_{iid} (each tap is a NxM matrix) where N is the number of receive antennas and M is the number of transmit antennas.

To generate temporally correlated Gaussian process that satisfies a specific Doppler spectrum, one implementation method is to use the summation of equal-power sinusoids where their frequencies are calculated numerically using either Method of Exact Doppler Spread (MEDS) or L_2-Norm Method (LNPM) [[22]]. Pre-computing the sinusoid frequencies for a set of quantized angle ϑ_n can be considered as a means to reduce simulation run time, comparing with computing the sinusoid frequencies on the fly.

Compute the correlated channel at each tap as

$$\mathbf{H}_n = unvec\left\{R_n^{1/2} vec(H_{iid})\right\}$$

where *vec(H)* denotes the column-wise stacking of matrix H and *unvec* is the reverse operation. $R_n^{1/2}$ denotes the square-root of matrix R.

Step 8 (Ray-based method only, Skip for correlation-based implementation): *Generate time-variant MIMO channels*.

For an *N* element linear BS array and a *M* element linear MS array, the channel coefficients for one of *L* multipath components are given by a *N*x*M* matrix of complex amplitudes. We denote the channel matrix for the *n*th multipath component (*n* = 1,…,*L*) as $\mathbf{H}_n(t)$. The (*u,s*)th component (*s* = 1,…,*N, u* = 1,…,*M*) of $\mathbf{H}_n(t)$ is given in the following, assuming polarized arrays (If polarization is not considered, the 2x2 polarization matrix can be replaced by scalar $\exp(\Phi_{n,m})$ and only vertically polarized field patterns applied)

$$h_{u,s,n}(t) = \sqrt{\frac{P_n \sigma_{SF}}{M}} \sum_{m=1}^{M} \left(\begin{bmatrix} \chi_{BS}^{(v)}(\theta_{n,m,AoD}) \\ \chi_{BS}^{(h)}(\theta_{n,m,AoD}) \end{bmatrix}^T \begin{bmatrix} \exp\left(j\Phi_{n,m}^{(v,v)}\right) & \sqrt{r_{n1}}\exp\left(j\Phi_{n,m}^{(v,h)}\right) \\ \sqrt{r_{n2}}\exp\left(j\Phi_{n,m}^{(h,v)}\right) & \exp\left(j\Phi_{n,m}^{(h,h)}\right) \end{bmatrix} \begin{bmatrix} \chi_{MS}^{(v)}(\theta_{n,m,AoA}) \\ \chi_{MS}^{(h)}(\theta_{n,m,AoA}) \end{bmatrix} \times \exp\left(jkd_s \sin(\theta_{n,m,AoD})\right) \times \exp\left(jkd_u \sin(\theta_{n,m,AoA})\right) \times \exp\left(jk\|\mathbf{v}\|\cos(\theta_{n,m,AoA} - \theta_v)\, t\right) \right)$$

where

P_n	is the power of the nth path
σ_{SF}	is the lognormal shadow factor
Q	is the number of subpaths per-path.

$\theta_{n,m,AoD}$ is the the AoD for the mth subpath of the nth path.

$\theta_{n,m,AoA}$ is the the AoA for the mth subpath of the nth path.

$G_{BS,s}(\theta_{n,m,AoD})$ is the BS antenna gain of each array element (including antenna imbalance).

$G_{MS,u}(\theta_{n,m,AoA})$ is the MS antenna gain of each array element (including antenna imbalance).

j is the square root of -1.

k is the wave number $2\pi/\lambda$ where λ is the carrier wavelength in meters.

d_s is the distance in meters from BS antenna element s from the reference (s = 1) antenna. For the reference antenna s = 1, d_1=0.

d_u is the distance in meters from MS antenna element u from the reference (u = 1) antenna. For the reference antenna u = 1, d_1=0.

$\Phi_{n,m}$ is the phase of the mth subpath of the nth path.

$\|\mathbf{v}\|$ is the magnitude of the MS velocity vector.

θ_v is the angle of the MS velocity vector.

$\chi_{BS}^{(v)}(\theta_{n,m,AoD})$ is the BS antenna complex response for the V-pol component.

$\chi_{BS}^{(h)}(\theta_{n,m,AoD})$ is the BS antenna complex response for the H-pol component.

$\chi_{MS}^{(v)}(\theta_{n,m,AoA})$ is the MS antenna complex response for the V-pol component.

$\chi_{MS}^{(h)}(\theta_{n,m,AoA})$ is the MS antenna complex response for the H-pol component.

r_{n1} is the random variable representing the power ratio of waves of the nth path leaving the BS in the vertical direction and arriving at the MS in the horizontal direction (v-h) to those leaving in the vertical direction and arriving in the vertical direction (v-v).

r_{n2} is the random variable representing the power ratio of waves of the nth path leaving the BS in the horizontal direction and arriving at the MS in the vertical direction (h-v) to those leaving in the vertical direction and arriving in the vertical direction (v-v).

$\Phi_{n,m}^{(x,y)}$ phase offset of the mth subpath of the nth path between the x component (either the horizontal h or vertical v) of the BS element and the y component (either the horizontal h or vertical v) of the MS element.]

Step 9: *If a non-zero K-factor wants to be enforced in a correlation based implementation (i.e., K≠0), adjust the LOS path power*

If a non-zero K-factor is to be enforced (i.e., K≠0), adjust the LOS path power. See Appendix -C for details.

Step 10: *Introduce receive antenna gain imbalance or coupling, if need.*

See Appendix-D.

3.3. Link Level Channel Model

A baseline link level channel model could be based on the spatial TDL or CDL models in order to be consistent with the system level models.

For various propagation scenarios, the corresponding CDL model can be directly used for link simulation, assuming the AOA and AOD are relative to the broadside direction of the receiver array, instead of assuming random orientation of the array in system simulations.

In the case of correlation-based implementation, the spatial correlation can be easily derived once the AOA/AOD is well defined based on either 20-ray approximation or numerical integration. The antenna configuration is assumed to either a linear array with a spacing of TBD-λ or a polarized antenna with an XPD of 8dB as assumed also in [23]

<Editor's notes: The text in [ ] has not been discussed on the call.> [The Doppler spectrum depends on traveling direction relative to the AOA. Instead of setting a random traveling direction with can vary from simulation to simulation, a worst case Jakes spectrum may be considered.]

4. Link-to-System Mapping

Editor: Louay Jalloul, jalloul@beceem.com

Sources	Document Reference
Sassan Ahmadi et al.	C80216m-07_069.doc
Alcatel-Dan Gal et al.	C80216m-07_063.doc
Robert Novak et al.	C80216m-07_074r1.doc
Wookbong Lee et al.	C80216m-07_075r1.doc C80216m-07_091.doc
Shiang-Jiun Lin et al	C802.16m-07_059r1.doc
Shirish Nagaraj et al.	C802.16m-07_096.doc
Krishna Sayana et al.	C802.16m-07_101.doc
Seung Joon Lee	C802.16m-07_107.doc

4.1. Background of PHY Abstraction

The objective of the physical layer (PHY) abstraction is to accurately predict link layer performance in a computationally simple way. The requirement for an abstraction stems from the fact that simulating the physical layer links between multiples BSs and MSs in a network/system simulator can be computationally prohibitive. The abstraction should be accurate, computationally simple, relatively independent of channel models, and extensible to interference models and multi-antenna processing.

In the past, system level simulations characterized the average system performance, which was useful in providing guidelines for system layout, frequency planning etc. For such simulations, the average performance of a system was quantified by using the topology and macro channel characteristics to compute a geometric (or average) SINR distribution across the cell. Each subscriber's geometric SINR was then mapped to the highest modulation and coding scheme (MCS), which could be supported based on link

level SINR tables that capture fast fading statistics. The link level SINR-PER look-up tables served as the PHY abstraction for predicting average link layer performance. Examples of this static methodology may be found in [25]-[26].

Current cellular systems designs are based on exploiting instantaneous channel conditions for performance enhancement. Channel dependent scheduling and adaptive coding and modulation are examples of channel-adaptive schemes employed to improve system performance. Therefore, current system level evaluation methodologies are based on explicitly modeling the dynamic system behavior by including fast fading models within the system level simulation (SLS). Here the SLS must support a PHY abstraction capability to accurately predict the instantaneous performance of the PHY link layer.

4.2. Dynamic PHY Abstraction Methodology

In system level simulations (SLS), an encoder packet may be transmitted over a time-frequency selective channel. For example, OFDM systems may experience frequency selective fading, and hence the channel gain of each sub-carrier may not be equal. In OFDM, the coded block is transmitted over several sub-carriers and the post-processing SINR values of the pre-decoded streams are thus non-uniform. Additionally, the channel gains of sub-carriers can be time selective, i.e. change in time due to the fading process and possible delays involved in HARQ re-transmissions. The result on a transmission of a large encoder packet is encoded symbols of unequal SINR ratios at the input of the decoder due to the selective channel response over the encoder packet transmission.

PHY abstraction methodology for predicting instantaneous link performance for OFDM systems has been an active area of research and has received considerable attention in the literature [27]-[36]. The role of a PHY abstraction method is to predict the coded block error rate (BLER) for given a received channel realization across the OFDM sub-carriers used to transmit the coded FEC block. In order to predict the coded performance, the post-processing SINR values at the input to the FEC decoder are considered as input to the PHY abstraction mapping. As the link level curves are generated assuming a frequency flat channel response at given SINR, an effective SINR, $SINR_{eff}$ is required to accurately map the system level SINR onto the link level curves to determine the resulting BLER. This mapping is termed *effective SINR mapping (ESM).* The ESM PHY abstraction is thus defined as compressing the vector of received SINR values to a single effective SINR value, which can then be further mapped to a BLER/PER number as shown in Figure 7.

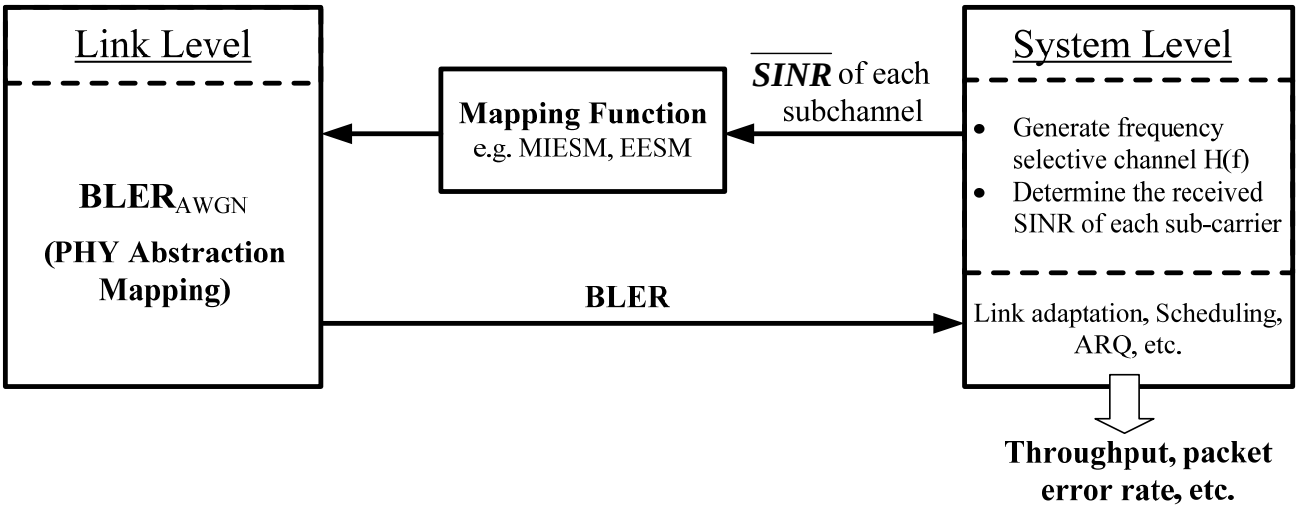

Figure 7: PHY link-to-system mapping procedure

Several ESM PHY abstractions to predict the instantaneous link performance have been proposed in the literature. Examples include mean instantaneous capacity ([27]-[29]), exponential-effective SINR (EESM, [30],[32]-[34]) and Mutual information effective SINR (MIESM, [35],[36]). With the class of MIESM there are two variants, one is based on the mutual information per received symbol normalized to yield the bit mutual information (referred to later as RBIR) and the other directly computes the bit mutual information (referred to later as MMIB). Each of these PHY abstractions uses a different function to map the vector of SINR values to a single number. Given the instantaneous EESM SINR, mean capacity or mutual information SINR, the PER (block error rate) for each MCS is calculated using a suitable mapping function for each MCS scheme.

In general, the ESM can be described as follows,

$$SINR_{eff} = \Phi^{-1}\left\{\frac{1}{N}\sum_{n=1}^{N}\Phi\left(SINR_n\right)\right\} \quad (1)$$

where N is the number of symbols in a coded block, and $\Phi(\bullet)$ is an invertible function.

In the case of the mutual information and capacity based ESM the function $\Phi(\bullet)$ is derived from the constrained capacity. While in the case of EESM, the function $\Phi(\bullet)$ is derived based on the Chernoff bound for the probability of error. In the next three sections, we describe these ESM methods.

4.3. PHY Abstraction Methods

4.3.1. Received Block Mutual Information (RBIR) ESM

A block diagram for the MIESM approach is shown in Figure 8. Given a set of *N* received encoder symbol SINRs from the system level simulations, denoted as $SINR_1$, $SINR_2$, $SINR_3$, …, $SINR_N$, the mutual information per symbol (*SI*) is computed as a function of the *M*-ary modulation scheme, with $m = \log_2 M$ bits/symbol, as follows:

$$SI\left(SINR_n, m(n)\right) = E_{XY}\left[\log_2\left(\frac{P(Y \mid X, SINR_n)}{\sum_X P(X)P(Y \mid X, SINR_n)}\right)\right] \quad (2)$$

In equation (2), $Y = \sqrt{\rho}X + U$ is the received symbol, $P(Y \mid X, SINR)$ is the channel transition probability density conditioned on the input symbol *X* for a given $SINR = \rho$. It is assumed that the transmitted symbols are equally likely, thus $P(X) = 1/M$, where *M* is the size of the modulation alphabet and that *U* is modeled as zero mean complex Gaussian with variance $1/2$ per component. The mutual information curves $SI(SINR, m)$ are generated, and stored once in the system simulator, for each of the modulation and coding formats.

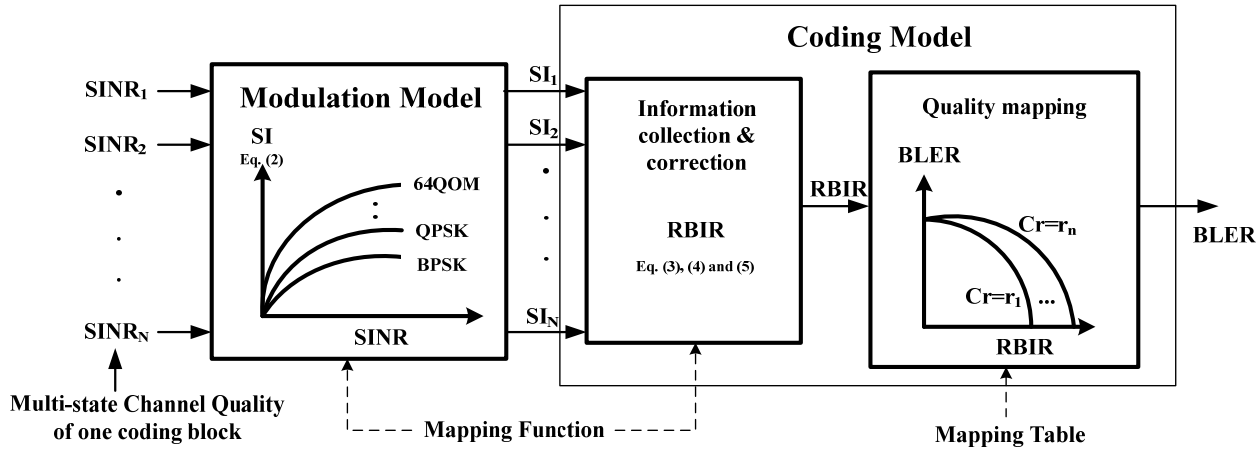

Figure 8: Computational procedure for mutual information ESM methods

Assuming *N* sub-carriers are used to transmit a coded block, the received mutual information over a coded block (*RBI*) is computed as:

$$RBI = \sum_{n=1}^{N} SI\left(SINR_n, m(n)\right) \quad (3)$$

We note that the even though we refer to the coded block being carried over a set of sub-carriers, in general, the coded block may be carried over multiple dimensions, including the spatial dimensions available with MIMO. Also, note that in the above, the

mutual information may be computed even with non-uniform modulation across the coded block. Next we compute the normalized mutual information per received bit (*RBIR*) which is given by

$$RBIR = \frac{\sum_{n=1}^{N} SI\left(SINR_n, m(n)\right)}{\sum_{n=1}^{N} m(n)} \quad (4)$$

The advantage of computing the *RBIR* is that the relationship between the *RBIR* and the PER is dependent only on the AWGN curves for the code rate and is independent of the modulation scheme. This feature is a very useful in computing the PHY abstraction for cases where the coded block comprises of mixed modulation symbols.

We further note that an adjustment parameter, $SINR_{adjust}$, may be specified with the RBIR metric that can account for deviations of the *RBIR* mapping with respect to the AWGN curves. This adjustment parameter is illustrated by the following equation.

$$RBIR = \frac{\sum_{n=1}^{N} SI\left(SINR_n / SINR_{adjust}, m(n)\right)}{\sum_{n=1}^{N} m(n)} \quad (5)$$

The exact specification of this adjustment parameter is determined through simulations and shall be specified along with the PHY abstraction tables, once the 802.16m numerology is specified.

The pervious computation of the mutual information per coded bit, RBIR, was derived from the symbol-level mutual information. Next we present an alternate method that directly arrives at the bit-level mutual information. This method called mean mutual information per bit (MMIB).

4.3.2. Mean Mutual Information Per Bit (MMIB) ESM

4.3.2.1. MMIB and its relation to other MI metrics

The accuracy of a mutual information based metric depends on the equivalent channel over which this metric is defined. Capacity is the mutual information based on a Gaussian channel with Gaussian inputs. Modulation constrained capacity metric is the mutual information of a “symbol channel” (i.e. constrained by the input symbols from a complex set). It is possible to obtain a mutual information per bit metric from the symbol channel by simply normalizing this constrained capacity (i.e. by dividing by the modulation order) as done in the RBIR method.

Note, however that the symbol channel does not account for the constellation mapping, i.e. the mapping of bits to symbols in the constellation, i.e. it is invariable to different bit-to-symbol mappings. An alternative metric is to define the mutual information on the bit

channel itself, which we will refer to as Mutual Information per coded Bit or MIB (or MMIB when a mean of multiple MIBs is involved). It is however possible that for certain constellation mappings (say Gray encoding) MMIB and RBIR functions may be similar.

More generally, given that our goal is to abstract the performance of the underlying binary code, the closest approximation to the actual decoder performance is obtained by defining an information channel at the coder-decoder level, i.e. defining the mutual information between bit input (into the QAM mapping) and LLR output (out of the LLR computing engine at the receiver), as shown in Figure 9. The concept of "bit channel" encompasses SIMO/MIMO channels and receivers. We will demonstrate that this definition will greatly simplify PHY abstraction by moving away from an empirically adjusted model and introducing instead MIB functions of equivalent bit channels.

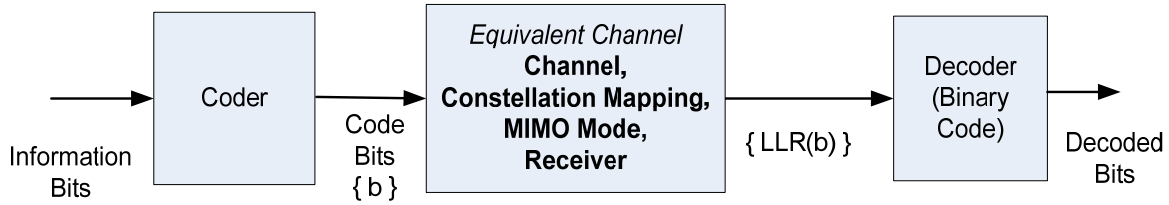

Figure 9: Bit-Interleaved Coded Modulation system

In the bit channel of Figure 9, the task now is to define efficient functions that capture the mutual information per bit. The following sections further develop an efficient approach for MIB computation by approximating the LLR PDF with a Gaussian mixture PDFs. We will begin with the development of explicit functions for MIBs in SISO and later extend to MIMO.

The concept of deriving mutual information between coded bits and their LLR values was also well known from work in MIESM for BPSK [3GPP contribution C30-20030429-010, Ericsson]. For BPSK, however, bit-level capacity is the same as symbol-level capacity.

4.3.2.2. MIB Mapping for SISO Systems

The mutual information of the coded bit is dependent on the actual constellation mapping. The MI of each bit-channel is obtained and averaged across the bits in a QAM symbol. After encoding (e.g. Turbo or CTC), a binary coded bit stream c_k is generated before QAM mapping. The QAM modulation can be represented as a labeling map $\mu : \mathrm{A} \to X$, where A is the set of m-tuples, $m \in \{2,4,6\}$ to represent QPSK, 16 and 64-QAM, of binary bits and X is the constellation. Given the observation y_n corresponding to the n^{th} QAM symbol in a codeword, the demodulator computes the log-likelihood ratio (LLR) $LLR(b_{i,n})$ of the i^{th} bit comprising the symbol via the following expression (where the symbol index n is dropped for convenience)

$$LLR(b_i) = \ln\left(\frac{P(y \mid b_i = 1)}{P(y \mid b_i = 0)}\right) \quad (6)$$

When the coded block sizes are very large in a bit-interleaved coded system (BICM), the bit interleaver effectively breaks up the memory of the modulator, and the system can be represented as a set of parallel independent bit-channels [38]. Conceptually, the entire encoding process can be represented as shown in Figure 9.

Due to the asymmetry of the modulation map, each bit location in the modulated symbol experiences a different 'equivalent' bit-channel. In the above model, each coded bit is randomly mapped (with probability $1/m$) to one of the m bit-channels. The mutual information of the equivalent channel can be expressed as:

$$I(b, LLR) = \frac{1}{m}\sum_{i=1}^{m} I(b_i, LLR(b_i)) \quad (7)$$

where $I(b_i, LLR(b_i))$ is the mutual information between input bit and output LLR for i^{th} bit in the modulation map. As can be seen, the bit LLR reflects the demodulation process to compute LLR, which was not reflected in the symbol-level MI and the RBIR defined above. This is the main difference between the bit- and symbol-level MI definitions. More generally, however, the mean mutual information – computed by considering the observations over N symbols (or channel uses) – over the codeword may be computed as

$$M = \frac{1}{mN}\sum_{n=1}^{N}\sum_{i=1}^{m} I(b_i, LLR(b_i)) \quad (8)$$

The mutual information function $I(b_i, LLR(b_i))$ is, of course, a function of the QAM symbol SINR, and so the mean mutual information M (MMIB) may be alternatively written as

$$M = \frac{1}{mN}\sum_{n=1}^{N}\sum_{i=1}^{m} I_{m,b_i}(SINR_n) = \frac{1}{N}\sum_{n=1}^{N} I_m\left(SINR_n\right) \quad (9)$$

The mean mutual information is dependent on the SINR on each modulation symbol (index n) and the code bit index i (or i-th bit channel), and varies with the constellation order m. Accordingly, the relationship $I_{m,b_i}(SINR)$ is required for each modulation type and component bit index in order to construct $I_m(SINR)$.[2]

For BPSK/QPSK, a closed from expression is given in [38]—[39], which is a non-linear function that can be approximated in polynomial form. For the particular case of

[2] *Note that in the 802.16e specification, bit indexing typically proceeds from 0.*

BPSK/QPSK, the function would be the same as that obtained by defining mutual information of a symbol channel (symbol channel is just a bit channel for BPSK).

4.3.2.3. Generalized LLR PDF Model and non-linear functions for MIB

For BPSK, conditional LLR PDF is Gaussian and the MIB can be expressed as

$$J(x) \approx \begin{cases} a_1 x^3 + b_1 x^2 + c_1 x, & \text{if } x \le 1.6363 \\ 1 - \exp(a_2 x^3 + b_2 x^2 + c_2 x + d_2) & \text{if } 1.6363 \le x \le \infty \end{cases} \quad (7)$$

where $a_1 = -0.04210661, b_1 = 0.209252$ and $c_1 = -0.00640081$ for the first approximation, and where $a_2 = -0.00181492, b_2 = -0.142675, c_2 = -0.0822054$ and $d_2 = 0.0549608$ for the second approximation.

It can be shown that the LLR PDFs for any other modulation can be approximated as a mixture of Gaussian distributions. Further they are non-overlapping at asymptotically high SINRs.

If the LLR distribution can be approximated by a mixture of Gaussian distributions (which are non overlapping), then it follows that the corresponding MIB can be expressed as a sum of *J(.)* functions,

$$\text{Mixture of Gaussians} \rightarrow I(x) = \sum_{i=1}^{K} a_i J(c_i x) \qquad \sum_{i} a_i = 1$$

We will use this parameterized function for expressing all non-linear MIB functions. The corresponding parameters themselves, would be a function of the modulation.
The optimized functions for QPSK, 16-QAM and 64-QAM are given by

MI Function	Numerical Approximation
$I_2(\gamma)$ (QPSK)	$M = J(2\sqrt{\gamma})$ $(Exact)$
$I_4(\gamma)$ (16-QAM)	$M = \frac{1}{2}J(0.8\sqrt{\gamma}) + \frac{1}{4}J(2.17\sqrt{\gamma}) + \frac{1}{4}J(0.965\sqrt{\gamma})$
$I_6(\gamma)$ (64-QAM)	$M = \frac{1}{3}J(1.47\sqrt{\gamma}) + \frac{1}{3}J(0.529\sqrt{\gamma}) + \frac{1}{3}J(0.366\sqrt{\gamma})$

Table 17: Numerical approximations for MMIB mappings

4.3.2.4. BLER Mapping Function – Detailed Description

Once the MMIB is computed over a set of subcarriers corresponding to coded symbols, a direct MMIB to BLER relationship can be used to obtain block error rate, without necessarily defining an effective SINR.

The BS can store the lookup tables for the AWGN reference curves for different MCS levels in order to map the MMIB to BLER. Another alternative is to approximate the reference curve with a parametric function. For example, we consider a Gaussian

cumulative model with 3 parameters which provides a close fit to the AWGN performance curve, parameterized as

$$y = \frac{a}{2}\left[1 - erf\left(\frac{x-b}{\sqrt{2}c}\right)\right], \quad c \neq 0 \tag{10}$$

where a is the "transition height" of the error rate curve, b is the "transition center" and c is related to the "transition width" (transition width = 1.349 c) of the Gaussian cumulative distribution. In the linear BLER domain, the parameter a can be set to 1, and the mapping requires only two parameters, which are given for each MCS index in the table below. The accuracy of the curve fit with this model is verified with MCS modes supported in 802.16e as shown in Figure 10. This parameterization of AWGN reference considerably simplifies the storage and simulation requirements.

So for each MCS the BLER is obtained as

$$BLER_{MCS} = \frac{1}{2}\left[1 - erf\left(\frac{x-b_{MCS}}{\sqrt{2}c_{MCS}}\right)\right], \quad c \neq 0 \tag{11}$$

Further, we can achieve an additional simplification. The following figure plots MMIB vs BLER for numerical results obtained in 802.16e simulations using 6 different MCS's with rates 1/2 and 3/4 on an AWGN channel.

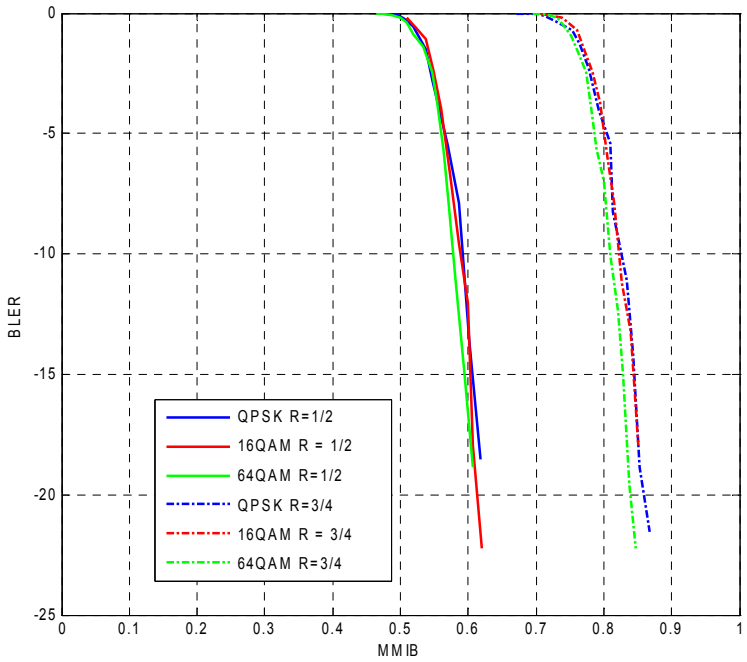

Figure 10: BLER mappings for MMIB from AWGN performance results

It can be seen from the figure that – to a first-order approximation – the mapping from MMIB to BLER can be assumed independent of the QAM modulation type. However, since code performance is strongly dependent on code sizes and code rates, $B_\varphi(M)$ will not be independent of these parameters.

Alternative: With the above result, we generalize the AWGN reference curves to be a function of the block size and coding rate (BCR)

$$BLER_{BCR} = \frac{1}{2}\left[1 - erf\left(\frac{x - b_{BCR}}{\sqrt{2}c_{BCR}}\right)\right], \quad c \neq 0 \tag{12}$$

With this simplification, a base station needs to store two parameters for each supported BCR mode.

Note: The choice of this particular MMIB to BLER mapping is due to the underlying physical interpretation. The parameter b is closely related to the binary code rate and will be equal to the code rate for an ideally designed code. Similarly, parameter c represented the rate of fall of the curve and is also related to the block size.

The table below is an example parameter table which can be determined based only on the performance on an AWGN channel. It can be further simplified only considering BCR modes instead of MCS, the latter being more useful for HARQ combining.

Modulation	Code Rate	b	c
QPSK	1/2	0.5512	0.0307
16QAM	3/4	0.7863	0.03375
64QAM	5/6	0.8565	0.02622
MCS4	..	..	..
MCS5	..	..	..

Table 18: Example: Parameters for Gaussian cumulative approximation

4.3.2.5. MIMO Receiver Abstraction

With linear receivers like MMSE, each 2 stream MIMO channel is treated as two equivalent SISO channels with SINRs given by post combining SINRs of the linear receiver. The MIB can be obtained as

$$M = \frac{1}{NN_t}\sum_{i=1}^{N}\sum_{j=1}^{N_t} I_m(\gamma_{ij})$$

and (13)

$$BLER = B_{BCR}(M)$$

where γ_{ij} is the post combining SINR of layer j on subcarrier i, N_t is the number of transmit antennas, N is the total number of coded subcarriers, and the mapping functions $I_m(.)$ and $B_{BCR}(.)$ are defined in sections on SISO for each MCS.

4.3.3. Exponential ESM (EESM)

The EESM is simply given by

$$SINR_{eff} = -\beta \ln\left(\frac{1}{N}\sum_{n=1}^{N}\exp\left(-\frac{SINR_n}{\beta}\right)\right) \quad (14)$$

where β is a value for optimization/adjustment that depends on the MCS and the encoding block length. A table of these β values will be provided once the numerology is decided.

4.4. Remarks on PHY Abstraction

The decision on which of the ESM PHY abstraction methods used in the final evaluation report shall be decided based on a rigorous set of comparisons using simulations and analyses.

4.5. Per-tone SINR Computation

All PHY abstraction metrics are computed as a function of post-processing per-tone SINR values across the coded block at the input to the decoder. The post-processing per-tone SINR is therefore dependent on the transmitter/receiver algorithm used to modulate/demodulate the symbols. As an illustration of how the post-processing per-tone SINR values can be computed, we consider the simple case of a single-input-single output (SISO) system with a matched filter receiver. Without loss of generality, let the target user/sector be denoted by the index 0. The received signal at the *n-th* sub-carrier for the target user is calculated as:

$$Y^{(0)}(n) = \sqrt{P_{tx}^{(0)}P_{loss}^{(0)}}H^{(i)}(n)X^{(0)} + \sum_{j=1}^{N_I}\sqrt{P_{tx}^{(j)}P_{loss}^{(j)}}G^{(j)}(n)X^{(j)} + U^{(0)}(n) \quad (15)$$

where

N_I is the number of interferers,

$P_{tx}^{(i)}$ is the total transmit power from *i-th* BS (per sector) or MS,

$P_{loss}^{(i)}$ is the distance dependent path loss including shadowing and antenna gain/loss and cable losses from the *i-th* sector or MS,

$H^{(i)}(n)$ is the channel gain for the desired MS for the *n*-th sub-carrier and *i-th* user/sector.

$X^{(j)}$ is the transmitted symbols by the *j*-th user/sector,

$U^{(0)}(n)$ is the receiver thermal noise, modeled as AWGN noise with zero mean and variance σ^2.

Using a matched filter (or maximum ratio combining) receiver, given by $H^{(0)}(n)^* Y^{(0)}(n)$, the post-processing SINR may be expressed as

$$SINR^{(0)}(n) = \frac{P_{tx}^{(0)} P_{loss}^{(0)} \left| H^{(0)}(n) \right|^2}{\sigma^2 + \sum_{j=1}^{N_I} P_{tx}^{(j)} P_{loss}^{(j)} \left| G^{(j)}(n) \right|^2} \quad (16)$$

In the above we assume that ideal knowledge of interference statistics per sub-carrier is available for post-processing SINR computation. For MIMO systems, post-processing SINR may be similarly calculated, especially if linear receivers are used for MIMO processing. We assume that linear minimum mean square (MMSE) receivers will be used asbaseline receivers for SLS methodology. Advanced receivers, such as the maximum likelihood receiver, and their associated PHY abstractions may be considered on an as needed basis and are for further study (FFS). The following section describes the post-processing SINR calculations for MIMO reception assuming the baseline linear MMSE receiver.

4.5.1. Per-Tone Post Processing SINR Calculation for MIMO

To illustrate the per-tone post processing SINR calculation for a MIMO system based on a linear MMSE receiver, we assume an *K* transmit and *L* receive antennas system for downlink transmission. Since these calculations are illustrative, for the sake of simplicity, we assume that *K* spatial streams are transmitted and $L \geq K$. We also assume that interferers and the desired signal use the same MIMO scheme for transmission. The simplified signal model is described as follows:

$$\underline{Y}^{(0)}(n) = \underline{H}^{(0)}(n)\underline{X}^{(0)}(n) + \sum_{j=1}^{N_I} \underline{G}^{(j)}(n)\underline{X}^{(j)}(n) + \underline{U}^{(0)} \quad (17)$$

where

$\underline{Y}^{(0)}(n)$ is a $L \times 1$ dimensional received signal vector at the MS for the *n*-th sub-carrier,

$\underline{H}^{(0)}(n)$ is a $L \times K$ channel gain matrix between the desired BS and the MS for the *n*-th sub-carrier,

$\underline{G}^{(j)}(n)$ is the $L \times K$ channel gain matrix between the interfering BS and the MS for the *n*-th sub-carrier,

$\underline{X}^{(0)}(n)$ and $\underline{X}^{(j)}(n)$ are the vectors ($K \times 1$) of the desired MS and the *j*-th interfering MS, with covariances $\sigma_0^2 \underline{I}$ *and* $\sigma_j^2 \underline{I}$ $j = 1, 2, \cdots, N_I$, respectively, and

$\underline{U}^{(0)}$ is modeled as zero mean AWGN noise vector with covariance $\sigma^2 \underline{I}$, $\underline{I}$ is the $K \times K$ identity matrix.

At the MS, a linear MMSE receiver is used to demodulate the transmitted signal vector, and

$$\underline{X}^{(0)}(n) = W(n)\underline{Y}^{(0)}(n) \tag{18}$$

Here, the non-interference-aware MMSE weights $W(n)$ are specified as

$$W(n) = \left(\underline{H}^{(0)^*} \underline{H}^{(0)} + \frac{\sigma^2}{\sigma_0^2} I \right)^{-1} \underline{H}^{(0)^*} \tag{19}$$

where (.)* is the Hermitian operator.

The post-processing SINR can be computed by defining the following two expressions:, $D(n) = diag\left[W(n)\underline{H}^{(0)}(n) \right]$ which denotes the desired signal component and $I_{self}(n) = W(n)\underline{H}^{(0)}(n) - D(n)$ which is the self interference between MIMO streams.

The post-processing SINR of the desired MS for *n-th* sub-carrier and the *k-th* MIMO stream is thus given as:

$$SINR_k^{(0)}(n) = \frac{diag\left[\sigma_0^2 D(n) D(n)^* \right]_{kk}}{diag\left[\sigma^2 W(n) W(n)^* + \sigma_0^2 I_{self} I_{self}^* + \sum_{j=1}^{N_I} \sigma_j^2 W(n) G^{(j)}(n) G^{(j)}(n)^* W(n)^* \right]_{kk}} \tag{20}$$

Here, ideal knowledge of the interfering statistics is assumed for the computation of the post-processing SINR, even though the MMSE receiver does not assume knowledge of the interference statistics.]

4.5.2. Interference Aware PHY Abstraction

Proponents should provide justification of assumptions related to knowledge of interference statistics used in system level simulations.

4.5.3. Practical Receiver Impairments

The evaluation should account for practical receiver implementation losses resulting from channel estimation errors, synchronization errors, coherence loss due to Doppler and inter-tone interference, etc. Inclusion of channel estimation losses and other receiver impairments is FFS; however the minimum level required is of adding a fixed implementation loss backed by analysis/simulation. The channel estimation algorithm that should be assumed as baseline is a linear channel estimation from known symbols (linear means each channel estimate is a linear function of the received pilots), with reasonable delay considering the link latency requirements.

4.6. Deriving Packet Error Rate from Block Error Rate

A packet comprises several FEC blocks. The packet error rate (PER) is the probability that an error occurs in at least one of FEC blocks comprising the packet. The PHY abstraction predicts the link performance, in terms of BLER, for a coded FEC block. Here we need to extrapolate the PER given the predicted BLER. If a packet is comprised of J blocks and the predicted BLERs are given by $BLER_1$, $BLER_2$, …, $BLER_J$, then the PER is derived as

$$PER = 1 - \prod_{j=1}^{J} \left(1 - BLER_j\right) \tag{21}$$

4.7. PHY Abstraction for H-ARQ

PHY abstraction of H-ARQ depends on the H-ARQ method and should be justified by link level simulations showing the PER forecast versus actual PER in each retransmission.

4.7.1. Baseline Modeling

The following abstraction is proposed as baseline:

- For Chase combining (CC): the SINR values of the sub-carriers are summed across retransmissions, and these combined SINR values will be fed into the PHY abstraction.
- For Incremental redundancy (IR): the transmission and retransmissions are regarded as a single codeword, and all the SINR values are fed into the PHY abstraction, which is calibrated according to link level PER curves of the entire transmission (including the retransmission).

For methods combining CC and IR the second approach is preferred but should be justified by link level simulations.

4.7.2. Chase Combining

For MMIB, the post-processing SINRs can be obtained as simple sum of the SINRs on the first transmission and subsequent retransmissions and thus

$$MMIB = \sum_{i=1}^{N} I_m \left(\sum_{j=1}^{q} \gamma_{ij} \right) \quad (22)$$

where γ_j is the i th symbol SINR during j th retransmission.

4.7.3. The Case of Repeated Bits/Symbols

This section details a method to handle symbol/coded bit repetitions accurately. Depending on the rate matching algorithm used, every H-ARQ transmission could have a set of new parity bits and other bits that are repeated. Accumulating the mutual information is appropriate as long as new parity bits are transmitted in every symbol. Otherwise, the receiver combines the demodulation symbols or, more typically, the LLRs. In this section, we consider a rate-matching approach that does pure IR transmissions and involves coded bit repetitions once all the coded bits from a base code rate are exhausted.

To handle this case, we consider a retransmission including a set of N_{NR} new coded bits, and a set of N_R coded bits that are repeated from pervious transmissions. Further, we assume there are N_{pre} coded bits that are not re-transmitted in this re-transmission. The averaged mutual information per bit from previous transmissions is $RBIR_{old}$. The averaged mutual information per bit in the this re-transmissions is $\overline{I}_b$.

We can then compute an updated RBIR after this retransmission as follows

$$RBIR_{new} = \frac{N_{pre} \cdot RBIR_{old} + N_{NR} \cdot \overline{I}_b + N_R \cdot f_1\left(f_1^{-1}\left(RBIR_{old} \right) + f_1^{-1}\left(\overline{I}_b \right) \right)}{N_{pre} + N_{NR} + N_R} \quad (23)$$

where $f_1(\cdot)$ is a mapping from bit SINR to RBIR function.

For MMIB the performance of the decoder at each stage is that corresponding to a binary code with the modified equivalent code rate and code size (as shown in Figure 11), and *neglecting any partial repetition* of previously sent packets for modeling purposes.

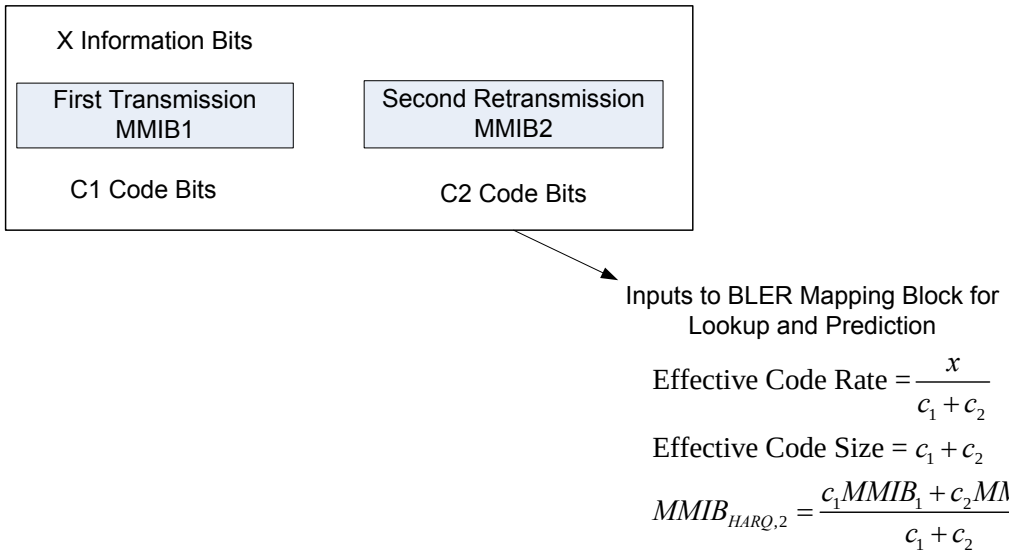

Figure 11: MMIB Update after a Retransmission and the Required Parameters for BLER Lookup

The performance prediction can be performed by combining the MMIBs on the transmissions as shown in Figure 11, and looking up the BLER relationship corresponding to the modified effective code rate and code size.

Note: A code rate-code size parameterized relationship for b,c parameters in the AWGN reference (see note below), is clearly very helpful to cover the new possible BCR combinations with IR.

Note: Express b,c parameters as simple 2-dimensional parameterized functions of block size and code rate as follows, which could further reduce storage requirements and streamline simulation methodology.

$$\begin{aligned} b &= f(R,L) = R + f'(R,L) \\ c &= g(R,L) \end{aligned}$$

where R is the code rate (Ex:1/2) and L is the block size (Ex: 500 bits)

In the case of EESM as a PHY abstraction method, the effective SINR for *k*th transmission can be calculated as follows:

$$SINR_{eff}^{1} = -\beta \ln\left(\frac{1}{|U_1|}\sum_{n\in U_1}\exp\left(-SINR_{n,1}/\beta\right)\right)$$

$$SINR_{eff}^{k} = -\beta \ln\left(\frac{1}{|U_k|}\left(|U_{k-1}|\sum_{n\in U_{k-1}}\exp\left(-\frac{1}{\beta}\left(SINR_{eff}^{k-1} + I_{n,k}SINR_{n,k}\right)\right) + \sum_{n\in V_k \setminus U_{k-1}}\exp\left(-SINR_{n,k}/\beta\right)\right)\right)$$

where $SINR_{eff}^{k}$ is *k*-th transmission's effective SINR, $SINR_{n,k}$ is *k*th transmission's post processed SINR for bit index *n*, V_k is the set of indices where a coded bit was

transmitted on *k*-th transmission, $I_{i,k}$ is an indicator function for codeword bit index *i* for the set V_k, ($I_{i,k}$ = 0 for $i \notin V_k$., and $I_{i,k}$ = 1 for $i \in V_k$), and U_k is the unique bit indices transmitted up to transmission *k*, $U_k = \bigcup_{j=1}^{k} V_j$.

4.8. PHY Abstraction for Repetition Coding

The SINR values of the sub-carriers are summed across repetition number, and these combined SINR values will be fed into the PHY abstraction.

5. Link Adaptation

Editor: Robert Novak, rnovak@nortel.com

Sources	Document Reference
Sassan Ahmadi et al.	C80216m-07_069.doc
Mark Cudak et al.	C80216m-07_061.pdf
Dan Gal et al.	C80216m-07_063.doc
Robert Novak et al.	C80216m-07_074r1.pdf
Wookbong Lee et al.	C80216m-07_075r1.doc
Liu Ying et al.	C80216m-07_064r1.doc

Link adaptation can enhance system performance by optimizing resource allocation in varying channel conditions. System level simulations should include adaptation of the modulation and coding schemes, according to link conditions.

The purpose of this section is to provide guidelines for link adaptation in system evaluations. The use of link adaptation is left to the proponent as it may not pertain to all system configurations. The link adaptation algorithms implemented in system level simulations are left to Individual proponents for each proposal. Proponents should specify link adaptation algorithms including power, MIMO rank, and modulation adaptation per resource block.

5.1. Adaptive Modulation and Coding

The evaluation methodology assumes that adaptive modulation and coding with various modulation schemes and channel coding rates is applied to packet data transmissions. In the case of MIMO, different modulation schemes and coding rates may be applied to different streams

5.1.1. Link Adaptation with H-ARQ

The link adaptation [algorithm] should be optimized to maximize the performance at the end of the H-ARQ process (e.g. maximize the average throughput under constraint on the delay and PER, or maximize number of users per service).

5.2. Channel Quality Feedback

A Channel Quality Indicator (CQI) channel is utilized to provide channel-state information from the user terminals to the base station scheduler. Relevant channel-state information can be fed back. For example, Physical CINR, effective CINR, MIMO mode selection and frequency selective sub-channel selection may be included in CQI feedback. Some implementations may use other methods, such as channel sounding, to provide accurate channel measurements. Proponents should describe the CQI feedback type and assumption of how the information is obtained.

5.2.1. Channel Quality Feedback Delay and Availability

Channel quality feedback delay accounts for the latency associated with the measurement of channel at the receiver, the decoding of the feedback channel, and the lead-time between the scheduling decision and actual transmission. The delay in reception of the channel quality feedback delay shall be modeled to accurately predict system performance.

Channel quality feedback may not be available every frame due to system constraints such as limited feedback overhead or intermittent bursts. The availability of the channel quality feedback shall be modeled in the system simulations.

The proponents should indicate the assumptions of channel quality feedback delay and availability for system proposals.

5.2.2. Channel Quality Feedback Error

System simulation performance should include channel quality feedback error by modeling appropriate consequences, such as misinterpretation of feedback or erasure.

The proposals should describe if CQI estimation errors are taken into account, and if so, how those errors are modeled.

6. HARQ

Editor: Robert Novak, rnovak@nortel.com

Sources	Document Reference
Sassan Ahmadi et al.	C80216m-07_069.doc
Mark Cudak et al.	C80216m-07_061.pdf
Dan Gal et al.	C80216m-07_063.doc
Robert Novak et al.	C80216m-07_074r1.pdf
Wookbong Lee et al.	C80216m-07_075r1.doc
Liu Ying et al.	C80216m-07_064r1.doc

The stop-and-wait Hybrid ARQ (HARQ) protocol can be implemented in system simulations. Multiple parallel HARQ streams may be present in each frame each

associated with a different packet transmission. Different MIMO configurations may also have an impact on the HARQ implementation.

Each HARQ transmission results in one of the following outcomes: successful decoding of the packet, unsuccessful decoding of the packet transmission requiring further re-transmission, or unsuccessful decoding of the packet transmission after maximum number of re-transmissions resulting in packet error. The effective SINR for packet transmissions after one or more HARQ transmissions used in system simulations is determined according to the PHY abstraction section of the evaluation methodology.

When HARQ is enabled, retransmissions are modeled based on the HARQ option chosen. For example, HARQ can be configured as synchronous/asynchronous with adaptive/non-adaptive modulation and coding schemes for Chase combining or incremental redundancy operation. Adaptive H-ARQ in which the parameters of the retransmission (e.g. power, MCS) are changed according to channel conditions reported by the MS may be considered.

The HARQ model and type shall be specified with chosen parameters, such as maximum number of retransmissions, incremental redundancy, chase combining, etc. HARQ overhead (associated control) should be accounted for in the system simulations on both the uplink and downlink

6.1. ACK/NACK Channel

The positive acknowledgement (ACK) and negative acknowledgement (NACK) channel is used to indicate whether or not a packet transmission was successfully received. An ACK/NACK indication is sent after each HARQ packet transmission.

Modeling of HARQ requires waiting for ACK/NACK feedback after each transmission prior to proceeding to the next HARQ transmission. The feedback delay should include the processing time which includes, decoding of the traffic packet, CRC check, and preparation of ACK and NAK transmissions. The amount of delay is determined by the system proposal.

Misinterpretation, missed detection, or false detection of the ACK/NACK message results in transmission (frame or encoder packet) error or duplicate transmission. Proponents for system each system proposal should justify the system performance in the presence of feedback error of the ACK/NACK channel.

7. Scheduling

Editor: Robert Novak, rnovak@nortel.com

Sources	Document Reference
Sassan Ahmadi et al.	C80216m-07_069.doc
Mark Cudak et al.	C80216m-07_061.pdf
Dan Gal et al.	C80216m-07_063.doc
Robert Novak et al.	C80216m-07_074r1.pdf

Wookbong Lee et al.	C80216m-07_075r1.doc
Liu Ying et al.	C80216m-07_064r1.doc
Arvind Raghavan et al.	C80216m-07_100.doc

The scheduler allocates system resources for different packet transmissions according to a set of scheduling metrics, which can be different for different traffic types. The same scheduling algorithm shall be used for all simulation runs. Various scheduling approaches will have performance and overhead impacts and will need to be aligned. System performance evaluation and comparison require that fairness be preserved or at least known in order to promote comparisons. The owner(s) of any proposal are also to specify the scheduling algorithm, along with assumptions on feedback. The scheduling will be done with consideration of reported metric where reported metric may include CQI and other information. . The scheduler shall calculate the available resources after accounting for all control channel overhead and protocol overhead.

Frequency selective scheduling can be applied by channel band selection for MSs. For this mode of scheduling with a contiguous permutation of subcarriers (as the Band Adaptive Modulation and Coding (AMC) mode in IEEE 802.16 systems), the sub-channels may experience different attenuation. A Channel Quality Indicator (CQI) is utilized to provide channel-state information from the user terminals to the base station scheduler.

7.1. DL scheduler

For the baseline simulation, a generic proportionally fair scheduler shall be used for full-buffer traffic model. The generic proportionally fair scheduler is defined in Appendix F.

In the general deployment case, the MAC scheduler should be capable of handling traffic mix on different QoS service classes that are enabled by the air interface. The proponent may present additional results with a more sophisticated scheduler other than proportionally fair scheduler and shall specify the scheduler algorithm in detail.

In its most generic form, a MAC scheduler may calculate a metric per flow at time t $M_i(t)$ that is a function of one or more attributes specific to the flow, and serve the flows in descending order of the metric values, where $M_i(t) = f(QoS_i(t), CQI_i(t), Delay_i(t), Throughput_i(t)...)$. There are several options for constructing the metric function, and each may serve a useful purpose depending on the design objectives.

7.2. UL scheduler

The UL scheduler is very similar to DL Scheduler. The UL scheduler maintains the request-grant status of various uplink service flows. Bandwidth requests arriving from various uplink service flows at the BS will be granted in a similar fashion as the downlink traffic.

8. Handover

Editor: Robert Novak, rnovak@nortel.com

Sources	Document Reference
Sassan Ahmadi et al.	C80216m-07_069.doc
Mark Cudak et al.	C80216m-07_061.pdf
Dan Gal et al.	C80216m-07_063.doc
Robert Novak et al.	C80216m-07_074r1.pdf
Wookbong Lee et al.	C80216m-07_075r1.doc
Liu Ying et al.	C80216m-07_064r1.doc
Rob Nikides et al.	C80216m-07_099r4.doc
Hyunjeong Hannah Lee et al.	C802.16m-07_103.doc

The system simulation defined elsewhere in the document deals with throughput, spectral efficiency, and latency. User experience in a mobile broadband wireless system is also influenced by the performance of handover. This section focuses on the methods to study the performance of handover which affects the end-users experience. Proponents of system proposals specifically relating to handover should provide performance evaluations according to this section.

For parameters such as cell size, DL&UL transmit powers, number of users in a cell, traffic models, and channel models; the simulation follows the simulation methodology defined elsewhere in the document. Only intra-radio access technology handover is considered; inter-radio access technology handover is not considered.

The handover procedure consists of cell reselection via scanning, handover decision and initiation, and network entry including synchronization and ranging with a target BS.

Latency is a key metric to evaluate and compare various handover schemes as it has direct impact on application performance perceived by a user. Total handover latency is decomposed into several latency elements. Further, data loss rate and unsuccessful handover rate are important metrics.

8.1. Handover Evaluation Procedure

TBD.

8.2. System simulation with Mobility

Two possible simulation models for mobility related performance are given in this section. The first is a reduced complexity model that considers the mobility of a single

MS along one of three trajectories with all other users at fixed locations, and a second simulation model that considers all mobiles in the system moving along random trajectories.

8.2.1. Single Mobile MS Model

For simplicity, one mobile MS and multiple fixed MSs can be modeled as a baseline for the mobility simulations. The mobility related performance metrics shall be computed only for this mobile terminal. [The mobile speed is fixed in every simulation drop and aligned with mobility mix associated with the specified channel models].

The trajectory of the mobile MSs can be chosen from the trajectories given in following section.

8.2.1.1. Trajectories

The movement of the single MS is constrained to one of the trajectories defined in this section. More detailed and realistic mobility models may be considered.

8.2.1.1.1. Trajectory 1

In this trajectory, the MS moves from Cell 1 to Cell 2 along the arrow shown in Figure 12. The trajectory starts from the center of Cell 1 to the center of Cell 2 while passing through the midpoint of the sector boundaries as shown in Figure 12. The purpose of this trajectory is to evaluate handover performance in a scenario where the signal strength from the serving sector continuously decreases whereas the signal strength from the target sector continuously increases.

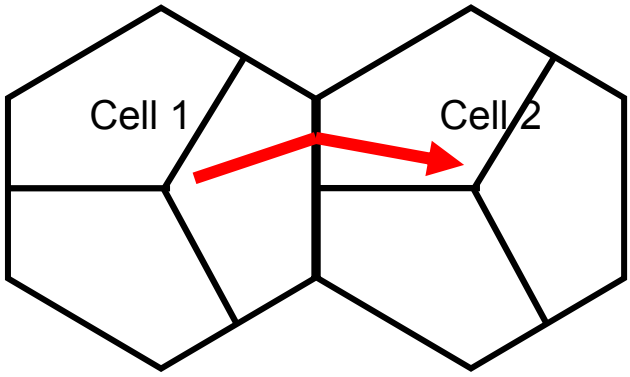

Figure 12: Trajectory 1

8.2.1.1.2. Trajectory 2

In this trajectory, the MS moves from Cell 1 to Cell 2 along the arrow shown in

Figure 13. The MS moves along the sector boundary between Cell 1 and Cell 2 until the midpoint of the cell boundary between Cell 1 and Cell 2. The purpose of this trajectory is to evaluate handover performance when the MS moves along the boundary of two adjacent sectors.

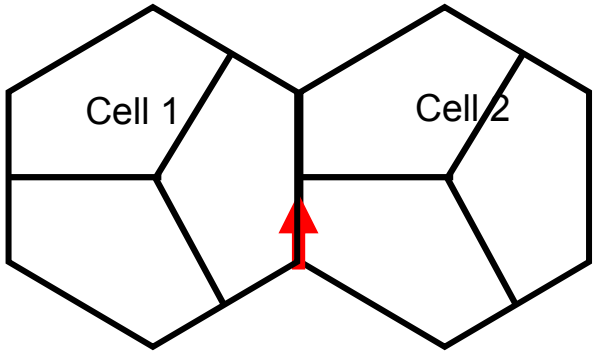

Figure 13: Trajectory 2

8.2.1.1.3. Trajectory 3

In this trajectory, the MS moves from Cell 1 to Cell 2 along the arrow shown in Figure 14. The MS starts from the center of Cell 2, moves along the boundary of two adjacent sectors of Cell 2 and towards the center of the Cell 1. The purpose of this trajectory is to evaluate a handover performance in the scenario where the MS traverses multiple sector boundaries.

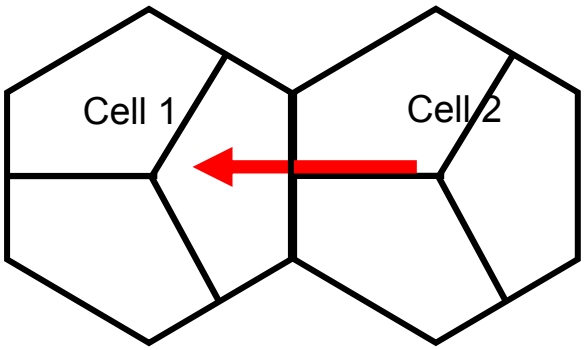

Figure 14: Trajectory 3

8.2.2. Multiple Mobile MS Model

In this model, multiple mobile MSs are uniformly placed over the simulation environment and given a random trajectory and speed. The parameters selected remain in effect until a drop is completed.

8.2.2.1. Trajectories

Each MS is assigned an angle of trajectory at the beginning of a call. The assigned angle is picked from a uniform distribution across the range of 0-359 degrees in one degree increments. The angle of zero degrees points directly North in the simulation environment. Movement of the MS is established by selecting a random speed for the users according to profiles in section 4.3.1 such that the population of MS users meets the desired percentages. The MS remains at the selected random speed and direction for the duration of the simulation drop. When a MS crosses a wrap around boundary point within the simulation space, the MS will wrap around to the associated segment identified within Appendix G, continuing to keep the same speed and trajectory. Figure 15 depicts an example of the movement process for a 19-cell system.

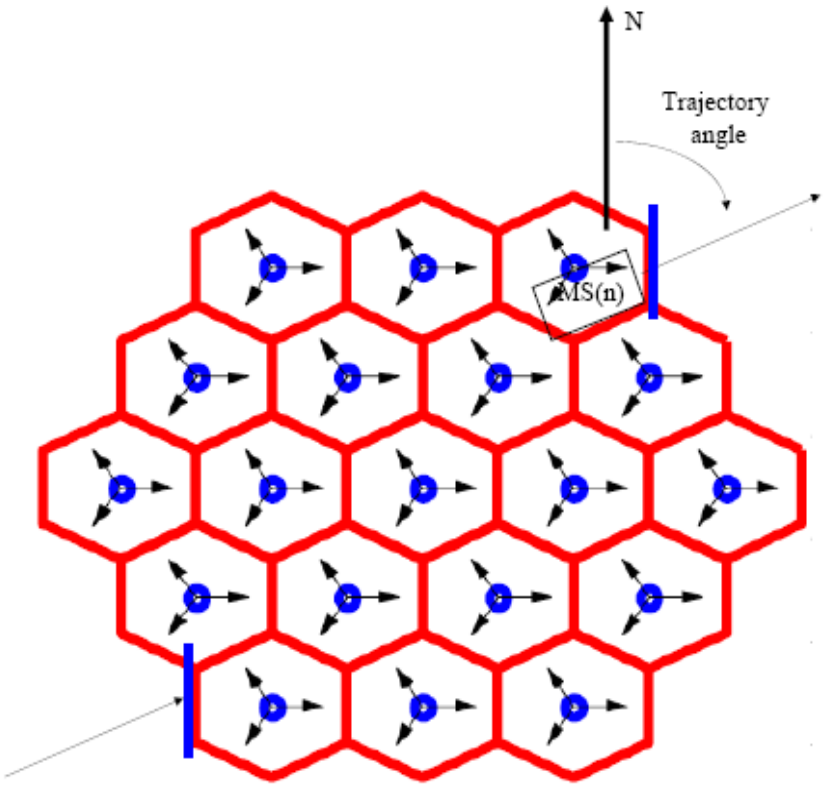

Figure 15: 19 cell abbreviated example of MS movement in a wrap around environment. Blue lines denote paired wrap around boundary segments.

8.3. Cell Topology

The simulation scenarios consider system level simulation parameters, channel models, interference modeling, and cellular layouts defined elsewhere in the evaluation methodology. [The time between handovers shall not be allowed to be less than a specified value. The minimum time between consecutive handovers is TBD.]

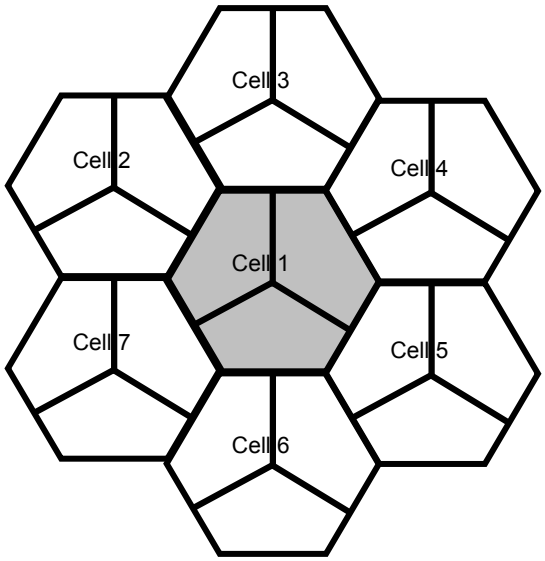

Figure 16: Seven Cell Topology

As a reduced complexity option for evaluating handover, a 7 cell topology may be evaluated. The 7 cell (first tier) network topology is shown in Figure 16.

The 7 cell topology can be used to evaluate the scenarios in which more than one potential target BSs are involved in the handover procedure. For the 7 cell topology, statistics will be collected only when mobile MSs had handover from or to the center cell (i.e. Cell 1 in Figure 16)

8.4. Handover Performance Metrics

The following parameters should be collected in order to evaluate the performance of different handover schemes. These statistics defined in this section should be collected in relation to the occurrence of handovers. A CDF of each metric may be generated to evaluate a probability that the corresponding metric exceeds a certain value.

For a simulation run, we assume:

- Total number of successful handovers occurred during the simulation time = $N_{HO\_success}$
- Total number of failed handover during the simulation time = N_{HO_fail}
- Total number of handover attempts during the simulation time = $N_{attempt}$, where $N_{attempt} = N_{HO\_success} + N_{HO\_fail}$

8.4.1. Radio Layer Latency

This value measures the delay between the time instance T1,i that an MS transmits a serving BS its commitment to HO (for a hard handover (HHO), this is the time that the MS disconnects from the serving BS) and the time instance T2,i that the MS achieves successfully achieves PHY layer synchronization at the target BS (i.e., frequency and DL timing synchronization) due to handover occurrence i. The exact thresholds for

successful PHY synchronization are for further study. For this metric, the following will be measured.

- Average Radio Layer Latency = $\frac{\sum_{i=1}^{N_{HO\_success}} (T_{2,i} - T_{1,i})}{N_{HO\_success}}$
- Maximum Radio Layer Latency = $\underset{1 \le i \le N_{HO\_success}}{Max}$ [*Radio Layer Latency of handover occurrence i*]

]

8.4.2. Network Entry Time

This value represents the delay between an MS's radio layer synchronization at $T_{2,i}$, and its completion of a Layer 2 network entry procedure at $T_{3,i}$ at the target BS due to handover occurrence i. This consists of ranging, UL resource request processes (contention or non-contention based), negotiation of capabilities, and registration. The transmission error rate of MAC messages associated with Network entry can be modeled dynamically or with a fixed value (e.g., 1%).

- Average Network Entry Time = $\frac{\sum_{i=1}^{N_{HO\_success}} (T_{3,i} - T_{2,i})}{N_{HO\_success}}$
- Maximum Network Entry Time = $\underset{1 \le i \le N_{HO\_success}}{Max}$ [*Network Entry Time of handover occurence i*]

8.4.3. Connection Setup Time

This value represents the delay between the completion of Layer 2 network entry procedure at the target BS at $T_{3,i}$ and the reception of first data packet from the target BS at $T_{4,i}$ due to handover occurrence i.. This consists of DL packet coordination and a path switching time. A path switching time, as a simulation input parameter, may vary depending on network architecture.

- Average Connection Setup Time = $\frac{\sum_{i=1}^{N_{HO\_success}} (T_{4,i} - T_{3,i})}{N_{HO\_success}}$
- Maximum Connection Setup Time = $\underset{1 \le i \le N_{HO\_success}}{Max}$ [*Connection Setup Time of handover occurence i*]

8.4.4. Service Disruption Time

This value represents time duration that a user can not receive any service from any BS. It is defined as the sum of Radio Layer Latency, Network Entry Time and Connection Setup Time due to handover occurrence i.

8.4.5. Data Loss

This value represents the number of lost bits during the handover processes. $D_{RX,i}$ and $D_{TX,i}$ denotes the number of received bits by the MS and the number of total bits transmitted by the serving and the target BSs during the MS performs handover occurrence *i,* respectively. Traffic profiles used for the simulation experiments to compare different handover schemes need to be identical.

$$\text{Data Loss} = \frac{\sum_{i=1}^{N_{HO\_success}} D_{TX,i} - D_{RX,i}}{N_{HO\_success}}$$

8.4.6. Handover Failure Rate

This value represents the ratio of failed handover to total handover attempts. Handover failure occurs if handover is executed while the reception conditions are inadequate on either the DL or the UL such that the mobile would have to go to a network entry state.

$$\text{Handover Failure Rate} = \frac{N_{HO\_fail}}{N_{attempt}}$$

9. Power Management (informative)

Sources	Document Reference
Sassan Ahmadi et al.	C80216m-07_069.doc

[The objective of power management is to minimize the power consumption by the subscriber stations (MSs) and thus, to maximize the battery life of the mobile devices. This is achieved through the use of idle mode and sleep mode operations. While idle mode is designed to use the periods of inactivity between calls to save battery power, the sleep mode is designed to use the periods of inactivity in between packets bursts of a call to reduce power consumption by the mobile devices. Thus, the simulation methodology should model sleep and idle mode operations. In addition, it should provide means to investigate the performance of idle and sleep mode operations. For example, some of the critical performance parameters to evaluate the power management in such networks are as follows: the duty cycle of idle and sleep mode operations; time it takes for an MS to return to active from idle and sleep mode. The details of these parameters are FFS.]

10. Traffic Models

Editor: Jeongho Park, jeongho.jh.park@samsung.com

Sources	Document Reference
Alcatel-Dan Gal et al.	IEEE C802.16m-07_063
Sassan Ahmadi et al.	IEEE C802.16m-07_072
Robert Novak et al.	IEEE C802.16m-07_074r1
Wookbong Lee et al.	IEEE C802.16m-07_075

Bong Ho Kim	IEEE C802.16m-07_105 IEEE C802.16m-07_106

This section describes traffic models in detail. A major objective of system simulations is to provide the operator a view of the maximum number of active users that can be supported for a given service under a specified configuration at a given coverage level. The traffic generated by a service should be accurately modeled in order to evaluate the performance of a system. This may be a time consuming exercise. Traffic modeling can be simplified, as explained below, by not modeling the user arrival process and assuming full queue traffic which is considered as the baseline. These two assumptions are further discussed proceeding paragraphs. Modeling non-full-queue traffic is also discussed in the next subsections.

Modeling of user arrival process: Typically all the users are not active at a given time and even the active users might not register for the same service. In order to avoid different user registration and demand models, the objective of the proposed simulation is restricted to evaluate the performance with the users who are maintaining a session with transmission activity. These can be used to determine the number of such registered users that can be supported. This document does not address the arrival process of such registered users, i.e. it does not address the statistics of subscribers that register and become active.

Full Queue model: In the full queue user traffic model, all the users in the system always have data to send or receive. In other words, there is always a constant amount of data that needs to be transferred, in contrast to bursts of data that follow an arrival process. This model allows the assessment of the spectral efficiency of the system independent of actual user traffic distribution type.

In the following sections, we will concentrate on traffic generation only for the non-full queue case. In addition, the interaction of the generated traffic with the higher layer protocol stack such as TCP is not included here. However, we will provide references to document which provide the detailed TCP transport layer implementation and its interaction with the various traffic models.

10.1. Web Browsing (HTTP) Traffic Model

HTTP traffic characteristics are governed by the structure of the web pages on the World Wide Web (WWW), and the nature of human interaction. The nature of human interaction with the WWW causes the HTTP traffic to have a bursty profile, where the HTTP traffic is characterized by ON/OFF periods as shown in Figure 17.

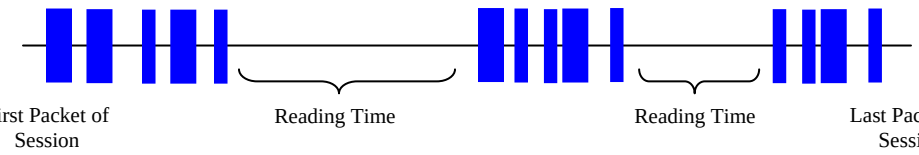

Figure 17: HTTP Traffic Pattern

The ON periods represent the sequence of packets in which the web page is being transferred from source to destination; while the OFF periods represent the time the user spends reading the webpage before transitioning to another page. This time is also known as Reading Time [43][44].

The amount of information passed from the source to destination during the ON period is governed by the web page structure. A webpage is usually composed of a main object and several embedded objects. The size of the main object, in addition to the number and size of the embedded objects define the amount of traffic passed from source to destination.

In summary, the HTTP traffic model is defined by the following parameters:

SM: Size of main object in page

Nd: Number of embedded objects in a page

SE: Size of an embedded object in page

Dpc: Reading time

Tp: Parsing time for the main page

In addition to the model parameters, HTTP traffic behavior is also dependent on the HTTP version used. Currently HTTP 1.0 and HTTP 1.1 are widely used by servers and browsers [45]-[48]. In HTTP 1.0, also known as burst mode transfer, a distinct TCP connection is used for each object in the page, thereby facilitating simultaneous transfer of objects. The maximum number of simultaneous TCP connections is configurable, with most browsers using a maximum of 4 simultaneous TCP connections. In HTTP/1.1, also known as persistent mode transfer, all objects are transferred serially over a single persistent TCP connection. Recent measurement and analysis for web page structures can be found in [58]. These measurements have been performed using a recent online-traffic analysis provided by market research firm ComScore Media Metrix, which examined the number of visitors among the 50 top Web sites on January 2007 [59]. The paper [58], includes web page sizes and compositions of the 50 top web sites after analyzing 25000 measurements, and each web site has been visited 500 times for three weeks from April 7 to April 23 in 2007. Web site visits are about one minute apart, and visits to the same website are about an hour apart.

Table 19 provides the model parameters for HTTP traffic for downlink and uplink connections based on the measurements in [59] and the model in [48]-[49].

Component	Distribution	Parameters		PDF
		Downlink	Uplink	
Main object size (SM)	Truncated Lognormal	Mean = 52390bytes SD= 49591bytes	Mean = 9055 bytes SD = 13265 bytes	$f_x = \frac{1}{\sqrt{2\pi}\sigma x}\exp\left[\frac{-(\ln x-\mu)^2}{2\sigma^2}\right], x \geq 0$

		Min = 1290bytes Max = 0.25Mbytes $\sigma = 0.8, \mu = 10.55$	Min = 100 bytes Max = 100 Kbytes $\sigma = 1.37, \mu = 8.35$	if x>max or x<min, discard and generate a new value for x
Embedded object size (SE)	Truncated Lognormal	Mean = 8551bytes SD = 59232bytes Min = 5bytes Max = 6Mbytes $\sigma = 1.97, \mu = 7.1$	Mean = 5958 bytes SD = 11376 bytes Min = 50 bytes Max = 100 Kbytes $\sigma = 1.69, \mu = 7.53$	$f_x = \frac{1}{\sqrt{2\pi}\sigma x}\exp\left[\frac{-(\ln x-\mu)^2}{2\sigma^2}\right], x \geq 0$ if x>max or x<min, discard and generate a new value for x
Number of embedded objects per page (Nd)	Truncated Pareto	Mean = 51.1 Max. = 165 $\alpha = 1.1, k = 2, m = 55$	Mean = 4.229 Max. = 53 $\alpha = 1.1, k = 2, m = 55$	$f_x = \frac{\alpha k^{\alpha}}{x^{\alpha+1}}, k \leq x < m$ $f_x = \left(\frac{k}{m}\right)^{\alpha}, x = m$ Subtract k from the generated random value to obtain Nd if x>max, discard and regenerate a new value for x
Reading time (Dpc)	Exponential	Mean = 30 sec	Mean = 30 sec λ = 0.033	$f_x = \lambda_e^{-\lambda x}, x \geq 0$
Parsing time (Tp)	Exponential	Mean = 0.13 sec	Mean = 0.13 sec $\lambda = 7.69$	$f_x = \lambda_e^{-\lambda x}, x \geq 0$

Table 19: HTTP Traffic Parameters

To request an HTTP session, the client sends an HTTP request packet, which has a constant size of 350 bytes.

From the statistics presented in the literature, a 50%-50% distribution of HTTP versions between HTTP 1.0 and HTTP 1.1 has been found to closely approximate web browsing traffic in the internet [49].

Further studies also showed that the maximum transmit unit (MTU) sizes most common to in the internet are 576 bytes and 1500 bytes (including the TCP header) with a distribution of 24% and 76% respectively. Thus, the web traffic generation process can be described as in
Figure **18**.

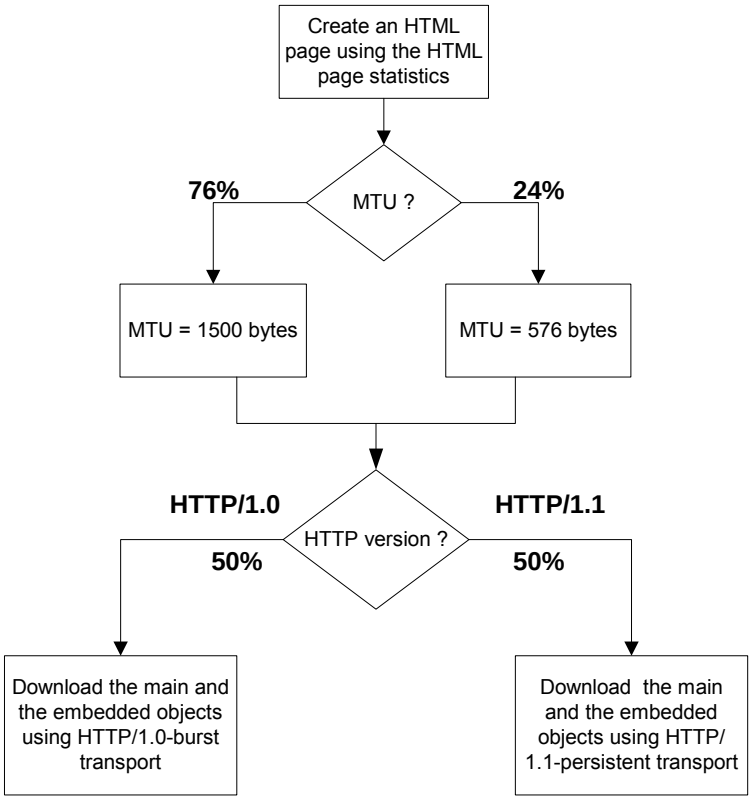

Figure 18: HTTP Traffic Profiles

A user is defined in outage for HTTP service if the average throughput is less the minimum average throughput requirement of [128] kbps. The system outage requirement is such that no more than [3]% of users can be in outage. The air link PER for HTTP traffic should be not be greater than [1]% after the HARQ process.

10.1.1. HTTP and TCP interactions for DL HTTP traffic

Two versions of the HTTP protocol, HTTP/1.0 and HTTP/1.1, are widely used by servers and browsers. Users shall specify 50% HTTP/1.0 and 50% HTTP/1.1 for HTTP traffic. For people who have to model the actual interaction between HTTP traffic and the underling TCP connection, refer to 4.1.3.2, 4.2.4.3 of [50] for details.

10.1.2. HTTP and TCP interactions for UL HTTP traffic

HTTP/1.1 is used for UL HTTP traffic. For details regarding the modeling of the interaction between HTTP traffic and the underling TCP connection, refer to 4.2.4.1, 4.2.4.2 of [50].

10.2. File Transfer Protocol Model

File transfer traffic is characterized by a session consisting of a sequence of file transfers, separated reading times. Reading time is defined as the time between end of transfer of the first file and the transfer request for the next file. The packet call size is

therefore equivalent to the file size and the packet call inter-arrival time is the reading time. A typical FTP session is shown in Figure 19.

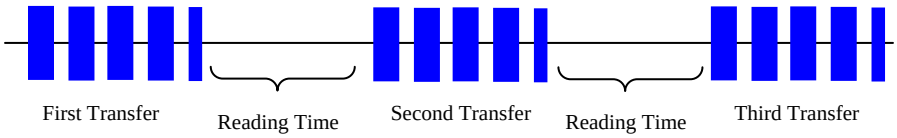

Figure 19: FTP Traffic Patterns

Table 20 provides the model parameters for FTP traffic that includes file downloads as well as uploads [51]-[52].In the case of file uploads, the arrival of new users is Poisson distributed and each user transfers a single file before leaving the network.

The FTP traffic generation process is described in Figure **20**. Based on the results on packet size distribution, 76% of the files are transferred using and MTU of 1500 bytes and 24% of the files are transferred using an MTU of 576 bytes. Note that these two packet sizes also include a 40 byte IP packet header and this header overhead for the appropriate number of packets must be added to the file sizes calculated from the probabilistic distributions in Table **20**. For each file transfer a new TCP connection is used whose initial congestion window size is 1 segment.

A user is defined in outage for FTP service if the average throughput is less the minimum average throughput requirement of [128] kbps. The system outage requirement is such that no more than [3]% of users can be in outage. The air link PER for FTP traffic should be not be greater than [1]% after the HARQ process.

Component	Distribution	Parameters		PDF
		DL	UL	
File size (S)	Truncated Lognormal	Mean = 2Mbytes SD = 0.722 Mbytes Max = 5 Mbytes $\sigma = 0.35$ $\mu = 14.45$	Min = 0.5 Kbytes Max = 500 Kbytes Mean = 19.5 Kbytes SD = 46.7 Kbytes $\sigma = 2.0899$ $\mu = 0.9385$	$f_x = \frac{1}{\sqrt{2\pi}\sigma x}\exp\left[\frac{-(\ln x-\mu)^2}{2\sigma^2}\right], x \geq 0$ if x>max or x<min, discard and generate a new value for x
Reading time (D_{pc})	Exponential	Mean = 180 sec. $\lambda = 0.006$	N/A	Download: $f_x = \lambda e^{-\lambda x}, x \geq 0$ Upload: N/A

Table 20: FTP Traffic Parameters

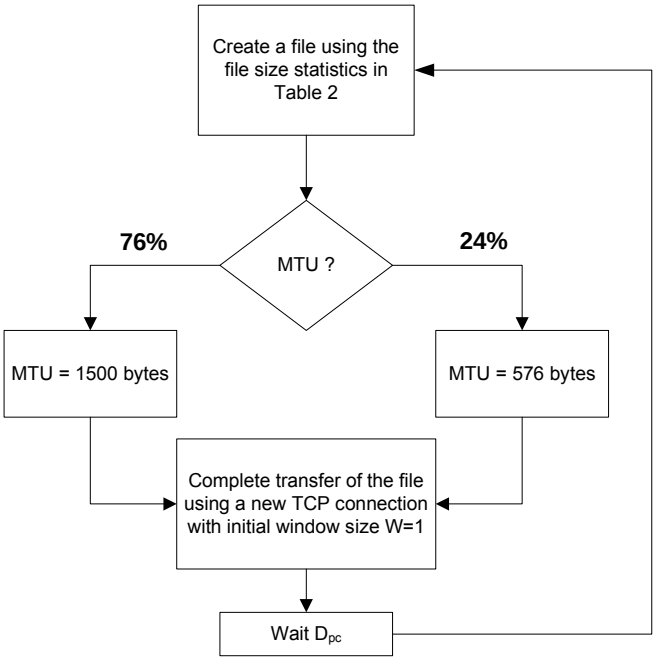

Figure 20: FTP Traffic Profiles

10.2.1. TCP Modeling

The widespread use of TCP as a transport protocol in the internet requires an accurate model of TCP behavior to better characterize traffic flow. The major behaviors that need to be accounted for in the TCP model are the session establishment and release and TCP slow start.

10.2.1.1. TCP Session Establishment and Release

TCP uses a 3-way handshake to establish and release a TCP session. The sequences of establishing and releasing a TCP session on the downlink and the uplink are shown in Figure 21 and Figure 22 respectively.

A TCP session is established by the transmitter sending a 40 byte SYNC control segment to the remote server. In response, the server sends a 40 byte SYNC/ACK control segment. The final acknowledgement is sent by the transmitter by setting the ACK flag in the first TCP segment of the TCP session, which is then started in slow start mode [62].

The TCP session is released by the transmitter setting the FIN flag in the last TCP segment. In response, the receiver sends by a FIN/ACK control segment. The session is concluded by the transmitter sending a final ACK message [62].

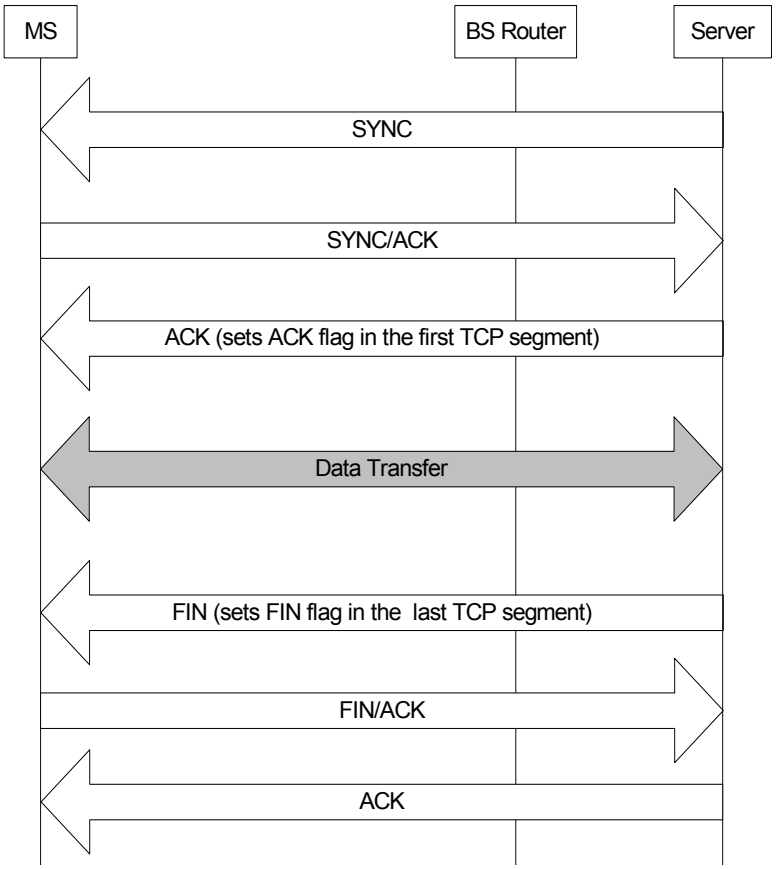

Figure 21: TCP Connection establishment and release on the downlink

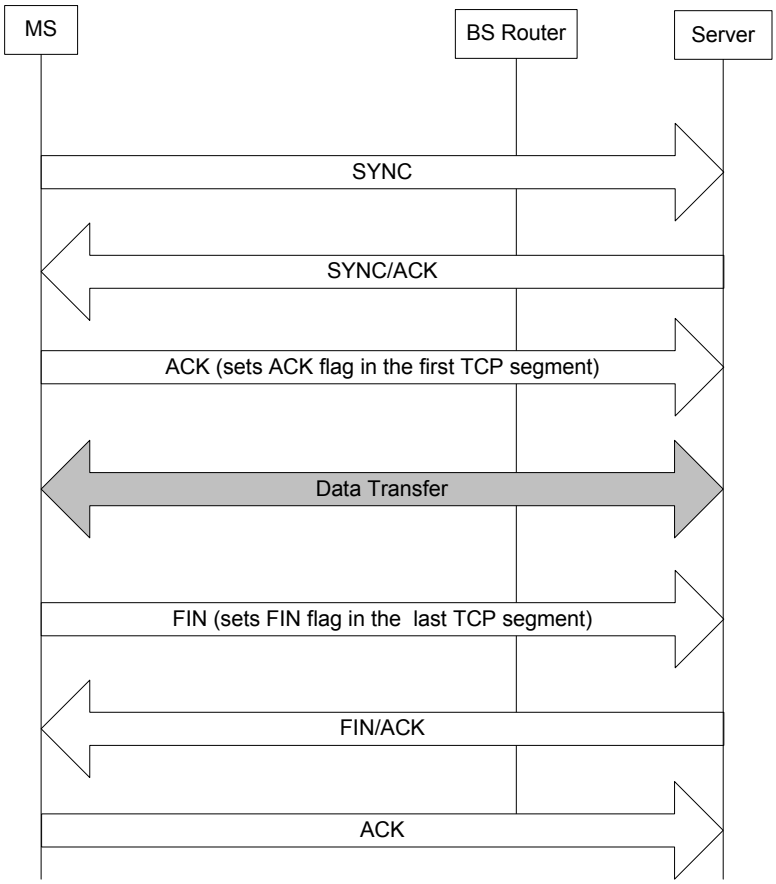

Figure 22: TCP Connection establishment and release on the uplink

10.2.1.2. TCP Slow Start Modeling

TCP slow start is part of the congestion control mechanism implemented in the TCP protocol. Congestion control is implemented using a window flow control mechanism, which tracks the maximum amount of unacknowledged or outstanding data at the transmitter.

The amount of outstanding data that can be sent without receiving an acknowledgement (ACK) is determined by the minimum of the congestion window size and the receiver window size. After the TCP session is established, the transfer of data starts in slow-start mode with an initial congestion window size of 1 segment. The congestion window size is subsequently increased by one with each arriving ACK for a successfully received packet. This increase occurs regardless of whether the packet is correctly received or not, and regardless of whether the packet is out of order or not. This results in an exponential growth of the congestion window.

Figure 23 explains the packet transmission sequence in a TCP session. The round trip time (RTT) for the TCP slow start model consists of:

RTT = $\tau 1 + \tau 2$

where:

$\tau 1$: Time taken by an ACK packet to travel from the client (server) to Base Station + Time taken by an ACK packet to travel from Base Station to server (client) + Time taken by TCP segment to travel from server (client) to Base Station.

$\tau 2$: Time taken by ACK segment to travel from Base Station to Client (server).

$\tau 1$ is assumed to be a random variable of exponential distribution, while $\tau 2$ is determined by the airlink throughput . This model only accounts for the slow start process, while congestion control and avoidance have not been modeled. Additionally, the receiver window size is assumed to be large, and thus not a limiting factor.

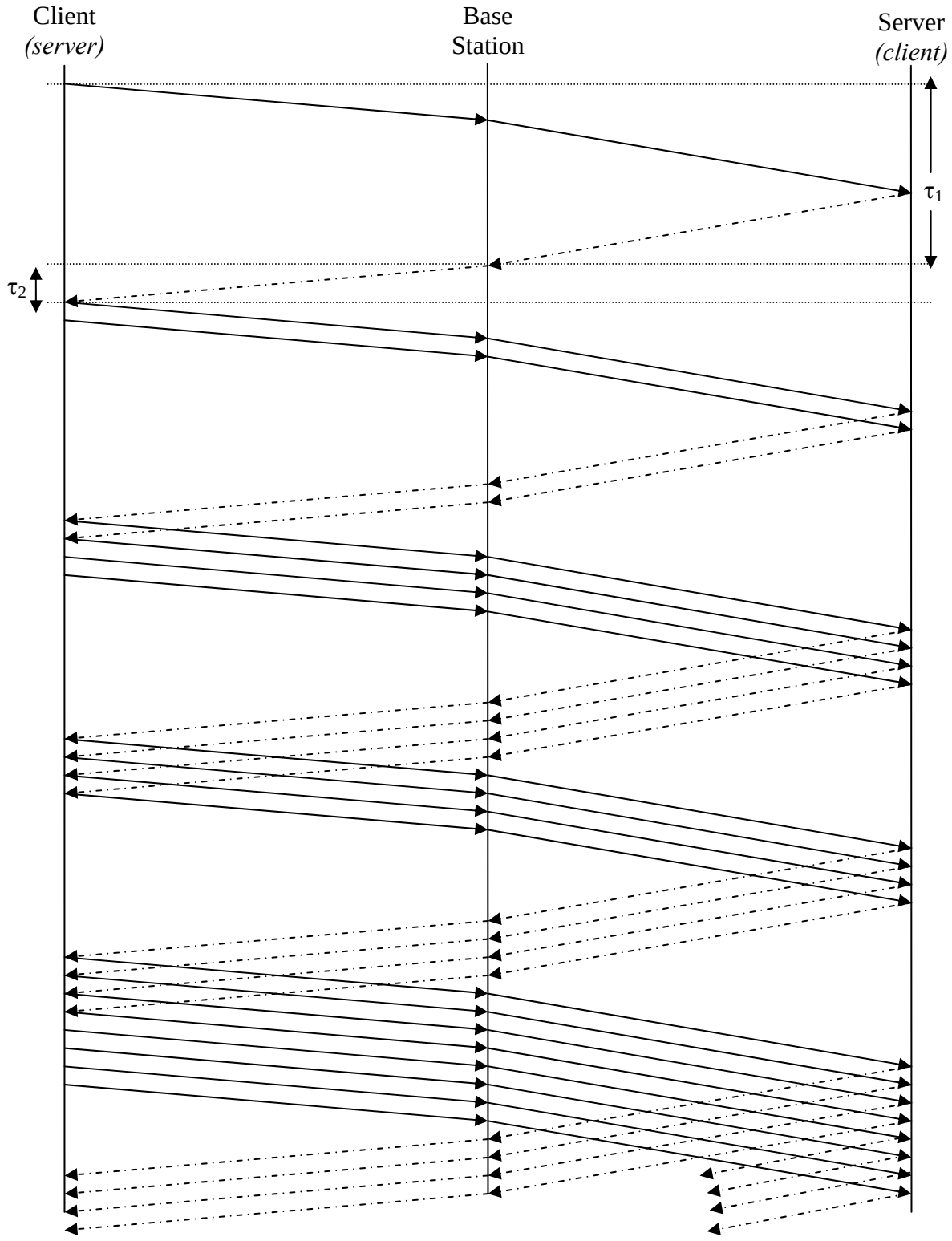

Figure 23: TCP Slow Start Process

10.3. Speech Source Model (VoIP)

Source Document Authors	Document Reference
Dan Gal, et al.	IEEE C802.16m-07/063
Sassan Ahmadi, et al.	IEEE C802.16m-07/072
Robert Novak, et al.	IEEE C802.16m-07/074r1
Wookbong Lee, et al.	IEEE C802.16m-07/075
Xin Chang, et al.	IEEE C802.16m-07/067

VoIP refers to real-time delivery of packet voice across networks using the Internet protocols. A VoIP session is defined as the entire user call time and VoIP session occurs during the whole simulation period.

There are a variety of encoding schemes for voice (i.e., G.711, G.722, G.722.1, G.723.1, G.728, G.729, and AMR) that result in different bandwidth requirements. Including the protocol overhead, it is very common for a VoIP call to require between 5 Kbps and 64 Kbps of bi-directional bandwidth.

10.3.1. Basic Voice Model

A typical phone conversation is marked by periods of active talking / talk spurts (ON periods) interleaved by silence / listening periods (or OFF periods) as shown in Figure 24.

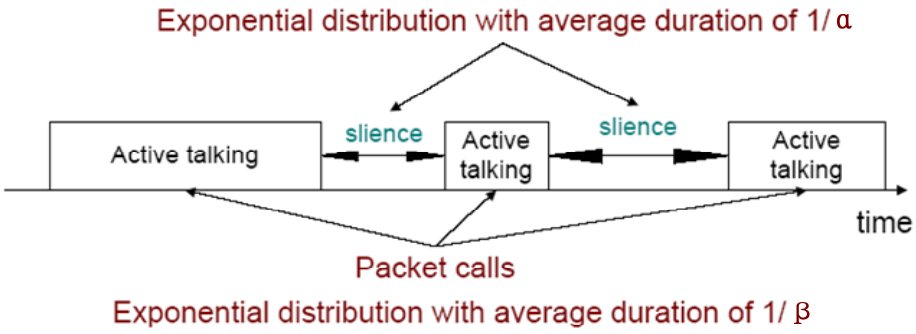

Figure 24: Typical phone conversation profile

Consider the simple 2-state voice activity Markov model shown in Figure 25 [54].

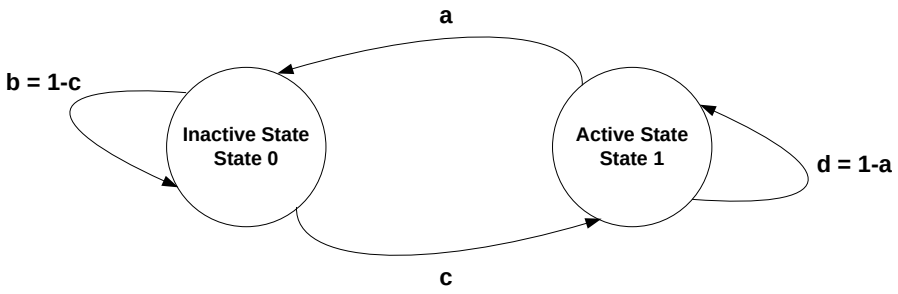

Figure 25: 2-state voice activity Markov model

In the model, the conditional probability of transitioning from state 1 (the active speech state) to state 0 (the inactive or silent state) while in state 1 is equal to a, while the conditional probability of transitioning from state 0 to state 1 while in state 0 is c. The model is assumed to be updated at the speech encoder frame rate R=1/T, where T is the encoder frame duration (typically, 20 ms). During the active state, packets of fixed sizes are generated at a regular interval. The size of packet and the rate at which the packets are sent depends on the corresponding voice codecs and compression schemes.

Table 21 provides information on some common vocoders.

Vocoder	EVRC	AMR	GSM 6.10	G.711	G.723.1		G.729A
Source Bit rate [Kb/s]	0.8/2/4/8.55	4.75-12.2	13	64	5.3	6.3	8
Frame duration [ms]	20	20	20	10	30	30	10
Information bits per frame	16/40/80/171	95-244	260	640	159	189	80

Table 21: Information on various vocoders

Among the various vocoders in
Table 21, a simplified AMR (adaptive multi-rate) audio data compression can be used to simplify the VoIP modeling process. AMR is optimized for speech coding and was adopted as the standard speech codec by 3GPP and widely used in GSM. The original AMR uses link adaptation to select from one of eight different bit rates based on link conditions. If the radio condition is bad, source coding is reduced (less bits to represent speech) and channel coding (stronger FEC) is increased. This improves the quality and robustness of the network condition while sacrificing some voice clarity. In our simplified version, we have chosen to disable the link adaptation and use the full rate of 12.2 kbps in the active state. This will give us the worst case scenario.

Description	AMR without Header Compression IPv4/IPv6	AMR with Header Compression IPv4/IPv6	G.729 without Header Compression IPv4/IPv6	G.729 with Header Compression IPv4/IPv6
Voice Payload (20 ms aggregation interval)	7 bytes for inactive 33 bytes for active	7 bytes for inactive 33 bytes for active	0 bytes for inactive 20 bytes for active	0 bytes for inactive 20 bytes for active
Protocol Headers (including UDP checksum)	40 bytes / 60 bytes	3 bytes / 5 bytes	40 bytes / 60 bytes	3 bytes / 5 bytes
RTP	12 bytes		12 bytes	
UDP	8 bytes		8 bytes	
IPv4 / IPv6	20 bytes / 40 bytes		20 bytes / 40 bytes	
802.16e Generic MAC Header	6 bytes	6 bytes	6 bytes	6 bytes
802.16e CRC for HARQ	2 bytes	2 bytes	2 bytes	2 bytes
Total VoIP packet size	55 bytes/ 75 bytes for inactive 81 bytes / 101 bytes for active	18 bytes/ 20 bytes for inactive 44 bytes / 46 bytes for active	0 bytes for inactive 68 bytes/ 88 bytes for active	0 bytes for inactive 31 bytes/ 33 bytes for active

Table 22: VoIP packet size calculation for simplified AMR and G. 729

Table 22 shows the VoIP packet size calculation for simplified AMR operation with or without header compression when using IPv4 or IPv6. In the table, the MAC CRC of 4B for ARQ is not included and only CRC for HARQ is included because the ARQ process can be assumed to be disabled for VoIP services.

To calculate the total packet size, MAC headers and CRC need to be accounted for (example: there are 6 bytes of MAC header and 2 bytes of HARQ CRC in IEEE 802.16e reference system). For example, without header compression, AMR payload of 33 bytes are generated in the active state for every 20 ms and AMR payload of 7 bytes are generated in the inactive state for every 160 ms, resulting in a packet size of 81 (55) bytes for the active (inactive) mode, respectively, assuming IPv4 and uncompressed headers.

The voice capacity shall be determined using the AMR 12.2. kbps codec with activity factor of 40%. VoIP capacity is defined as maximum number of user that can be serviced such that the percentage of users in outage is less than 3%. A VoIP user is in

outage if more than 3% of the VoIP packets are not delivered successfully to the user within the delay bound of 80 ms. [Dropped packets are assigned infinite delay.]

10.3.2. VoIP Traffic Model Parameters

During each call (each session), a VoIP user will be in the Active or Inactive state. The duration of each state is exponentially distributed. In the Active/Inactive state, packets of fixed sizes will be generated at a fixed interval. Hence, both the datagram size and datagram arrival intervals are fixed within a packet call.

Table 23 shows parameters associated with the VoIP traffic model.

Component	Distribution	Parameters	PDF
Active state duration	Exponential	Mean = 1 second	$f_x = \lambda e^{-\lambda x}$, $x \geq 0$ $\lambda = 1/Mean$
Inactive state duration	Exponential	Mean = 1.5 second.	$f_x = \lambda e^{-\lambda x}$, $x \geq 0$ $\lambda = 1/Mean$
Probability of transition from active to inactive state	N/A	0.02	N/A
Probability of transition from inactive to active state	N/A	0.0133	N/A

Table 23: VoIP traffic model parameters specification

Link adaptation of AMR codec is disabled in order to evaluate performance under worst case, and to simplify the voice traffic model.

During the inactive state, we have chosen to generate comfort noise with smaller packet sizes at regular intervals instead of no packet transmission. This simplified model does not include a feature called hangover, which generates additional seven frames at the same rate as speech to ensure the correct estimation of comfort noise parameters at the receiver side even if there is a silence period at the end of a talk spurt (ON state), and after the hangover period, a SID_FIRST frame is sent. The voice traffic model specifies only one rate during the ON state (talk spurt) of the AMR codec (12.2 kbps) and another rate for the comfort noise (SID_UPDATE) during the OFF state of the AMR codec. SID_UPDATE frames are generated every 8th frame during the silence period.

Table 24 provides the relevant parameters of the VoIP traffic that shall be assumed in the simulations. The details of the corresponding traffic model are described below:

Parameter	Characterization
Codec	RTP AMR 12.2, Source rate 12.2 kbps
Encoder frame length	20 ms
Voice activity factor (VAF)	40%
Payload	Active: 33 bytes (Octet alignment mode)Inactive: 7 bytes SID packet every 160 ms during silence
Protocol Overhead with compressed header	RTP/UDP/IP (including UDP check sum): 3 bytes 802.16 Generic MAC Header: 6 bytes CRC for HARQ: 2 bytes
Total voice payload on air interface	Active: 44 bytes Inactive: 18 bytes

Table 24: Detailed description of the VoIP traffic model for IPv4

10.4. Near Real Time Video Streaming

This section describes a model for streaming video traffic for DL direction. Figure 26 describes the steady state of video streaming traffic from the network as observed by the base station. Call setup latency and overhead is not considered in this model.

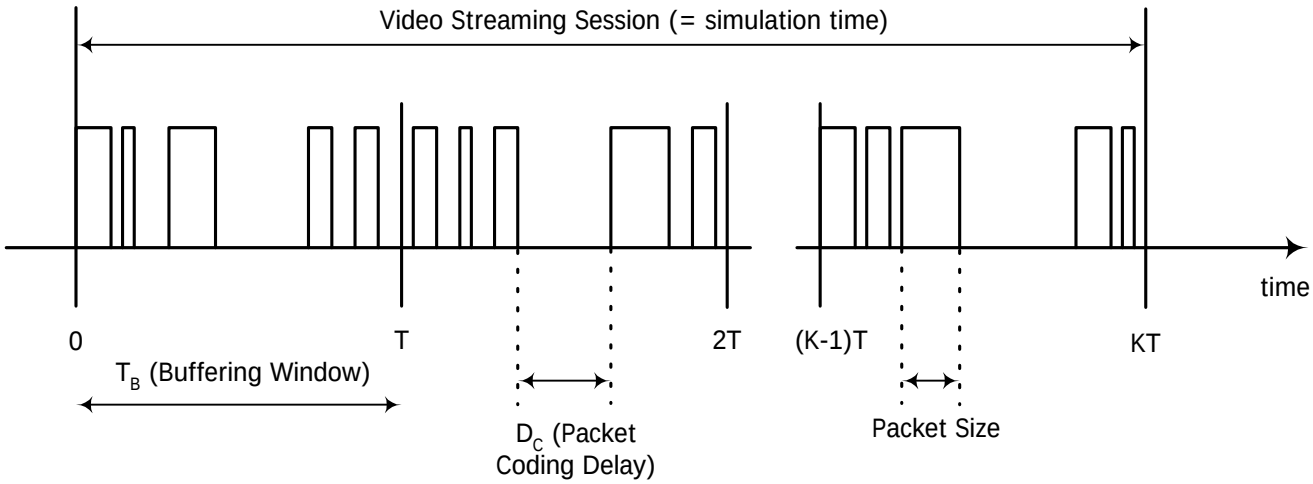

Figure 26: Video Streaming Traffic Model

[Editor's note: We need to choose text from one of the two following bracketed proposals]

[

Each frame of video data arrives at a regular interval T. Each frame can be treated as a packet call and there will be zero OFF duration within a session. Within each frame (packet call), packets (or datagrams) arrive randomly and the packet sizes are random as well.

To counter the jittering effect caused by the random packet arrival rate within a frame at the MS, the MS uses a de-jitter buffer window to guarantee a continuous display of video streaming data. The de-jitter buffer window for video streaming service is 5 seconds. At the beginning of the simulation, the MS de-jitter buffer shall be full with video data. During simulation, data is leaked out of this buffer at the source video data rate and filled as DL traffic reaches the MS from the BS. As a performance criterion, the simulation shall record the length of time, if any, during which the de-jitter buffer runs dry.

The packet sizes and packet inter-arrival rate can be found in when using a source rate of 64 kbps.

Information types	Inter-arrival time between the beginning of each frame	Number of packets (slices) in a frame	Information types	Packet (slice) size
Distribution	Deterministic (Based on 10 fps)	Deterministic	Truncated Pareto (Mean=50 bytes, Max=125 bytes)	Truncated Pareto (Mean=6 ms, Max=12.5 ms)
Distribution parameters	100 ms	8	K=20 bytes α = 1.2	K = 2.5 ms α = 1.2

Figure 27: Near Real Time Video Streaming Traffic Model Parameters

]

[

A typical business-quality video streaming run can deliver TV-quality video at 25 to 30 frames per second. There are several types of video compression technologies such as H.264, H.263 and H.261. H.264 is the next-generation video compression technology in the MPEG-4 standard, and it surpasses H.261 and H.263 in terms of video quality, effective compression and resilience to transmission losses, giving it the potential to halve the required bandwidth for digital video services over the internet or wireless networks. H.264 is likely to be used in applications such as Video Streaming, Video Conferencing Mobile devices, Tele-Medicine etc and current 3G mobiles use a derivate of MPEG-4.

MPEG compressed videos are composed of pictures (frames) that are separated into three different types: I, B, and P. I frames are intraframes that encode the current picture, while B and P frames interpolate from previous and future frames. MPEG-4

video traffic modeling with separate set of I, B, and P frames form a final model that looks very similar to the original [63][64].

An important feature of common MPEG encoders is the manner in which frame types are generated. Although not required by the standards, typical encoders use a fixed Group-of-Pictures (GOP) pattern when compressing a video sequence (the GOP pattern specifies the number and temporal order of P and B frames between two successive I frames). Quite often the fixed GOP pattern is “regular” in the sense that the number of B frames between two reference frames (I or P) is fixed. Such a GOP pattern can be characterized by two parameters: the I-to-I frame distance (N), and the I-to-P frame distance (M) (if no P frames are used, then M = N).

10.4.1. I Frame

It is observed that I frames exhibit different VBR dynamics at different time scales. At a time scale of the order of few seconds, the bit rate fluctuates in small amounts about some mean level, which itself varies drastically at a larger time scale. The fluctuations in the mean levels at the larger time scale are often attributed to “scene” changes. Incorporating a “scenic” component in a traffic model gives the VBR dynamics a physical interpretation and often leads to better performance predictions, and the scene length distribution can be appropriately fitted by an exponential (or geometric) distribution [65]. Summary statistics of the computed scene lengths for the trace of Silence of the Lambs are given in Table 25.

Trace	Number of Computed Scenes	Scene Length Statistic (in consecutive I frames)			
		Mean	Std. dev	Max	Min
Silence of the Lambs	327	10.2 (5.1 sec)	18.1	209	1

Table 25: Summary statistics of the computed scene lengths (Source: [63])

10.4.2. P and B Frames

The sizes of P and B frames can be appropriately characterized by lognormal distributions with parameters (μ_P, σ_P) and (μ_B, σ_B) respectively. Although the empirical frame sizes for P frames (also B frames) are correlated, these correlations are negligible compared to the correlations between different types of frames [63].

10.4.3. Video Streaming Traffic Model

For the video streaming traffic model, a high quality movie trace, Silence of the Lambs [66], is used and two different resolutions for the display have been considered; 176x144 for a small device and 320x240 for a large device. The required bandwidth for the uncompressed video stream with 176x144 pixels and 8 bit color depth is about 7.6

Mbps and with 320x240 pixels and 8 bit color depth is about 23 Mbps. To minimize the effects of the non-uniform delay between the packets, a buffer is used at the user device to guarantee a continuous and smooth display of the video streaming data. For video streaming services, this buffer is set to 5 seconds. The algorithm generating synthetic MPEG stream is described in [63].

Service	Movie Streaming	
Video Codec	MPEG-4	
Protocols	TCP	
Scene Length (sec)	Lognormal(μ=5.1 sec , σ =9.05 sec)	
Direction	Uni-direction (DL only)	
Buffering (sec)	5 sec	
Frames/sec	25 frames/sec	
GOP	N=12, M=3	
Display size	176x144	320x240
Color depth (bit)	8	8
Subsampling method	4:1:1	4:1:1
Mean BW for uncompressed stream	7.6 Mbps	23 Mbps
Compression ratio	13.22	13.22
Mean BW for compressed stream	0.58 Mbps	1.74 Mbps
I frame size (byte)	Lognormal(μ=5640 , σ=2632)	Lognormal(μ=17068 ,σ=7965)
P frame size (byte)	Lognormal(μ=3037 , σ=2315)	Lognormal(μ=9190 ,σ=7005)
B frame size (byte)	Lognormal(μ=2260 ,σ=1759)	Lognormal(μ=6839 ,σ=5323)

Table 26: Video Streaming Traffic Model

<references [63] to[66] correspond to this section only>

]

10.4.4. Performance Criteria for Near Real Time Video

Video playout buffers introduce a delay between the receipt of frames and the frame playout. This absorbs variations in the data arrival pattern and permits a continuous playout of the frames. The actual design of these playout buffers involves a number of factors (including reset policies when the buffer runs dry) and is specific to the mobile.

To avoid modeling such implementation details, we focus on what the BS scheduler must do to generally accommodate this continuous playout. Therefore, the scheduler should transmit an entire video frame within 5 second of receipt of the entire frame (i.e., receipt of the last octet of the last slice of the frame). If a frame exceeds the 5-second requirement, the scheduler discards the remainder of the frame that has not yet been transmitted. The size and arrival statistics for the video frames are defined in Table 26.

The performance requirement is that the fraction of video frames that are not completely transmitted within 5 seconds of their arrival at the scheduler shall be less than 2% for each user. The system outage requirement is such that no more than 3% of users can be in outage.

10.5. Video Telephony

[

Based on the compression efficiency and market acceptance as described in the section 10.4, MPEG 4 has been selected for the video codec. The estimated values for the parameters to model a video stream, vary from one trace to another. For parameters associated with the statistical distributions, the estimates depend strongly on the dimensions of the captured frames. For the video telephony traffic model, medium quality of an Office Cam trace is used and the trace library is available at [60]. For the traffic model two different qualities for the video have been considered; high and medium quality. For the medium quality encoding the quantization parameters for all three frame types were fixed at 10, and for the high quality encoding the quantization parameters for all three frame types were fixed at 4 [61].

The scene length for the video telephony is assumed to be the entire application session since the background or the main subject may not be so dynamic.

Service	Video Telephony	
Video Codec	MPEG-4	
Protocols	UDP	
Scene Length (sec)	Session duration	
Direction	Bi-direction (DL and UL)	
Frames/sec	25 frames/sec	
GOP	N=12, M=3	
Display size	176x144	
Color depth (bit)	8	
Video Quality	Medium	High
Mean BW	110 kbps	400 kbps
I frame size (byte)	Weibull($\alpha =$ 5.15, $\beta =$ 863), shift=3949, μ= 4742 , σ=178 , min=4034, max=5184	Weibull($\alpha =$ 5.2, $\beta =$ 1439), shift=7775, μ= 9098 , σ=296, min=7926, max=9911
P frame size (byte)	Lognormal(μ=259 , σ=134), min=100, max=1663	Lognormal(μ=1615 , σ=342), min=1085, max=4357
B frame size (byte)	Lognormal(μ=147 ,σ=74), min=35, max=882	Lognormal(μ=1233 ,σ=236), min=112, max=3076

Table 27: Video Telephony Traffic Model

]

10.6. Gaming traffic model

Gaming is a rapidly growing application embedded into communication devices, and thus wireless gaming needs to be considered.

Packet size in gaming traffic is modeled by the Largest Extreme Value distribution. The starting time of a network gaming mobile is uniformly distributed between 0 and 40 m to simulate the random timing relationship between client traffic packet arrival and reverse link frame boundary.

For both the downlink and uplink, a packet is dropped if any part of the packet (including HARQ operation) has not started within 160 ms of the time the packet entered the transmitting station's buffer. Packet delay of a dropped or erased packet is counted as 180 ms. It is widely accepted that 50 ms lag is considered excellent quality while 100 ms lag is considered good quality. Ping times above 150 ms are often reported to be intolerable but many players claim to have no problems with ping times around 200 ms

[55] . A user is in outage in wireless gaming if the per user average packet delay is greater than 60 ms, where average delay includes the delay of packets delivered and the delay of packets dropped or erased between MS and BS. Some studies show that many players who experience high ping times of over 225 ms do not quit and continue to play. The impact of packet loss is rarely discussed as it is experienced as lag as well. However, a high ping time without packet loss is preferable to a small ping time with packet loss of around 10%. As per general system outage requirements, no more than [3]% of users can be in outage. Table 28 provides the traffic model parameters for 'Counter Strike' internet gaming.

Component	Distribution		Parameters		PDF
	DL	UL	DL	UL	
Initial packet arrival	Uniform	Uniform	a=0, b=40 ms	a=0, b=40 ms	$f(x)=\frac{1}{b-a} \quad a \le x \le b$
Packet arrival time	Extreme	Deterministic	a=55 ms, b=6 ms	40 ms	$f(x)=\frac{1}{b}e^{\frac{x-a}{b}}e^{-e^{\frac{x-a}{b}}},b>0$ $[X=\lfloor a-b\ln(-\ln Y)\rfloor]$ $Y \in U(0,1)$
Packet size	Extreme	Extreme	a=120 bytes, b=36 bytes	a=80 bytes, b = 5.7 bytes	$f(x)=\frac{1}{b}e^{\frac{x-a}{b}}e^{-e^{\frac{x-a}{b}}},b>0$ $[X=\lfloor a-b\ln(-\ln Y)\rfloor+2,]$ $[X=\lfloor a-b\ln(-\ln Y)\rfloor]$ $Y \in U(0,1)$

Table 28: Counter Strike Internet Gaming Traffic Model

Note:

[1. To account for UDP header, 2 was added to the size of the packet size]

2. Because packet size has to be integer number of bytes, the largest integer less than or equal to X is used as the actual packet size.

10.7. Traffic Mixes

A mobile broadband wireless system is expected to support a mix of simultaneous traffic types. There can be different types of usage scenarios (multi-service v. single-type), different types of devices (notebook PCs, vs. PDAs or smart phones), different usage levels (intense vs. light) and different delay/latency requirements (real-time vs. best-effort).

The previous sections are primarily concerned with the traffic models for each of the potential traffic types. As discussed in the previous section, these models are based on

statistical analysis of measured traffic that yielded some invariant patterns that are not very dependant on the specific system. It is more difficult to describe a similar invariant mix of traffic types since these tend to depend more heavily on the type of system and the actual deployment mix of user device types.

In the context of system performance evaluation, using traffic models, the specific traffic-mix should emphasize different aspects of the system performance, e.g. sustained throughput for file downloads v. faster response times for interactive applications.

Table 29 contains traffic mixes that should be used in system evaluations
For system level simulation purposes, “traffic mix” refers to the percentage of users in the system generating a particular type of traffic. In this context, each user is assumed to be generating only one type of traffic, recognizing that in an actual network a single user’s terminal could support multiple applications and generate several types of traffic simultaneously.

	VoIP	FTP	HTTP	NRTV	Gaming	VT	Full Buffer	Mandatory/ Optional
Voice only	100% [#users = Nv*]	0%	0%	0%	0%	0%	0%	Mandatory
FTP only	0%	100%	0%	0%	0%	0%	0%	[TBD]
Full Buffer only	0%	0%	0%	0%	0%	0%	100%	Mandatory
HTTP only	0%	0%	100%	0%	0%	0%	0%	[TBD]
NRTV only	0%	0%	0%	100%	0%	0%	0%	[TBD]
Gaming only	0%	0%	0%	0%	100%	0%	0%	[TBD]
VT only	0%	0%	0%	0%	0%	100%	0%	[TBD]
Traffic Mix	30%	10%	20%	20%	20%	0%	0%	Mandatory
VoIP & Full Buffer Mix 1	0.5 of Nv	0%	0%	0%	0%	0%	16 Users	Mandatory
VoIP & Full Buffer Mix 2	0.75 of Nv	0%	0%	0%	0%	0%	16 Users	[TBD]

Table 29: Traffic Mixes

* Nv is the system voice capacity that satisfy outage criteria at system and user level

11. Simulation Procedure and Flow

Editor: Roshni Srinivasan, roshni.m.srinivasan@intel.com

Sources	Document Reference
Sassan Ahmadi et al.	C80216m-07_069.doc

Dan Gal et al.	C80216m-07_063.doc
Robert Novak et al.	C80216m-07_074r1.pdf
Wookbong Lee et al.	C80216m-07_075r1.doc

The nineteen-cell network topology with wrap-around (as shown in the Appendix G) shall be used as the baseline network topology for all system-level simulations. The system simulation flow required in this evaluation methodology is illustrated in Figure 28.

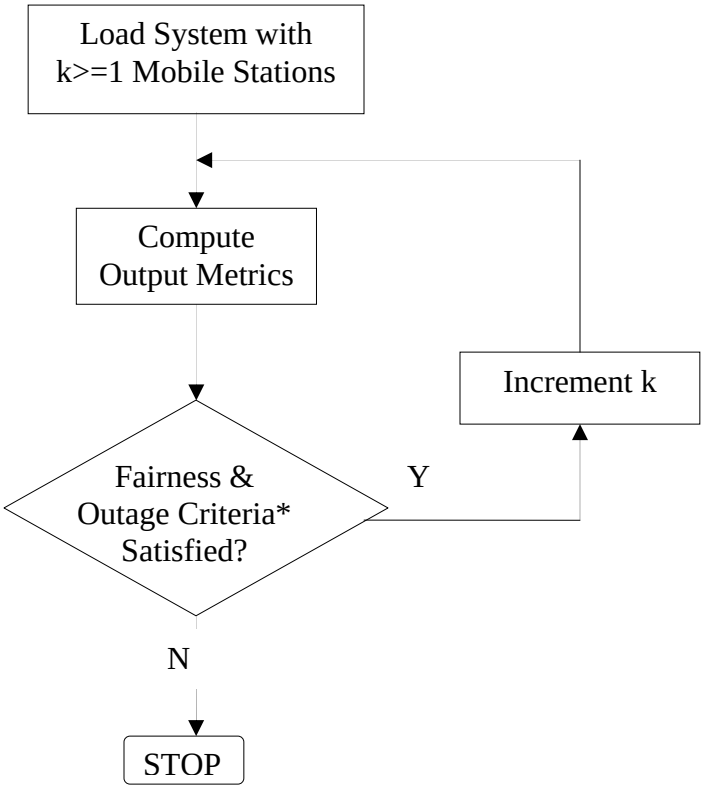

Figure 28: Simulation Procedure

** As defined in Sections 10 and 13*

1. The system is modeled as a network of 7 clusters. Each cluster has 19 hexagonal cells with six cells of the first tier and twelve cells of the second tier surround the central cell of each cluster. Each cell has three sectors. Frequency reuse is modeled by planning frequency allocations in different sectors in the network
2. MSs are dropped uniformly throughout the system. Each mobile corresponds to an active user session that runs for the duration of the drop.
3. Mobiles are randomly assigned channel models. Depending on the simulation, these may be in support of a desired channel model mix, or separate statistical realizations of a single type of channel model.

4. MSs are dropped according to the specified traffic mix. The simulation runs are done with an increment of MSs per sector until a termination condition is met as shown in Figure 28.
5. For sectors belonging to the center cluster, sector assignment to an MS is based on the received power at an MS from all potential serving sectors. The sector with best path to MS, taking into account slow fading characteristics (path loss, shadowing, and antenna gains) is chosen as the serving sector.
6. Mobile stations are randomly dropped over the 57 sectors such that each sector has the required numbers of users. Although users may be in regions supporting handover each user is assigned to only one sector for counting purposes. All sectors of the system shall continue accepting users until the desired fixed number of probe and load users per sector is achieved everywhere. Users dropped within 35 meters of a sector antenna shall be redropped. MS locations for six wrapping clusters are the same as the center cluster.
7. Fading signal and fading interference are computed from each mobile station into each sector and from each sector to each mobile for each simulation interval.
8. Packets are not blocked when they arrive into the system (i.e. queue depths are infinite).Users with a required traffic class shall be modeled according to the traffic models defined in this document. Start times for each traffic type for each user should be randomized as specified in the traffic model being simulated.
9. Packets are scheduled with a packet scheduler using the required fairness metric. Channel quality feedback delay, PDU errors and ARQ are modeled and packets are retransmitted as necessary. The ARQ process is modeled by explicitly rescheduling a packet as part of the current packet call after a specified ARQ feedback delay period.
10. .Simulation time is chosen to ensure convergence in user performance metrics. For a given drop the simulation is run for this duration, and then the process is repeated again, with the MSs dropped at new random locations. A sufficient number of drops are simulated to ensure convergence in the system performance metrics.
11. Performance statistics are collected for MSs in all cells according to the output matrix requirements.
12. All 57 sectors in the system shall be dynamically simulated

12. Interference Modeling

The reuse of frequencies through planned allocation enables a cellular system to increase capacity with a limited number of channels. Frequency reuse 1 and 3 shall be modeled in 802.16m network.

The interference model due to frequency reuse should accurately represent the time-frequency selective nature of OFDMA interference. The channel matrices for the desired and interfering signals shall be generated according to the models in Section 3 which account for the pathloss, shadowing, and fast fading variations. For simplicity, the same fast fading channel model but a different realization shall be assigned to each link between an MS & all BSs in the network. This time-frequency modeling can create

significant computational complexity in network simulations. To reduce complexity, pathloss and shadowing are calculated to determine the I_{strong} strongest interferers. The strongest interferers are modeled as spatially correlated processes and their channel matrices include pathloss, shadowing and fast fading components. The remaining I_{weak} interferers are modeled as spatially white spectrally flat processes. It has been shown that this modeling procedure results in negligible loss in performance. The procedure is summarized below:

1. Determine the pathloss and shadowing from all interfering sectors to MS.
2. Rank the interfering sectors in order of received power (based on pathloss and shadowing).
3. Model the strongest (I_{strong}) interfering sectors as spatially correlated processes whose covariances are determined by their channel matrices. These channel matrices account for the pathloss, shadowing, and fast fading variations. A typical value for I_{strong} is 14.
4. Model the remaining sectors as spatially white Gaussian noise processes whose variances are based on a spectrally flat Rayleigh fading process. The power of the Rayleigh fading process includes the effects of pathloss and shadowing. The fading processes for all links between MS and BS are assumed to be independent, and the Doppler rate is determined by the speed of the mobile. At any instant in time, the total received interference power is the summation of the receive power from of all weak interferers. Hence, the interference power is varying in time during a simulation drop.

Multi-cell scheduling shall be modeled to capture dynamics of interference in the 19-cell network as described in Appendix G. The scheduler at each base station sector allocates OFDMA resources to MS associated with that BS. The resource allocation can be independent or jointly optimized across the network to mitigate interference. If BS co-operation is implemented, the information exchanged across the network, and scheduling algorithm shall be disclosed. The MIMO mode (beamforming, spatial multiplexing, transmit diversity, etc) between the BS and an MS shall be determined by scheduler at each BS.

13. Performance Metrics

Section Editor: Roshni Srinivasan, roshni.m.srinivasan@intel.com

Sources	Document Reference
Sassan Ahmadi et al.	C80216m-07_069.doc
Dan Gal et al.	C80216m-07_063.doc
Robert Novak et al.	C80216m-07_074r1.pdf
Wookbong Lee et al.	C80216m-07_075r1.doc
Liu Ying et al.	C80216m-07_064r1.doc
Mark Cudak et al.	C80216m-07_061.pdf

13.1. Introduction

Performance metrics may be classified as single-user performance metrics or multi-user performance metrics.

13.1.1. Single User Performance Metrics

13.1.1.1. Link Budget and Coverage Range (Noise Limited) – single-cell consideration

Link budget evaluation is a well known method for initial system planning that needs to be carried out for BS to MS links. Although a link budget can be calculated separately for each link, it is the combination of the links that determines the performance of the system as a whole. The parameters to be used needs to be agreed upon after obtaining consensus. Using the margins in the link budget, the expected signal to noise ratio can be evaluated at given distances. Using these results, the noise limited range can be evaluated for the system. The link budget template is TBD.

Coverage range is defined as the maximum radial distance to meet a certain percentage of area coverage (x%) with a signal to noise ratio above a certain threshold (target SINR) over y% of time, assuming no interference signals are present. It is proposed that x be 99 and y be 95.

13.1.1.2. C/I Coverage – interference limited multi-cell consideration

The C/I coverage is defined as the percentage area of a cell where the average C/I experienced by a stationary user is larger than a certain threshold (target C/I).

13.1.1.3. Data Rate Coverage – interference limited multi-cell consideration

The percentage area for which a user is able to transmit/receive successfully at a specified mean data rate using single-user analysis mentioned above. No delay requirement is considered here.

13.1.2. Multi-User Performance Metrics

Although a user may be covered for a certain percentage area (e.g. 99%) for a given service, when multiple users are in a sector/BS, the resources (time, frequency, power) are to be shared among the users. It can be expected that a user's average data rate may be reduced by a factor of N when there are N active users (assuming resources are equally shared and no multi-user diversity gain), compared to a single user rate.

For example, assume that there is a system, where a shared channel with a peak rate of 2 Mbps can serve 99% of the area. If a user wants to obtain a video streaming service at 2 Mbps, that particular user will be able to obtain the service, but no other user will be able to get any service during the whole video session (which may extend for more than an hour). Therefore, in this example although 99% area is covered for the video service, this service is not a viable service for the operator and performance of coverage need to be coupled with the capacity in order to reflect viable service solutions. Coverage performance assessment must be coupled with capacity (# of MSs), to obtain a viable metric.

The users having poor channel quality may be provided more resources so that they would get equal service from the cellular operator. This could adversely impact the total cell throughput. Thus, there is a trade-off between coverage and capacity. Any measure of capacity should be provided with the associated coverage. .

Since an operator should be able to provide the service to multiple users at the same time, an increase in the area coverage itself does not give an operator the ability to offer a given service

Therefore, the number of users that can be supported under a given coverage captures actual coverage performance for a given service from a viability point of view.

The suggested performance metric is the number of admissible users (capacity), parameterized by the service (R_{min}), and the coverage (allowable outage probability).

13.2. Definitions of Performance Metrics

It is assumed that simulation statistics are collected from sectors belonging to the test cell(s) of the 19-cell deployment scenario. Collected statistics will be traffic-type (thus traffic mix) dependent.

In this section, we provide a definition for various metrics collected in simulation runs. For a simulation run, we assume:

1] Simulation time per drop = T_{sim}
2] Number of simulation drops = D
3] Total number of users in sector(s) of interest= N_{sub}
4] Number of packet calls for user u = p_u
5] Number of packets in i^{th} packet call = $q_{i,u}$

13.2.1. Throughput Performance Metrics

For evaluating downlink (uplink) throughput, only packets on the downlink(uplink) are considered in the calculations. Downlink and uplink throughputs are denoted by upper case DL and UL respectively (example: R_u^{DL}, R_u^{UL}). The current metrics are given per a single simulation drop.

The throughput metrics below shall be measured at the following layers:

- PHY Layer
- MAC Layer
- TCP Layer

The throughput for those layers is measured at the points identified in Figure 29 where the throughput refers to the payload throughput without the overhead.

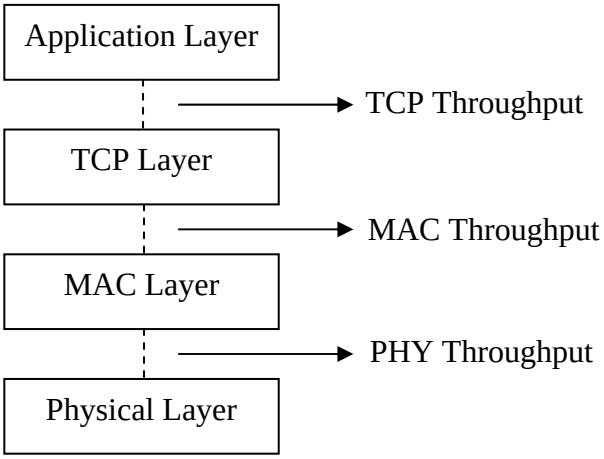

Figure 29: Throughput Metrics Measurement Points

13.2.1.1. Average Data Throughput for User u

The data throughput of a user is defined as the ratio of the number of information bits that the user successfully received divided by the amount of the total simulation time. If user *u* has $p_u^{DL(UL)}$ downlink (uplink) packet calls, with $q_{i,u}^{DL(UL)}$ packets for the i[th] downlink (uplink) packet call, and $b_{j,i,u}$ bits for the *j*[th] packet; then the average user throughput for user *u is*

$$R^{DL(UL)} = \frac{\sum_{i=1}^{p_u^{DL(UL)}} \sum_{j=1}^{q_{i,u}^{DL(UL)}} b_{j,i,u}}{T_{Sim}}$$

13.2.1.2. Sector Data Throughput

Assuming N_{sub} users in sector(s) of interest, and *u*[th] user where $u \in N_{sub}$ has throughput $R_u^{DL(UL)}$, then sector(s) data throughput is :

$$R_{\text{sec}}^{DL(UL)} = \sum_{u=1}^{N_{sub}} R_u^{DL(UL)}$$

13.2.1.3. Average packet call throughput

Packet call throughput is the total bits per packet call divided by total packet call duration. If user *u* has $p_u^{DL(UL)}$ downlink (uplink) packet calls, with $q_{i,u}^{DL(UL)}$ packets for the i[th] downlink (uplink) packet call, and $b_{j,i,u}$ bits for the *j*[th] packet; then the average packet call throughput is

$$R_u^{pc,DL(UL)} = \frac{1}{p_u^{DL(UL)}} \left(\sum_{i=1}^{p_u^{DL(UL)}} \frac{\sum_{j=1}^{q_{i,u}^{DL(UL)}} b_{j,i,u}}{(T_{i,u}^{end,DL(UL)} - T_{i,u}^{start,DL(UL)})} \right)$$

13.2.1.4. The histogram of users' average packet call throughput

The histogram will display the distribution of the downlink (uplink) average packet call throughput observed at the MS (BS) for the subscribed users.

13.2.1.5. Throughput Outage

Throughput outage ($O_{thpt}(R_{min})$) is defined as the percentage of users with data rate R_u^{DL}, less than a predefined minimum rate R_{min} (TBD).

13.2.1.6. Cell edge user throughput

The cell edge user throughput is defined as the 5th percentile point of the CDF of users' average packet call throughput

13.2.1.7. Geographical Distribution of Average Packet Call Throughput per User (optional)

The plot will show the geographical distribution of the average packet call throughput observed on the downlink (uplink) by the MS (BS). It provides insight into the throughput variation as a function of distance from the BS. This allows for easy comparison between different reuse scenarios, network loading conditions, smart antenna algorithms, etc.

13.2.2. Performance Metrics for Delay Sensitive Applications

For evaluating downlink (uplink) delay, only packets on the downlink (uplink) are considered in the calculations. Downlink and uplink delays are denoted by upper case DL and UL respectively (example: D_u^{DL}, D_u^{UL}) .

13.2.2.1. Packet Delay

Assuming the j^{th} packet of the i^{th} packet call destined for user u arrives at the BS (SS) at time $T_{j,i,u}^{arr,DL(UL)}$ and is delivered to the MS (BS) MAC-SAP at time $T_{j,i,u}^{dep,DL(UL)}$, the packet delay is defined as

$$Delay_{j,i,u}^{DL(UL)} = T_{j,i,u}^{dep,DL(UL)} - T_{j,i,u}^{arr,DL(UL)}$$

Packets that are dropped or erased may or may not be included in the analysis of packet delays depending on the traffic model specifications. For example, in modeling traffic from delay sensitive applications, packets may be dropped if packet transmissions are not completed within a specified delay bound. The impact of such

dropped packets can be captured in the packet loss rate. In addition to the delay corresponding to successfully transmitted packets, delay corresponding to such dropped packets may also be included in the packet delay distribution by assigning a fixed large value to the packet delay for dropped or erased packets. This fixed value of delay for dropped packets depends on the traffic type should be specified in the traffic model. Including a delay value for dropped packets in the distribution permits the outage criterion to be specified simply in terms of a percentile of delay values within a delay bound, without specifying any bounds on the packet error rate.

13.2.2.2. The CDF of packet delay per user

CDF of the packet delay per user provides a basis in which maximum latency, x%-tile, average latency as well as jitter can be derived.

13.2.2.3. X%-tile Packet delay per user

The x%-tile packet delay is simply the packet delay value for which x% of packets have delay below this value.

13.2.2.4. The CDF of X%-tile Packet Delays

The CDF of x%-tiles of packet latencies is used in determining the y%-tile latency of the x%-tile per user packet delays.

13.2.2.5. The Y%-tile of X%-tile Packet Delays

The y%-tile is the latency number in which y% of per user x%-tile packet latencies are below this number. This latency number can be used as a measure of latency performance for delay sensitive traffic. A possible criteria for VoIP, for example, is that the 98th %-tile of the 98%-tile of packet latencies per user is 30ms.

13.2.2.6. User Average Packet Delay

The average packet delay is defined as the average interval between packets originated at the source station (either MS or BS) and received at the destination station (either BS or MS) in a system for a given packet call duration. The average packet delay for user *u*, $D_u^{avg,DL(UL)}$ is given by:

$$D_u^{avg,DL(UL)} = \frac{\sum_{i=1}^{p_u}\sum_{j=1}^{q_{i,u}}\left(T_{j,i,u}^{dep,DL(UL)} - T_{j,i,u}^{arr,DL(UL)}\right)}{\sum_{i=1}^{p_u} q_{i,u}}$$

13.2.2.7. CDF of Users' Average Packet Delay

The CDF will reflect the cumulative distribution of the average packet delay observed by all users.

13.2.2.8. Packet Loss Ratio

The packet loss ratio per user is defined as

$$Packet\ Loss\ Ratio = 1 - \frac{Total\ Number\ of\ Successfully\ \mathrm{Re}ceived\ Packets}{Total\ Number\ of\ Successfully\ Transmitted\ Packets}$$

13.2.3. System Level Metrics for Unicast Transmission

13.2.3.1. System data throughput

The data throughput of a BS is defined as the number of information bits per second that a site can successfully deliver or receive via the air interface using the scheduling algorithms.

13.2.3.2. Spectral Efficiency

Both physical layer spectral efficiency and MAC layer spectral efficiency should be evaluated. Physical layer spectral efficiency should represent the system throughput measured at the interface from the physical layer to the MAC layer, thus including physical layer overhead but excluding MAC and upper layer protocols overhead. MAC layer spectral efficiency should represent the system throughput measured at the interface from the MAC layer to the upper layers, thus including both physical layer and MAC protocols overhead.

The MAC efficiency of the system should be evaluated by dividing the MAC layer spectral efficiency by the physical layer spectral efficiency.

The average cell/sector spectral efficiency is defined as

$$r = \frac{R}{BW_{eff}}$$

Where R is the aggregate cell/sector throughput, BW_{eff} is the effective channel bandwidth i.e., the total spectrum utilized by the system (corresponding to the reuse pattern being simulated). The effective channel bandwidth is defined as

$$BW_{eff} = BW \times TR$$

where BW is the used channel bandwidth, and TR is time ratio of the link. For example, for FDD system TR is 1, and for TDD system with DL:UL=2:1, TR is 2/3 for DL and 1/3 for UL, respectively

13.2.3.3. CDF of SINR

For uplink simulations, this is defined as the cumulative distribution function (CDF) for the signal to interference and noise ratio (SINR) observed by the BS for each MS on the uplink channel. For downlink simulations, this is defined as the CDF for the SINR observed by each MS on the downlink. This metric allows for a comparison between different reuse scenarios, network loading conditions, smart antenna algorithms, resource allocation and power control schemes, etc.

13.2.3.4. Histogram of MCS

The histogram will display the distribution of MCS for all subscribed users.

13.2.3.5. Application Capacity

Application capacity *(C_{app})* is defined as the maximum number of application users that the system can support without exceeding the maximum allowed outage probability.

13.2.3.6. System Outage

System outage is defined as when the number of users experiencing outage exceeds 3% of the total number of users. The user outage criterion is defined based on the application of interest in Section 10.

13.2.4. System Level Metrics for Multicast Broadcast Service

In order to evaluate the performance of multicast broadcast services, two cases should be considered. The first case consists of all 57 sectors transmitting the same MBS service. In the second case, which is used to evaluate the performance at the MBS zone edge, only the centre cell and the first tier of cells are transmitting the same MBS service. The remaining cells are either transmitting unicast data or a different MBS service. Both cases should be evaluated with the performance metrics given in the following subsections.

13.2.4.1. Maximum MBS Data Rate

The maximum MBS data rate is defined as the maximum data rate for 95% coverage with a target packet error rate of 1%.

13.2.4.2. Coverage versus Data Rate Trade-off

The coverage versus data rate trade-off can be evaluated through a plot of the coverage percentage versus the data rate for a target packet error rate of 1%.

13.2.4.3. Impact of Multicast/Broadcast resource size on Unicast Throughput

As the MBS resource size increases, the impact on unicast throughput should be provided. Given the total resource budget, the impact of multicast/broadcast resource size on unicast throughput can be evaluated through a plot of the unicast throughput versus the multicast/broadcast throughput for 95% coverage with a target PER of 1%.

13.3. Fairness Criteria

It may be an objective to have uniform service coverage resulting in a fair service offering for best effort traffic. A measure of fairness under the best effort assumption is important in assessing how well the system solutions perform.

The fairness is evaluated by determining the normalized cumulative distribution function (CDF) of the per user throughput. The CDF is to be tested against a predetermined fairness criterion under several specified traffic conditions. The same scheduling algorithm shall be used for all simulation runs. That is, the scheduling algorithm is not

to be optimized for runs with different traffic mixes. The owner(s) of any proposal are also to specify the scheduling algorithm.

Let $T_{put}[k]$ be the throughput for user k. The normalized throughput with respect to the average user throughput for user k, $\tilde{T}_{put}[k]$ is given by

$$\tilde{T}_{put}[k] = \frac{T_{put}[k]}{\underset{i}{\text{avg}}\, T_{put}[i]}$$

13.3.1. Moderately Fair Solution

The CDF of the normalized throughputs with respect to the average user throughput for all users is determined. This CDF shall lie to the right of the curve given by the three points in Table 30.

Normalized Throughput w.r.t average user throughput	CDF
0.1	0.1
0.2	0.2
0.5	0.5

Table 30: Moderately Fair Criterion CDF

14. Template for Reporting Results

Sources	Document Reference
Sassan Ahmadi et al.	C80216m-07_069.doc
Dan Gal et al.	C80216m-07_063.doc

[The link-level and system-level simulation results shall be reported in the format exemplified in the following tables and graphs. Where applicable, one table and figure per simulation case should be provided. Models and assumptions should be aligned with those listed in this document. Any deviations should be highlighted.

Metric	Peak Rate (Mbps)	C-plane latency (ms)	U-plane delay (ms)	Intra- FA HO delay (ms)	Inter-FA HO delay (ms)
IEEE 802.16e Reference System					
IEEE 802.16m DL					
IEEE 802.16m UL					

Table 31: System Analysis Results

Metric	Average cell throughput and spectrum efficiency (x IEEE 802.16e Reference System)	Average user throughput and spectrum efficiency	Cell-edge user throughput and spectrum efficiency
IEEE 802.16e Reference System			
IEEE 802.16m baseline SU-MIMO			
IEEE 802.16m baseline MU-MIMO			
IEEE 802.16m			
IEEE 802.16m			

Table 32: Downlink full buffer system evaluation

Metric	Average cell throughput and spectral efficiency (x IEEE 802.16e Reference System)	Average user throughput and spectral efficiency	Cell-edge user throughput and spectral efficiency
IEEE 802.16e Reference System			
IEEE 802.16m baseline			
IEEE 802.16m MU-MIMO			
IEEE 802.16m SU-MIMO			
IEEE 802.16m …			

Table 33: Uplink full queue system evaluation results.

Metric	VoIP Capacity
IEEE 802.16m DL	
IEEE 802.16m UL	

Table 34: VoIP Results

]

14.1. Evaluation Report

[The 802.16m evaluation report may be submitted as two separate reports. A summary of the items to be simulated and submitted in each report is defined in Table 35. The items marked with an 'X' are included in the corresponding report.

The goals of the first report are, first, to achieve confidence that different simulation models are calibrated and, second, to present fundamental performance metrics for the physical and link layer of various proposals.
The system level calibration shall follow the procedures described in this document.

Items		Evaluation Report 1	Evaluation Report 2
Link Level Simulation		X	
System simulations with 19 tri-sector cells layout		X	X
System Simulation calibration		X	-
Applications	Full Buffers	X	-
	Traffic Type Mix		X
Channel Models	Suburban macro, 3 Km/h pedestrian B[3], 100% (No channel mix)	X	X
	Suburban macro, 120Km/h Vehicular B, 100% (No channel mix)	X	X
	Link-level 250 Km/h suburban macro model and system level Channel Mix Models		X
Network delay and loss model			X
Mobility (i.e. Handover) model			X
Overhead Channels model			X
RF characteristics		X	
Link Budget		X	-

Table 35: Evaluation Reports

]

[3] *Link curves should be provided for the considered channel models*

Appendix-A: Spatial Correlation Calculation

In order to compute the spatial correlation, two methods can be considered here:

Method-1: Using 20 subpaths to approximate the Laplacian PDF

For each path, generate 20 subpaths with some angular offsets from the per-path AOD_n and AOA_n. The angular offsets of the k-th (k=1..20) subpath are determined by (the offsets are the same for all paths)

$$\psi_{k,BS} = \Delta_k AS_{BS,Path}$$
$$\psi_{k,MS} = \Delta_k AS_{MS,Path}$$

where the values of Δ_k are given below.

Sub-path number *k*	Δ_k
1,2	± 0.0447°
3,4	± 0.1413°
5,6	± 0.2492°
7,8	± 0.3715°
9,10	± 0.5129°
11,12	± 0.6797°
13,14	± 0.8844°
15,16	± 1.1481°
17,18	± 1.5195°
19,20	± 2.1551°

Table 36: Value of Δ_k

Derive the antenna spatial correlation at the BS and MS between the p-th and q-th antenna as:

$$r_{n,BS}(p,q) = \frac{1}{20}\sum_{k=1}^{20}\exp\left\{j\frac{2\pi d_{BS}}{\lambda}(p-q)\sin(AOD_n + \psi_{k,BS})\right\}$$
$$r_{n,MS}(p,q) = \frac{1}{20}\sum_{k=1}^{20}\exp\left\{j\frac{2\pi d_{MS}}{\lambda}(p-q)\sin(AOA_n + \psi_{k,MS})\right\}$$

where d_{BS} (d_{MS}) is the antenna spacing at BS (MS) and λ is the wavelength.

Method-2:Pre-compute the correlation values with quantized AOA, AOD

Pre-calculate the BS spatial correlation matrices for a set of $AOD \in \{-90^o, -80^o, \cdots, 0^o, \cdots, 80^o, 90^o\}$ and the MS spatial correlation matrices for a set of $AOA \in \{-90^o, -80^o, \cdots, 0^o, \cdots, 80^o, 90^o\}$

$$R_{BS}(m,p,q) = \int_{-\infty}^{\infty} p(\alpha)\exp\left\{j\frac{2\pi d_{BS}}{\lambda}(p-q)\sin(AOD[m]+\alpha)\right\}d\alpha$$
$$R_{MS}(m,p,q) = \int_{-\infty}^{\infty} p(\beta)\exp\left\{j\frac{2\pi d_{MS}}{\lambda}(p-q)\sin(AOA[m]+\beta)\right\}d\beta$$

where m is the quantization step index, α, β are the angular offset at BS and MS, respectively with Laplacian PDF as defined.

For each path, determine the index m_{BS} corresponding to AOD_n,

$$m_{BS} = \left\lfloor \frac{AOD_n}{10} \right\rfloor$$

and the index m_{MS} corresponding to AOA_n

$$m_{MS} = \left\lfloor \frac{AOA_n}{10} \right\rfloor$$

The spatial correlation matrix for this path is then

$$r_{n,BS}(p,q) = R_{BS}(m_{BS}, p, q)$$
$$r_{n,MS}(p,q) = R_{MS}(m_{MS}, p, q)$$

Appendix-B: Polarized Antenna

Correlation between polarized antennas results from the cross polarization power ratio (XPR). The polarization matrix is given by:

$$\mathbf{S} = \begin{bmatrix} s_{vv} & s_{vh} \\ s_{hv} & s_{hh} \end{bmatrix},$$

where *v* denotes vertical and *h* horizontal polarization, the first index denoting the polarization at BS and the second the polarization at MS. In the ITU scenarios we assume -8 dB per-tap power ratio between vertical-to-horizontal and vertical-to-vertical polarisations (also P_{hv}/P_{hh} = -8dB). The -8dB value was adopted from [1]. The following derivation of antenna correlation due to polarization with -8dB XPD can also be found in [1]. This results in the following mean power per polarization components

$$p_{vv} = E\left\{\left|s_{vv}\right|^2\right\} = 0\,\text{dB} = 1$$

$$p_{vh} = E\left\{\left|s_{vh}\right|^2\right\} = -8\,\text{dB} = 0.1585$$

$$p_{hv} = E\left\{\left|s_{hv}\right|^2\right\} = -8\,\text{dB} = 0.1585$$

$$p_{hh} = E\left\{\left|s_{hh}\right|^2\right\} = 0\,\text{dB} = 1$$

If the MS polarizations are assumed to be vertical and horizontal, but the BS polarizations are slant +45° and -45°. The MS and BS polarization matrices $\mathbf{P}_{MS}$ and $\mathbf{P}_{BS}$ respectively are rotation matrices, which map vertical and horizontal polarizations to MS and BS antenna polarizations.

$$\mathbf{P}_{MS} = \begin{bmatrix} 1 & 0 \\ 0 & 1 \end{bmatrix}$$

$$\mathbf{P}_{BS} = \frac{1}{\sqrt{2}} \begin{bmatrix} 1 & 1 \\ 1 & -1 \end{bmatrix}$$

The total channel is the matrix product of the BS polarization, the channel polarization, and the MS polarization:

$$\mathbf{Q} = \mathbf{P}_{BS}\,\mathbf{S}\,\mathbf{P}_{MS} = \frac{1}{\sqrt{2}} \begin{bmatrix} s_{vv} + s_{hv} & s_{vh} + s_{hh} \\ s_{vv} - s_{hv} & s_{vh} - s_{hh} \end{bmatrix}$$

The covariance matrix of the channel is

$$\boldsymbol{\Gamma}_{UL} = E\left\{vec(\mathbf{Q})\cdot vec(\mathbf{Q})^{H}\right\}$$

$$= E\left\{\frac{1}{2}\begin{bmatrix} (s_{vv}+s_{hv})(s_{vv}+s_{hv})^{*} & (s_{vv}+s_{hv})(s_{vv}-s_{hv})^{*} & (s_{vv}+s_{hv})(s_{vh}+s_{hh})^{*} & (s_{vv}+s_{hv})(s_{vh}-s_{hh})^{*} \\ (s_{vv}-s_{hv})(s_{vv}+s_{hv})^{*} & (s_{vv}-s_{hv})(s_{vv}-s_{hv})^{*} & (s_{vv}-s_{hv})(s_{vh}+s_{hh})^{*} & (s_{vv}-s_{hv})(s_{vh}-s_{hh})^{*} \\ (s_{vh}+s_{hh})(s_{vv}+s_{hv})^{*} & (s_{vh}+s_{hh})(s_{vv}-s_{hv})^{*} & (s_{vh}+s_{hh})(s_{vh}+s_{hh})^{*} & (s_{vh}+s_{hh})(s_{vh}-s_{hh})^{*} \\ (s_{vh}-s_{hh})(s_{vv}+s_{hv})^{*} & (s_{vh}-s_{hh})(s_{vv}-s_{hv})^{*} & (s_{vh}-s_{hh})(s_{vh}+s_{hh})^{*} & (s_{vh}-s_{hh})(s_{vh}-s_{hh})^{*} \end{bmatrix}\right\}$$

$$= \frac{1}{2}\begin{bmatrix} p_{vv}+p_{hv} & p_{vv}-p_{hv} & 0 & 0 \\ p_{vv}-p_{hv} & p_{vv}+p_{hv} & 0 & 0 \\ 0 & 0 & p_{vh}+p_{hh} & p_{vh}-p_{hh} \\ 0 & 0 & p_{vh}-p_{hh} & p_{vh}+p_{hh} \end{bmatrix}$$

Here the property of uncorrelated fading between different elements in **S** (i.e. $E\left\{s_{ij}s_{kl}^{*}\right\}=0, \quad i\neq k, j\neq l$) has been used to simplify the expressions. Plugging the numerical example of -8dB XPD, we have

$$\boldsymbol{\Gamma}_{UL} = \frac{1}{2}\begin{bmatrix} 1+0.1585 & 1-0.1585 & 0 & 0 \\ 1-0.1585 & 1+0.1585 & 0 & 0 \\ 0 & 0 & 0.1585+1 & 0.1585-1 \\ 0 & 0 & 0.1585-1 & 0.1585+1 \end{bmatrix} = \begin{bmatrix} 0.5793 & 0.4208 & 0 & 0 \\ 0.4208 & 0.5793 & 0 & 0 \\ 0 & 0 & 0.5793 & -0.4208 \\ 0 & 0 & -0.4208 & 0.5793 \end{bmatrix}$$

When all of the diagonal elements are equal, the covariance matrix can be further normalised to correlation matrix:

$$\Gamma_{UL} = \begin{bmatrix} 1 & \gamma & 0 & 0 \\ \gamma & 1 & 0 & 0 \\ 0 & 0 & 1 & -\gamma \\ 0 & 0 & -\gamma & 1 \end{bmatrix}$$

Value of γ depends only on XPR and it is obtained from the previous matrix after the normalization of the diagonal values to “1”. With different orientations of MS and BS antenna polarizations, also the covariance matrix structure will be different.

Note that the channel matrix **Q** is defined from an uplink perspective (i.e., from MS to BS). From the downlink perspective, the matrix $\mathbf{Q}^{T}$ should be used and the corresponding polarization correlation matrix should be

$$\boldsymbol{\Gamma} = \begin{bmatrix} 1 & 0 & \gamma & 0 \\ 0 & 1 & 0 & -\gamma \\ \gamma & 0 & 1 & 0 \\ 0 & -\gamma & 0 & 1 \end{bmatrix}$$

Appendix-C: LOS Option with a K-factor

A single-tap MIMO channel can be added to the TDL channels in this case and then modify the time-domain channels as:

$$\mathbf{H}_n = \begin{cases} \sqrt{\frac{1}{K+1}}\mathbf{H}_n + \sqrt{\frac{K}{K+1}}\mathbf{H}^{LOS} & n = 1(\text{first tap}) \\ \sqrt{\frac{1}{K+1}}\mathbf{H}_n & n \neq 1 \end{cases}$$

where the K-factor is in decimal and the LOS component is defined as, between p-th BS antenna and q-th MS antenna

$$\mathbf{H}^{LOS}(p,q) = \exp\left(j\frac{2\pi d_{BS}(p-1)}{\lambda}\sin(\theta_{BS})\right) \times \exp\left(j\frac{2\pi d_{MS}(q-1)}{\lambda}\sin(\theta_{MS})\right)$$

where d_{BS} and d_{MS} are antenna spacing at the BS and MS, respectively, assuming uniform linear array in this case.

Appendix-D: Antenna Gain Imbalance and Coupling

Overall receive correlation matrix is

$$\mathbf{H}_n^{'} = \begin{bmatrix} \sqrt{\frac{1}{c+1}} & \sqrt{\frac{c}{c+1}} \\ \sqrt{\frac{c}{c+1}} & \sqrt{\frac{1}{c+1}} \end{bmatrix} \begin{bmatrix} 1 & 0 \\ 0 & \sqrt{a} \end{bmatrix} \mathbf{H}_n$$

where antenna-1 to antenna-2 coupling coefficient (leakage of ant-1 signal to ant-2) is "c" (linear) and the antenna-1 and antenna gain ratio is "a" (linear).

Appendix-E: WINNER Primary Model Description

<Editor's note: The following text is the proposed text from Electrobit to the drafting subgroup>

This appendix describes the primary model from which the CDL models were derived. The primary model is an accurate representation of the true MIMO radio channel. The CDL modes are a simplification of the primary model in order to save simulation time. The use of the primary model is optional but encouraged for further simulation.

The proposed channel model is a geometry-based stochastic model. Geometric based modeling of the radio channel enables separation of propagation parameters and antennas.
The channel parameters for individual snapshots are determined stochastically, based on statistical distributions extracted from channel measurement. Antenna geometries and field patterns can be defined properly by the user of the model. Channel realizations are generated with geometrical principle by summing contributions of rays (plane waves) with specific small scale parameters like delay, power, angle-of-arrival (AoA) and angle-of-departure (AoD). Superposition results to correlation between antenna elements and temporal fading with geometry dependent Doppler spectrum.

A number of rays constitute a cluster. In the terminology of this document we equate the cluster with a propagation path diffused in space, either or both in delay and angle domains. Elements of the MIMO channel, i.e. antenna arrays at both link ends and propagation paths, are illustrated in Figure 30

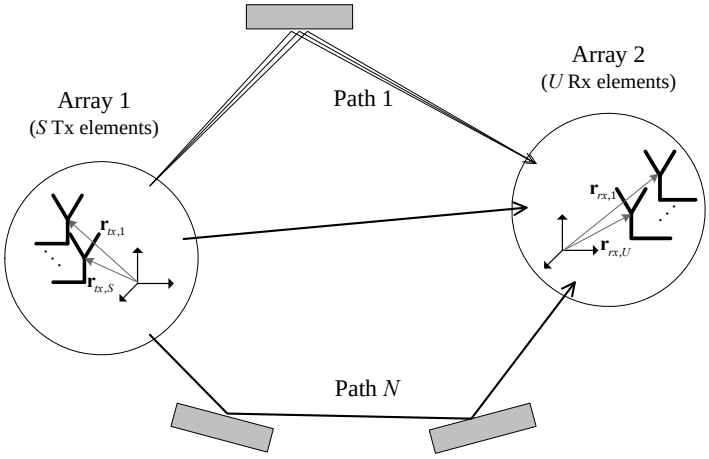

Figure 30: MIMO Channels

Transfer matrix of the MIMO channel is

$$\mathbf{H}(t;\tau)=\sum_{n=1}^{N}\mathbf{H}_n(t;\tau)$$

It is composed of antenna array response matrices $\mathbf{F}_{tx}$ for the transmitter, $\mathbf{F}_{rx}$ for the receiver and the propagation channel response matrix $\mathbf{h}_n$ for cluster *n* as follows

$$\mathbf{H}_n(t;\tau)=\iint \mathbf{F}_{rx}(\varphi)\mathbf{h}_n(t;\tau,\phi,\varphi)\mathbf{F}_{tx}^{T}(\phi)\,d\phi d\varphi$$

The channel from Tx antenna element *s* to Rx element *u* for cluster *n* is

$$\begin{aligned}H_{u,s,n}(t;\tau)=\sum_{m=1}^{M}&\begin{bmatrix}F_{rx,u,V}(\phi_{n,m})\\F_{rx,u,H}(\phi_{n,m})\end{bmatrix}^{T}\begin{bmatrix}\alpha_{n,m,VV} & \alpha_{n,m,VH}\\ \alpha_{n,m,HV} & a_{n,m,HH}\end{bmatrix}\begin{bmatrix}F_{tx,s,V}(\varphi_{n,m})\\F_{tx,s,H}(\varphi_{n,m})\end{bmatrix}\\ &\times\exp\left(j2\pi\lambda_0^{-1}(\bar{\phi}_{n,m}\cdot\bar{r}_{rx,u})\right)\exp\left(j2\pi\lambda_0^{-1}(\bar{\varphi}_{n,m}\cdot\bar{r}_{tx,s})\right)\\ &\times\exp\left(j2\pi\upsilon_{n,m}t\right)\delta(\tau-\tau_{n,m})\end{aligned}$$

where $F_{rx,u,V}$ and $F_{rx,u,H}$ are the antenna element *u* field patterns for vertical and horizontal polarizations respectively, $\alpha_{n,m,VV}$ and $\alpha_{n,m,VH}$ are the complex gains of vertical-vertical and vertical-horizontal polarizations of ray *n*,*m* respectively. Further λ_0 is the wave length on carrier frequency, $\bar{\phi}_{n.m}$ is AoD unit vector, $\bar{\varphi}_{n.m}$ is AoA unit vector, $\bar{r}_{tx,s}$ and $\bar{r}_{rx,u}$ are the location vectors of element *s* and *u* respectively, and $\upsilon_{n,m}$ is the Doppler frequency component of ray *n,m*. If the radio channel is modeled as dynamic, all the above mentioned small scale parameters are time variant, i.e. function of *t*.

WINNER generic model is a system level model, which can describe an infinite number of propagation environment realizations. The generic model can describe single or multiple radio links for all the defined scenarios and arbitrary antenna configurations. This is done by applying different parameter sets to a single common mathematical framework. The generic model is a stochastic model with two (or three) levels of randomness. The first level, known as large scale (LS), parameters like Shadow fading, delay and angular spreads are drawn randomly from tabulated distribution functions. LS parameters have cross-correlation between different parameters and auto-correlation between different transceiver locations. Next, the small scale parameters like delays, powers and directions arrival and departure are drawn randomly according to tabulated distribution functions and the random LS parameters (second moments). At this stage the geometric setup is fixed and the only free variables are the random initial phases of the scatterers. By picking (randomly) different initial phases, an infinite number of different realizations of the model can be generated. When the initial phases are also fixed, there is no further randomness.

Channel segment (drop) represents period of quasi-stationarity in witch probability distributions of low-level parameters are not changed. During this period all large-scale control parameters, as well as velocity and direction-of-travel for mobile station (MS), are held constant. Motion within a segment is only virtual and causes fast fading and the Doppler effect by superposition of rotating phasors, rays. To be physically feasible, the

channel segment must be relatively confined in distance. The size depends on the environment, but it can be at maximum few meters. Although the large scale parameters can be correlated between the channel segments, the radio channel is discontinuous from segment to segment.

Detailed description of the WINNER model is given in [12] An implementation of the primary model is available at [24]

Appendix-F: Generic Proportionally Fair Scheduler for OFDMA

The proportionally fair scheduler (PFS), in its simplest form, computes a metric for all active users at for a given scheduling interval. The user with the highest metric is allocated the resource available in the given interval, the metrics for all users are updated before the next scheduling interval, and the process repeats. To adapt this simple algorithm for OFDMA systems, the definition of scheduling interval and scheduling resource must be extended to apply to a two-dimensional OFDMA frame resource. Furthermore, this PFS applies only to full buffer traffic simulations and zones which use a distributed subcarrier permutation such as PUSC.

For OFDMA systems, the scheduling interval is typically a frame, and multiple users may be allocated in the same frame. Therefore, in the simplest extension to OFDMA systems, two modifications must be made to the PFS: (i) Frames must be equi-partitioned into regular, fixed scheduling resources that must be scheduled sequentially until all available resources are assigned. [(ii) The metric must be updated after scheduling each resource. Note that the number of resources eventually allocated to a user depends on the metric update process, and does not preclude a single user from getting multiple or all the resources in a frame.]

To promote fair comparison, each proponent should evaluate system performance with full-buffer traffic using this generic PFS. If this scheduler is not used, the proponent must justify the use of an alternate scheduler, and describe the algorithm in detail. The number of partitions, $N_{partitions}$, , the time constant of the filter used in the metric computation, and number of active users are all simulation parameters that must be specified by the proponent.

For informative purposes, the metric for a simple proportionally fair scheduler, in which a single user is scheduled in a given scheduling interval, is described in the remainder of this appendix.

At any scheduling instant t, the scheduling metric $M_i(t)$ for subscriber i used by the proportional fair scheduler is given by

$$M_i(t) = \frac{T\_inst_i(t)}{T\_smoothed_i(t)}$$

where $T\_inst_i(t)$ is the data rate that can be supported at scheduling instant t for subscriber i $T\_inst_i(t)$ is a function of the instantaneous SINR, and consequently of the modulation and coding scheme that can meet the PER requirement. $T\_smoothed_i(t)$ is throughput smoothed by a low-pass filter at the scheduling instant t for user i. For the scheduled subscriber, $T\_smoothed_i(t)$ is computed as

$$T\_smoothed_i(t) = \frac{1}{T_{PF}} * T\_inst_i(t) + (1 - \frac{1}{T_{PF}}) * T\_smoothed_i(t-1)$$

and for unscheduled subscriber,

$$T\_smoothed_i(t) = (1 - \frac{1}{T_{PF}}) * T\_smoothed_i(t-1)$$

where $T_{PF} > 1$ represents the latency time scale of the PF scheduler.

[The trade-off between spectral efficiency and delay is implicit in the choice of the latency time scale. Larger values of T_{PF} make it possible for the scheduler to wait longer to schedule subscribers when channel conditions are most favorable.

Shorter time scales reduce the opportunities the scheduler has in scheduling a particular subscriber since the smoothed throughput, which diminishes each time a subscriber is not scheduled, becomes the dominant factor in the value of the metric. Although the smoothed throughput for an unscheduled subscriber drops with every scheduling opportunity that is missed, the metric for the same subscriber increases, ultimately forcing the subscriber to be scheduled within the latency time scale of operation.]

In some implementations, the scheduler may give priority to HARQ retransmissions.

Appendix-G: 19-Cell Wrap-Around Implementation

G-1. Multi-Cell Layout

In Figure 31, a network of cells is formed with 7 clusters and each cluster consists of 19 cells. Depending on the configuration being simulated and required output, the impact of the outer 6 clusters may be neglected. In such cases, only 19 cells of the center cluster may be modeled.

For the cases where modeling outer-cells are necessary for accuracy of the results, the wrap around structure with the 7 cluster network can be used. In the wrap around implementation, the network is extended to a cluster of networks consisting of 7 copies of the original hexagonal network, with the original hexagonal network in the middle while the other 6 copies are attached to it symmetrically on 6 sides, as shown in Figure 31. The cluster can be thought of as 6 displacements of the original hexagon. There is a one-to-one mapping between cells/sectors of the center hexagon and cells/sectors of each copy, so that every cell in the extended network is identified with one of the cells in the central (original) hexagonal network. Those corresponding cells have thus the same antenna configuration, traffic, fading etc. except the location. The correspondence of those cells/sectors is illustrated in Figure 32.

An example of the antenna orientations in case of a sectorized system is defined in . The distance from any MS to any base station can be obtained from the following algorithm: Define a coordinate system such that the center of cell 1 is at (0,0). The path distance and angle used to compute the path loss and antenna gain of a MS at (x,y) to a BS at (a,b) is the minimum of the following:

a. Distance between (x,y) and (a,b);
b. Distance between (x,y) and $(a+3R, b+8\sqrt{3}R/2)$;
c. Distance between (x,y) and $(a-3R, b-8\sqrt{3}R/2)$;
d. Distance between (x,y) and $(a+4.5R, b-7\sqrt{3}R/2)$;
e. Distance between (x,y) and $(a-4.5R, b+7\sqrt{3}R/2)$;
f. Distance between (x,y) and $(a+7.5R, b+\sqrt{3}R/2)$;
g. Distance between (x,y) and $(a-7.5R, b-\sqrt{3}R/2)$,

Where, R is the radius of a circle which connects the six vertices of the hexagon.

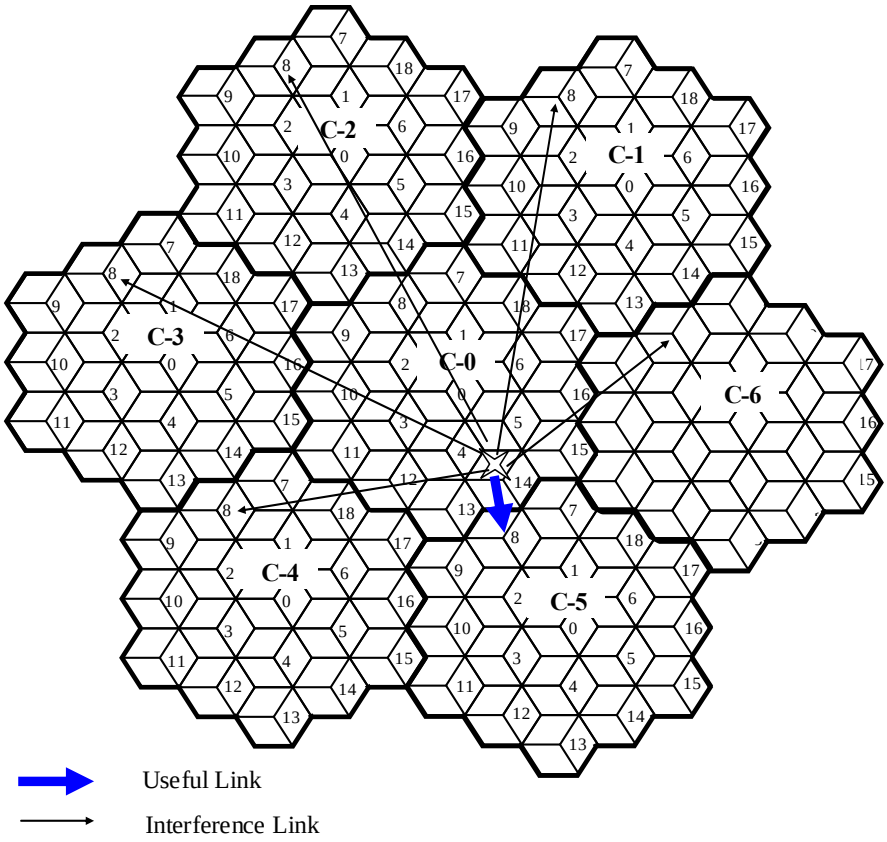

Figure 31: Multi-cell Layout and Wrap Around Example

G-2. Obtaining virtual MS locations

The number of MSs is predetermined for each sector, where each MS location is uniformly distributed. The MS assignment is only done for the cluster-0 from where the decided MSs are replicated in the other six clusters. The purpose to employ this wrap-around technique, as will be discussed in later section, is to easily model the interferences from other cells.

G-3. Determination of serving cell/sector for each MS in a wrap-around multi-cell network

The determination of serving cell for each MS is carried out by two steps due to the wrap-around cell layout. The first step is to determine the 19 shortest distance cells for each MS from all seven logical cells clusters, and the second step is to determine the serving cell/sector among the nearest 19 cells for each MS based on the strongest link according to the path-loss and shadowing.

To determine the shortest distance cell for each MS, the distances between the target MS and all logical cell clusters should be evaluated and the 19 cells with a shortest distance in all 7 cell clusters should be selected. Figure 31 illustrates an example for determination of the shortest distance cell for the link between MS and cell-8. It can be

seen that the cell-8 located in cluster-5 generates the shortest distance link between MS and cell-8.

To determine the serving cell for each MS, we need to determine 19 links, whereby we may additionally determine the path-loss, shadowing and transmit/receive antenna gain in consideration of antenna pattern corresponding to the nearest 19 cells/sectors. The serving cell for each MS should offer a strongest link with a strongest received long-term power. It should be noted that the shadowing experienced on the link between MS and cells located in different clusters is the same.

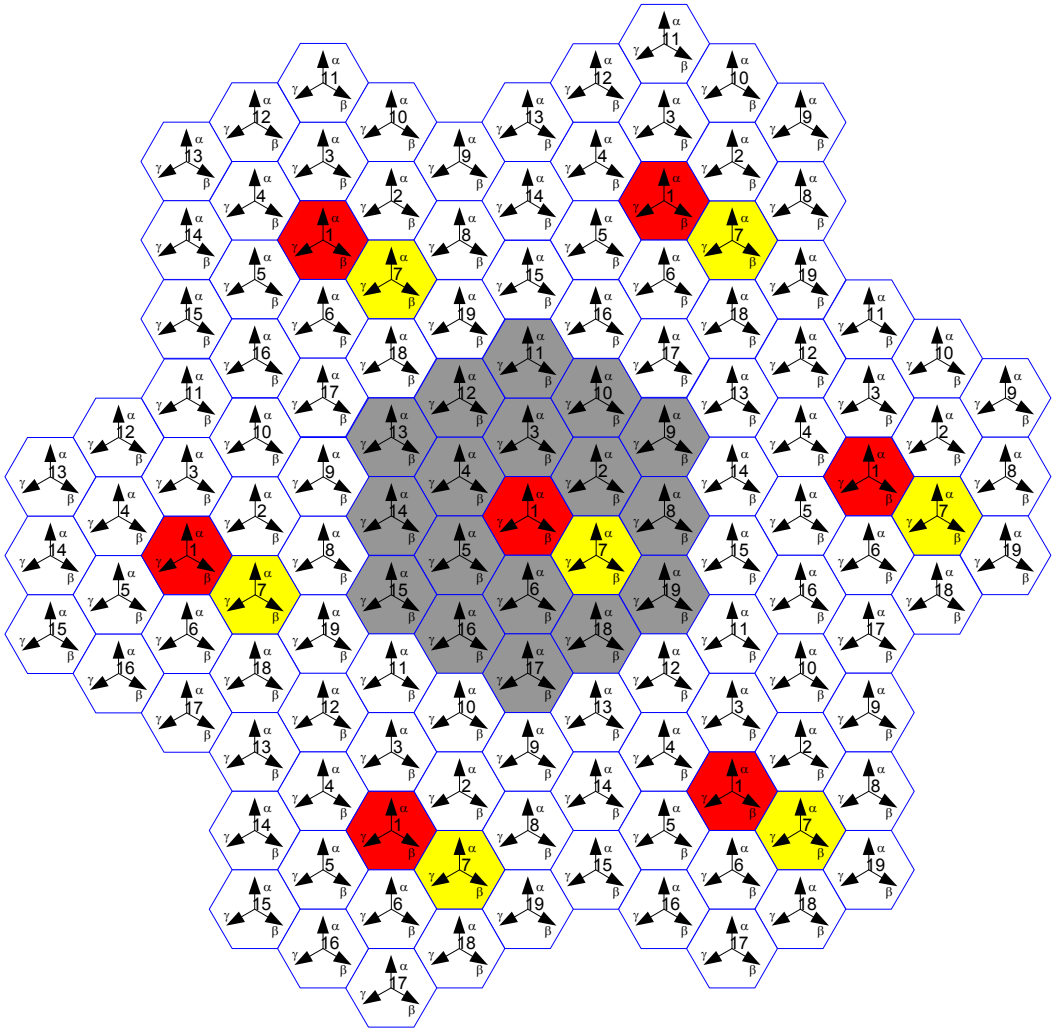

Figure 32: An example of the antenna orientations for a sectorized system to be used in the wrap-around simulation. The arrows in the Figure show the directions that the antennas are pointing

Appendix-H: Calculation of PAPR and Cubic Metric

Sources	Document Reference
Sassan Ahmadi et al. Jeff Zhuang et al.	C80216m-07_069.doc

When power amplifier and radiated spectrum performance related subjects are discussed, for example to evaluate the amount of backoff needed to achieve a certain radiated spectrum requirement (e.g., Adjacent Channel Loss Ratio or ACLR), PAPR and CM are two options that are commonly used.

[

H-1. Peak to Average Power Ratio (PAPR)

PAPR could be used to calculate the TX power amplifier back-off value. Since it is not desirable to change the back-off value at every symbol, the rms transmit power should be evaluated over a long period of time. For the calculation of average power, the worst case assumption, which causes maximum average power, should be made; e.g., maximum loading of data. In addition it is desirable for the P_{av1} defined below to have a similar value from symbol-to-symbol.

P_{av1} denotes the average power over one OFDM symbol duration defined by

$$P_{av1} = \frac{1}{T}\int_0^T |s(t)|^2 dt$$

where s(t) is the time domain OFDM signal. Note that s(t) may include a weight matrix to take into account the transmit beamforming, and closed-loop MIMO if any. Note that the weight matrix is a function of channel and can increase the peak power.

P_{av} is an ensemble average of OFDM symbols over all possible random data, and channel

$$P_{av} = E\left\{|s(t)|^2\right\}$$

In transmit antenna selection, the average power should be evaluated only when the antenna is selected in order to get the maximum (or worst case) average power.

P_{max} is the peak power measured over one OFDM symbol duration and it is defined as

$$P_{max} = \max_{0 \le t < T} |s(t)|^2$$

Then, the PAPR1 and PAPR are defined as follows

$$PAPR_1 = \frac{P_{\max}}{P_{av1}}$$

$$PAPR = \frac{P_{\max}}{P_{av}},$$

The CCDF of PAPR1 and PAPR should be evaluated over all possible channel conditions, and random OFDM signals. In the PAPR simulations, the signal shall be over-sampled at least 8 times. The guard interval can be included in the OFDM symbol duration (T). From P_{av} and CCDF of PAPR, the back-off value and operating point of PA can be obtained.

H-2. Instantaneous PAPR

The instantaneous power can be written as

$$P_i = |s(t)|^2.$$

We can define two different instantaneous PAPR by normalizing using either P_{av1} or P_{av}

$$PAPR_{i1} = \frac{P_i}{P_{av1}}, \text{ and}$$

$$PAPR_i = \frac{P_i}{P_{av}}.$$

Note that we should look at lower probability in CCDF of $PAPR_i$ than that in PAPR case depending on the number of samples during one OFDM symbol.
]

[

H-3. Cubic Metric

The cubic metric is a well established approach ([56], Section 6.2.2) to assessing the impact of the peak excursions of a power amplifier transmitted waveform. Originally specified for direct sequence spread CDMA waveforms (such as 3GPP WCDMA), the cubic metric method has been further studied in the specification of variable bandwidth OFDM systems [57], where it has again been found to be an accurate predictor of critical power amplifier and radiated spectrum performance criteria such as Adjacent Channel Loss Ratio (ACLR).

A larger CM denotes a more difficult waveform type for power amplification, leading to greater spectrum expansion or adjacent channel power insertion. Alternatively, CM can be used to compute the amount of “power back-off” required to achieve the same ACLR. A waveform CM value which is greater by 1dB than the CM for a second

waveform implies the first waveform, for the same PA and current drain, can be radiated at 1dB higher mean power level.

The cubic metric (CM) of a waveform $v(t)$ is formally defined as

$$CM\,(dB) = \frac{20\log_{10}\{rms\left[v_{norm}^{3}(t)\right]\} - 20\log_{10}\{rms\left[v_{ref}^{3}(t)\right]\}}{K}$$

where $rms(x) = \sqrt{\frac{x^T x}{N}}$ (where x is sampled as a length-N vector), and $v_{norm}(t) = \frac{|v(t)|}{rms[v(t)]}$.

In the above equation, the reference CM of $20\log_{10}\{rms\left[v_{ref}^{3}(t)\right]\}$ and the coefficient K are determined empirically by studying the behavior of contemporary mobile station power amplifiers [57].

For the present purpose, the following expression is applicable

$$CM = \frac{20\log_{10}\left\{rms\left[v_{norm}^{3}(t)\right]\right\} - 1.52}{1.56} + 0.77 \quad dB$$

]

Appendix-I: Overhead Calculations

Sources	Document Reference
Sassan Ahmadi et al.	C80216m-07_069.doc
Dan Gal et al.	C80216m-07_063.doc

[

I-1. Overhead Channels

I-1.1. Dynamical Simulation of the Downlink Overhead Channels

Dynamically simulating the overhead channels is essential to capture the dynamic nature of these channels. The simulations shall be done as follows:

The performance of the overhead channels shall be included in the system level simulation results unless the overhead channel is taken into account as part of fixed overhead e.g., if an overhead channel is time division multiplexed, and takes all the bandwidth, the percentage of time used translates into the same percentage decrease of throughput.

There are two possible types of overhead channels depending on the proposal: static and dynamic. A static overhead channel requires fixed base station power. A dynamic overhead channel requires dynamic base station power.

The demodulation performance (i.e., frame error rate) of the downlink control channel could be assessed using the link abstraction method used to model traffic channels, with proper modifications, if necessary, to reflect any difference in the transmission or coding format of the control channel.

[The link level performance should be evaluated off-line by using separate link-level simulations. The performance is characterized by curves of detection, miss, false alarm, and error probability (as appropriate) versus Eb/No (or some similar metric depending on the interface between the link and system simulations).

The system level simulations need not directly include the coding and decoding of overhead channels. There are two aspects that are important for the system level simulation: the required Ec/Ior (or some similar metric depending on the interface between the link and system simulations) during the simulation interval, and demodulation performance (detection, miss, and error probability — whatever is appropriate).]

For static overhead channels, the system simulation should compute the received [Eb/No (or similar metric)] [SINR] and predict the demodulation performance.

For dynamic overhead channels with open-loop control (if used), the simulations should take into account the estimate of the required downlink power that needed to be transmitted to the mobile station for the overhead channels. During the reception of overhead information, the system simulation should compute the received [SINR] [Eb/No (or similar metric)].

Once the received [SINR] [Eb/No (or similar metric)] is obtained and the frame error rate is predicted, then the various miss error events should be determined. The impact of these events should then be modeled. The false alarm events are evaluated in link-level simulation, and the simulation results shall be included in the evaluation report. The impact of false alarm, such as delay increases and throughput reductions for both the downlink and uplink, shall be appropriately taken into account in system-level simulation.

All overhead channels should be modeled or accounted for.

If a proposal adds messages to an existing channel (for example sending control on a data channel), the proponent shall justify that this can be done without creating undue loading on this channel. The system level and link level simulation required for this modified overhead channel as a result of the new messages shall be performed according to 3) and 4), respectively.

I-1.2. Uplink Modeling in Downlink System Simulation

The proponents shall model feedback errors (e.g. power control, acknowledgements, rate indication, etc.) and measurements (e.g. C/I measurement). In addition to supplying the feedback error rate average and distribution, the measurement error model and selected parameters, the estimated power level required for the physical reverse link channels shall be supplied.

I-1.3. Signalling Errors

Signaling errors shall be modeled and specified as in the following table.

Signaling Channel	Errors	Impact
ACK/NACK channel (if proposed)	Misinterpretation, missed detection, or false detection of the ACK/NACK message	Transmission (frame or encoder packet) error or duplicate transmission
Explicit Rate Indication (if proposed)	Misinterpretation of rate	One or more Transmission errors due to decoding at a different rate (modulation and coding scheme)
User identification channel (if proposed)	A user tries to decode a transmission destined for	One or more Transmission errors due to HARQ/IR

	another user; a user misses transmission destined to it.	combining of wrong transmissions
Rate or C/I feedback channel (if proposed)	Misinterpretation of rate or C/I	Potential transmission errors
Transmit sector indication, transfer of H-ARQ states etc. (if proposed)	Misinterpretation of selected sector; misinterpretation of frames to be retransmitted.	Transmission errors

Table 37: Signaling Errors

Proponents shall quantify and justify the signaling errors and their impacts in the evaluation report.
]

[

I-2. Calculation of Overhead

I-2.1. Calculation of L1 overhead

The L1 overhead shall be accounted for the purpose of calculation of system performance metrics such as spectral efficiency, user throughput, etc. The following are the list of L1 overhead that shall be accounted for in the overhead calculation:

1. Number of sub-carriers that carry preamble ($N_{preamble}$)
2. Number of sub-carriers that are used as the guard carriers and DC sub-carrier (N_{guard}).
3. Number of sub-carriers that are assigned to the TX/RX switching points (N_{gap}) (for TDD duplex scheme only).
4. Number of sub-carriers that are used to carry pilots (N_{pilot}) in downlink or uplink sub-frame.
5. The cyclic prefix (CP) or the guard interval (GI) is accounted for through the actual number of OFDM symbols within a frame.

Given transmission bandwidth (BW) and sub-carrier spacing (1/T when there is no cyclic prefix), the ideal number of sub-carriers per OFDM symbol becomes $BW \cdot T$. The number of OFDM symbols over frame duration (T_f) excluding L1 overhead can be expressed as $\frac{T_f}{T}$. Hence, the total number of available sub-carriers over BW and T_f becomes $M = BW \cdot T_f$.

However, due to L1 overhead, the actual number of available sub-carriers (N) over a frame and the transmission bandwidth will be smaller than M.

$$L1_{overhead} = \frac{M - N}{M} \times 100 \text{ in \%}$$

As an example in IEEE 802.16e reference system, M=10 MHz * 5 ms = 50000. Using DL PUSC, 47 OFDM symbols are available (including the preamble and cyclic prefix overhead). The number of usable sub-carriers for both data and pilot is 840*47 including the effect of guard sub-carriers. In PUSC, the number of pilots is 840*47/56*8=5640. Thus, N is equal to 840*47*48/56=33840. Hence, the L1 overhead becomes 32.3%.

I-2.2. Calculation of L1+L2 overhead

The L2 overhead includes the following:

1. The number of OFDM symbols (or sub-carriers) that are used for MAP
2. The average number of ODFM symbols (or sub-carriers) that are used for system configuration information (FCH, DCD/UCD).
3. The number of OFDM symbols (or sub-carriers) that are used for ACK/NACK,
4. The number of OFDM symbols (or sub-carriers) that are used for CQICH,
5. The number of OFDM symbols (or sub-carriers) that are used for Ranging

Let L denote the number of sub-carriers over a frame and the bandwidth excluding L2 overhead such as MAP, control channel, etc. Then, the L1+L2 overhead is defined

$L1 + L2_{overhead} = \frac{M - L}{M} \times 100$ in %.

The L2 overhead can be written as

$$L2_{overhead} = \frac{N - L}{N} \times 100 \text{ in \%.}$$

Note that $L1 + L2_{overhead} \neq L1_{overhead} + L2_{overhead}$.

]